



Ferdowsi University  
of Mashhad

Vol.13

No.6

2018

# Iranian Food Science and Technology Research Journal



ISSN:1735-4161

## Contents

- Optimization of textural characteristics of analogue UF-Feta cheese made from dairy and non-dairy ingredients..... 80**  
A. A. Gholamhosseinpour, M. Mazaheri Tehrani, S. M. A. Razavi
- Effect of pulsation period and microwave power on paddy drying ..... 92**  
H. Jafari, D. Kalantari, M. Azadbakht
- Changes in the surface tension and viscosity of fish oil nanoemulsions developed by sonication during storage..... 105**  
M. Nejadmansouri, S. M. H. Hosseini, M. Niakosari, Gh. H. Yousefi, M. T. Golmakani
- Effect of ultrasound bath and probe combined to brine and brine- polyphosphate solutions on the qualitative and textural properties of beef meat ..... 117**  
M. H Naeli, R. Esmailzadeh Kenari
- Development of a chitosan-montmorillonite nanocomposite film containing *Satureja hortensis* essential oil..... 131**  
V. Alizadeh, H. Barzegar, B. Nasehi, V. Samavati
- Study on the effects of sucrose and lactose on the rheological properties of *Alyssum homolocarpum* seed gum in dilute solutions ..... 144**  
M. A. Hesarinejad, S. M. A. Razavi, A. Koocheki, M. A. Mohammadifar

# Iranian Food Science and Technology Research Journal

Vol. 13

No. 6

2018

**Published by:** Ferdowsi University of Mashhad

**Executive Manager:** Shahnoushi, N.

**Editor-in-Chief:** Razavi, Seyed M. A.

**Executive Director:** Taghizadeh, M.

## Editorial Board:

Ehsani, M.R.	Prof. in Dairy Technology
Farahnaki, A.	Assoc. Prof. in Food Engineering
Farhoosh, R.	Prof. in Food Chemistry
Fazli Bazzaz, S.	Prof. in Microbiology
Habibi najafi, M.	Prof. in Microbiology
Kadivar, M.	Assoc. Prof. in Food Chemistry
Kashaninejad, M.	Assoc. Prof. in Food Engineering
Khomeiri, M.	Assoc. Prof. in Microbiology
Khosroshahi, A.	Prof. in Dairy Technology
Mortazavi, Seyed A.	Prof. in Microbiology and Biotechnology
Pourazerang, H.	Prof. in Food Chemistry
Razavi, Seyed M. A.	Prof. in Food Engineering
Sahari, M. A	Prof. in Food Chemistry
Sedaghat, N.	Assoc. Prof. in Food Packaging
Shahidi, F.	Prof. in Microbiology
Varidi, M.J.	Assoc. Prof. in Food technology

**Printed by:** Ferdowsi University of Mashhad Press, Iran.

**Address:** The Iranian Food Science & Technology Research Journal, Scientific Publication Office, Food Science and Technology Department, Agriculture Faculty, Ferdowsi University of Mashhad, Iran.

**P.O.BOX:** 91775- 1163

**Phone:** (98)511-8795618-20(321)

**Fax:** (98)511-8787430

**E-Mail:** ifstrj@um.ac.ir

**Web Site:** [http://jm.um.ac.ir/index.php/food\\_tech/index](http://jm.um.ac.ir/index.php/food_tech/index)

This journal is indexed in ISC, SID, and MAGIRAN.

## Contents

<b>Optimization of textural characteristics of analogue UF-Feta cheese made from dairy and non-dairy ingredients</b>	80
A. A. Gholamhosseinpour, M. Mazaheri Tehrani, S. M. A. Razavi	
<b>Effect of pulsation period and microwave power on paddy drying</b>	92
H. Jafari, D. Kalantari, M. Azadbakht	
<b>Changes in the surface tension and viscosity of fish oil nanoemulsions developed by sonication during storage</b>	105
M. Nejadmansouri, S. M. H. Hosseini, M. Niakosari, Gh. H. Yousefi, M. T. Golmakani	
<b>Effect of ultrasound bath and probe combined to brine and brine- polyphosphate solutions on the qualitative and textural properties of beef meat</b>	117
M. H Naeli, R. Esmailzadeh Kenari	
<b>Development of a chitosan-montmorillonite nanocomposite film containing <i>Satureja hortensis</i> essential oil</b>	131
V. Alizadeh, H. Barzegar, B. Nasehi, V. Samavati	
<b>Study on the effects of sucrose and lactose on the rheological properties of <i>Alyssum homolocarpum</i> seed gum in dilute solutions</b>	144
M. A. Hesarinejad, S. M. A. Razavi, A. Koocheki, M. A. Mohammadifar	

## Optimization of textural characteristics of analogue UF-Feta cheese made from dairy and non-dairy ingredients

A. A. Gholamhosseinpour<sup>1</sup>, M. Mazaheri Tehrani<sup>2\*</sup>, S. M. A. Razavi<sup>2</sup>

Received: 2016.10.05

Accepted: 2017.07.04

### Abstract

In this study, a mixture of milk protein concentrate, whey protein concentrate, skim milk powder, soymilk, margarine, butter and water was used for production of recombined UF-Feta cheese analogue. Variables were milk protein concentrate (8%, 9%, 10%), whey protein concentrate (0%, 1.5%, 3%), soymilk (5%, 10%, 15%) and margarine (0%, 5%, 10%). Textural properties of Samples were analyzed 3 days post-manufacture. The central composite design was employed and the results were modeled and analyzed using response surface methodology. Coefficients of determination,  $R^2$ , of fitted regression models for different variables were varied in the range of 89.59-97.80 and the lack-of-fit was not significant for all responses at 95%. Hence, the models for all the response variables were highly adequate. The results showed that the optimum processing conditions for producing cheese with suitable hardness and cohesiveness and lowest adhesiveness were: 9.13% milk protein concentrate, 3% whey protein concentrate, 15% soymilk and 7.65% margarine.

**Keywords:** Milk protein concentrate; Whey protein concentrate; Soymilk; Margarine; Analogue cheese; Texture profile.

### Introduction

Cheese is the generic name for a group of fermented dairy products, produced throughout the world in a wide range of flavours, textures and forms (Fox *et al.* 2000). It is commonly believed that cheese evolved in the 'Fertile Crescent' between the Tigris and Euphrates rivers, that run through modern-day Iraq, about 8000 years ago (Fox 2011). It is estimated that more than 2000 varieties exist and the list may still be growing (Gunasekaran and Mehmet 2003). The broad range of different cheeses available is based mainly on regional conditions and production technology, which has been repeatedly adapted and optimized (Isam *et al.* 2010).

UF-Feta cheese is a cheese with soft and spreadable texture that is produced from milk which has been concentrated by ultrafiltration,

to achieve total solids of 35 %, and then enzymatically coagulation of retentate. This type of cheese contains 45-60% fat (on dry basis), 28% protein (on dry basis) and max. 3% salt and its final pH after 72 hours is 4.8. UF-Feta cheese is a fresh cheese that can be consumed 3 days after production. The shelf life of UF-Feta cheese is max. 2 months (Iran standards 12736 and 6629).

Analogue cheese is generally manufactured from dairy and non-dairy proteins, various edible fat or oil sources, types of starches, other ingredients and water (Fox *et al.* 2000; McSweeney 2007). The main advantages of Analogue cheeses over natural cheeses are lower cost and relatively high functional stability during storage (Fox *et al.* 2000).

According to Abou El Nour *et al.* (1998), the replacement of rennet casein by milk protein concentrate (MPC, 85% protein) powders increase the firmness but decrease the meltability of spread-type cheese analogue. Shakeel-Ur-Rehman *et al.* (2003) found that using a mixture of cream and liquid MPC in low fat Cheddar cheese formulation increase the yield.

Whey protein concentrate (WPC) and skim milk powder (SMP) are used in variety of

1. Assistant professor, Department of Food Science and Technology, Faculty of Agriculture, Jahrom University, Jahrom, Iran.

2. PhD Student and Professor, Department of Food Science and Technology, Faculty of Agriculture, Ferdowsi University of Mashhad, Mashhad, Iran.

(\* - Corresponding Author Email: mmtehrani@um.ac.ir)

DOI: 10.22067/ifst.v1396i0.59349

process cheeses and analogues (Guinee *et al.* 2004). El-Neshawy *et al.* (1988) showed that increase in WPC caused an improvement in consistency and spreadability of the resultant processed cheese analogue. The addition of WPC increases the moisture content of cheese (Guinee *et al.* 2004). Gelation and water binding properties for WPC has also been implied (Harper 1991).

In spite of technological problems, Soymilk is one of soybean products that used in cheesemaking industry as a low cost substitute for milk protein. Ahmed *et al.* (1995) studied the feasibility of using soy protein as a partial replacement for casein in manufacturing of imitation cheeses and showed that increase of soy protein caused a decrease in firmness of cheeses. According to Metwalli *et al.* (1982), 20% of soymilk would be the maximum proportion of mixing with milk for cheese making. They observed that the higher concentration of soymilk (25-30%), resulted in the formation of a very weak curd. They also showed that autoclaving soymilk at 120°C for 15 min before mixing with milk, greatly improved curd firmness.

Attempts to reduce cheese costs have led to the use of vegetable fat and oil to replace the more costly milk fat (Mounsey and O'Riordan 2001; Chavan and Jana 2007). Fat and oil, apart from their nutritional significance in cheeses, are two of the most important ingredients affecting the sensory and textural properties of cheese (Miočinović *et al.* 2011). Metzger and Mistry (1995) studied the effect of fat on cheese structure and reported that the weakness of protein matrix was affected by the fat globule distribution. The use of vegetable fats in cheese formulations resulted in analogues that were harder or similar to cheeses manufactured with butter (Cunha *et al.* 2013). Soybean fat conferred hardness and adhesiveness to the cheese analogues, but decreased their cohesiveness and springiness (Lobato-Calleros *et al.* 1997).

The objective of the current study was to produce a mixture similar to retentate to produce a recombined cheese like UF-Feta cheese after addition of Enzyme, starter and

salt and evaluation of its textural properties.

### Material and Methods

Calcium chloride (food-grade) was obtained from Kemira Agro Ltd. (Helsinki, Finland). Milk protein concentrate containing 75% protein (MPC-75) was supplied by Milei GmbH (Stuttgart, Germany). Whey protein concentrate (WPC-35), skim milk powder (SMP) and butter were prepared from the Khorasan Pegah Dairy Co. (Mashhad, Iran). Margarine was obtained from BehinehWazin Co. (Mahgol<sup>TM</sup>) (Tehran, Iran). Full fat soy flour was purchased from Soyan Toos Co. (Mashhad, Iran).

The chemical composition of the MPC (proteins: 75%, water: 5%, ash: 7.6%, lactose: 10.9%, fat: 1.5%), WPC (proteins: 35%, water: 4.6%, ash: 7.2%, lactose: 50.2%, fat: 3%), SMP (proteins: 36%, water: 4%, ash: 7.85%, lactose: 50.8%, fat: 1.35%), Butter (proteins: 0.49%, water: 16%, fat: 82%), Margarine (proteins: 0.5%, water: 18%, fat: 80%) and soy flour (proteins: 38%, water: 13.7%, soluble carbohydrate: 15%, non-soluble carbohydrate: 15, fat: 18%) were declared by their producers.

Safelt 2, as a Blend of mesophilic and thermophilic bacteria, was obtained from Chr. Hansen A/S (Hørsholm, Denmark). This culture contains specially selected strains chosen for their phage resistance and ability to produce lactic acid quickly. This culture does not produce CO<sub>2</sub>. As coagulant, Fromase<sup>®</sup> 2200 TL granulate (microbial rennet from *Rhizomucor miehei* obtained from DSM Co., Netherland) was used.

### Preparation of soymilk, enzyme and starter

Full fat soy flour was used to make soymilk. For this purpose, soy flour and boiling water were poured into a blender (Model A707A, Kenwood MFG, Surrey, UK) in the ratio of one part soy flour to six parts boiling water and then mixed for 10 minutes. This mixture, was then poured into sealed glass containers and heated to 100°C and kept at this temperature for 15 minutes before

mixing with other components. After conditioning, soymilk was not filtered and wholly used in cheese formulation.

Rennet was added at a concentration of 30 mg per kg of recombined retentate. Rennet was diluted in sterile water. The dilution was standardized so that 5 mL of solution would deliver 30 mg of chymosin to 1 kg of recombined retentate.

0.1 mg of freeze-dried culture was dispersed in 50 mL sterile water and 5 mL was then added directly into 1 kg of recombined retentate.

#### **Cheese manufacture**

To achieve homogenous mixture, initially, MPC, WPC and SMP powders were mixed with warm water (60°C) in a laboratory blender for 5 minutes. Then, the previously prepared soymilk was added and mixed thoroughly. After cooling to 40°C, melted (40°C) margarine and butter were added and mixed completely. To prevent separation of fat globules during process, the mixture was homogenized using an Ultra-Turrax® T25 homogenizer (IKA® Werke, Janke & Kunkel GmbH & Co KG, Staufen, Germany) at a speed of 20000 rpm for 1.5 min (Day *et al.* 2007). After adding salt (1.4%), the resulting mixture was pasteurized and cooled to approximately 34°C. Rennet, starter culture and calcium chloride (0.02%) were then mixed with the mixture. Rennet includes the enzyme chymosin, which makes the casein in mixture coagulate (Bylund 1995). After addition of mentioned materials, the mixture was thoroughly stirred and poured into 100-ml sterile cups and covered with aluminum foils and then incubated at 34°C for 25 min to coagulate. After completion of coagulation, cheese samples were incubated at 27-28°C for 19 h to achieve pH 4.8 and finally stored at 5°C for 3 days. Textural analyses were performed on 3-day-old cheeses.

#### **Texture profile analysis (TPA)**

Texture profile analysis (being the most

commonly used method for assessment of cheese texture) has been found to be effective for evaluating cheese texture (International Dairy Federation 1991). TPA parameters were determined by using Universal Testing Machine, Model QTS-25 (CNS Farnell, Ltd., Hertfordshire, England) equipped with a 5-25 kg load cell. A flat plate probe with 36 mm of diameter was attached to moving crosshead. Six Cubic samples (20×20×20 mm) were prepared from each cheese block using a metal borer at 4–6°C. Samples were compressed to 70% of their original height at a speed of 60 mm min<sup>-1</sup>. For reducing friction at the sample – compression plate interface, plates were lubricated with mineral oil. The results of hardness (N), cohesiveness, adhesiveness (Ns), springiness (mm) and gumminess (N) were presented as an average of six analyses.

#### **Experimental design and statistical analysis**

A four-factor, three-level Central Composite Design (CCD) was used for obtaining optimum levels of MPC, WPC, Soymilk and margarine. The central composite design with a quadratic model was employed. Four independent variables namely MPC (X<sub>1</sub>), WPC (X<sub>2</sub>), Soymilk (X<sub>3</sub>) and margarine (X<sub>4</sub>) were chosen. Each independent variable had 3 levels which were -1, 0 and +1. A total of 30 different combinations (including six replicates of center point) were chosen in random order according to a CCD configuration for four factors. The coded values of independent variables are shown in Table 1. Analysis was performed by using Design-Expert, Version 8.0.7.1 program. A significance level of 0.05 was used in the statistical evaluations. Results of the optimization analysis were validated by producing a trial cheese with the optimized formula. The Kolmogorov–Smirnov's test was applied to verify if the experimental data had a normal distribution (p>0.05). Mean values of experimental and predicted data were then compared using parametric one sample t-test.

**Table 1. Uncoded and coded levels of the independent variables**

Independent variables	Index	Coded levels		
		+1	0	-1
MPC (%)	X <sub>1</sub>	10	9	8
WPC (%)	X <sub>2</sub>	3	1.5	0
Soymilk (%)	X <sub>3</sub>	15	10	5
Margarine (%)	X <sub>4</sub>	10	5	0

The study was carried out according to the central composite design and the experimental points used according to the design are shown in Table 2. A second-order polynomial

equation was used to express Y (dependent variable or response) as a function of independent variables.

$$Y = K + AX_1 + BX_2 + CX_3 + DX_4 + ABX_1X_2 + ACX_1X_3 + ADX_1X_4 + BCX_2X_3 + BDX_2X_4 + CDX_3X_4 + A^2X_1^2 + B^2X_2^2 + C^2X_3^2 + D^2X_4^2 \quad (1)$$

**Table 2. Central composite design used for preparation of UF-Feta cheese analogues**

Sample run	Coded level				Real levels (%)			
	1	2	3	4	MPC	WPC	Soymilk	Margarine
1	-1	-1	1	-1	8	0	15	0
2	-1	1	-1	-1	8	3	5	0
3	-1	-1	-1	1	8	0	5	10
4	-1	0	0	0	8	1.5	10	5
5	-1	-1	1	1	8	0	15	10
6	-1	1	1	-1	8	3	15	0
7	-1	-1	-1	-1	8	0	5	0
8	-1	1	-1	1	8	3	5	10
9	-1	1	1	1	8	3	15	10
10	0	1	0	0	9	3	10	5
11	0	0	0	0	9	1.5	10	5
12	0	0	0	0	9	1.5	10	5
13	0	0	0	1	9	1.5	10	10
14	0	0	-1	0	9	1.5	5	5
15	0	0	0	0	9	1.5	10	5
16	0	0	0	0	9	1.5	10	5
17	0	-1	0	0	9	0	10	5
18	0	0	0	-1	9	1.5	10	0
19	0	0	0	0	9	1.5	10	5
20	0	0	0	0	9	1.5	10	5
21	0	0	1	0	9	1.5	15	5
22	1	1	-1	1	10	3	5	10
23	1	-1	-1	1	10	0	5	10
24	1	1	1	-1	10	3	15	0
25	1	-1	1	-1	10	0	15	0
26	1	-1	-1	-1	10	0	5	0
27	1	-1	1	1	10	0	15	10
28	1	1	-1	-1	10	3	5	0
29	1	1	1	1	10	3	15	10
30	1	0	0	0	10	1.5	10	5

Samples contained MPC in the range of 8-10%, 0-3% WPC, 6% SMP, 0-15% soymilk, 0-10% margarine, 1.4% NaCl, 0.02% calcium chloride and water. The proportion of fat was held constant (16%) and the amount of butter was adjusted according to the proportion of fat in the formula.

## Results and Discussion

### Effects of MPC, WPC, Soymilk and margarine on textural properties of UF-Feta cheese analogues

UF-Feta cheese analogues were prepared by using a basic formula and manufacturing method which was developed in the preliminary studies. Four ingredients, MPC, WPC, Soymilk and margarine, were found to be the major components effective on physical properties of the cheeses. The upper and lower levels of mentioned ingredients that could give a cheese-like structure were determined in the preliminary studies.

The amount of fat was kept constant at a value of 16% and the reduction or addition in the amount of margarine was compensated by increasing or decreasing the level of butter in the formula, respectively.

### Hardness

Hardness is the force required to penetrate the sample with the molar teeth or force necessary to attain a given deformation (Gunasekaran and Mehmet 2003). The linear

effects of MPC, WPC and Soymilk levels on hardness were found significant ( $P < 0.05$ ). A significant interaction effect between MPC and WPC was also observed ( $P < 0.05$ ). According to Fig. 1, hardness increased with increasing levels of MPC and WPC significantly because of the increase in dry solids content. Hennelly *et al.* (2005) also observed that an increase in the hardness of imitation cheese was associated with an increase in dry solids. The increase in hardness was more obvious at higher MPC and WPC concentrations so that the highest hardness was related to 10% MPC and 3% WPC. Addition of soymilk to mixture followed by heat treatment at approximately 100°C for 15-20 min caused an increase in hardness. This is probably due to the more denaturation of the soy proteins at higher temperatures as compared to the lower temperatures. Hardness was also significantly influenced by margarine content ( $P < 0.05$ ; result not shown). Cunha *et al.* 2010 also found that the substitution of 25% and 50% of the dairy fat by vegetable fat resulted in increased hardness.

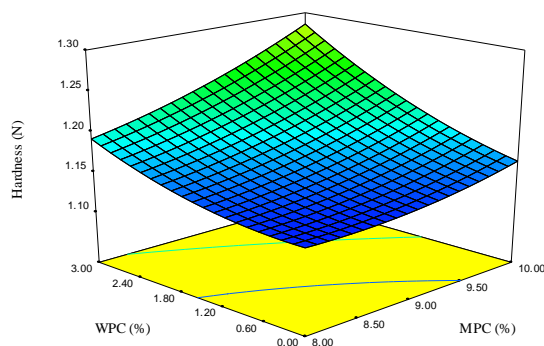


Fig.1. The response surface for hardness of cheese as function of MPC and WPC concentrations in TPA test.

### Cohesiveness

Cohesiveness is the amount of deformation undergone by a material before rupture when biting completely through the sample using molars or strength of the internal bonds making up the body of the product (Gunasekaran and Mehmet 2003). The amount of cohesiveness significantly increased with increasing MPC, WPC and soymilk concentrations ( $P < 0.05$ ) (Fig. 2). Furthermore, the effect of MPC on increasing cohesiveness

was higher as compared with WPC. By increasing MPC, WPC and soymilk, the amount of protein was increased and resulted in reinforced the gel structure and cohesiveness. In comparison, the cohesiveness values of the cheese made from UF milk were higher than those made from un-concentrated milk (Toufeili and Özer 2006). Scanning electromicrograms of traditional and UF Urfa cheese (a white-brined Turkish cheese) also showed that the cheese made from UF

concentrated milk had a more compact structure than the cheese manufactured from

un-concentrated milk (Özeret *et al.* 2003).

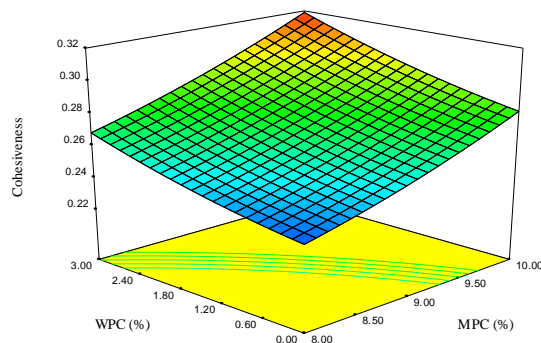


Fig.2. The response surface for cohesiveness of cheese as function of MPC and WPC concentrations in TPA test.

### Adhesiveness

Adhesiveness is described as the force required to remove the food from the palate during eating or work necessary to overcome the attractive forces between the surface of the food and surface of other materials with which the food comes in contact (Gunasekaran and Mehmet 2003). Adhesiveness values were significantly decreased by increasing MPC and WPC concentrations ( $P < 0.05$ ) because of increasing total solids. The highest value of

adhesiveness was found for 8% MPC and 0% WPC (Fig. 3). Adhesiveness decreased with decreasing moisture content (Bryant *et al.* 1995). Watkinson *et al.* (2002) reported that an increase in the moisture content of model Cheddar-like cheeses, from 40 to 48%, w/w, resulted in a large increases in adhesiveness. Addition of soymilk also significantly reduced adhesiveness ( $P < 0.05$ ) and this may be due to the increased protein and dry solids contents.

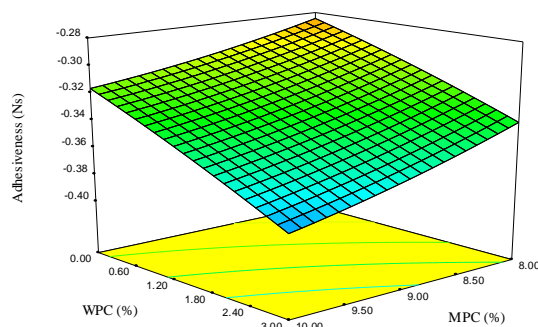


Fig.3. The response surface for adhesiveness of cheese as function of MPC and WPC concentrations in TPA test.

### Springiness

Springiness is degree or rate at which the sample returns to its original size/shape after partial compression between the tongue and palate or the distance recovered by the sample during the time between end of first bite and start of second bite (Gunasekaran and Mehmet 2003). WPC and Soymilk had significant linear effects on springiness ( $P < 0.05$ ). Significant interaction effects between MPC

and WPC and between soymilk and WPC were also observed ( $P < 0.05$ ). As seen from Fig. 4, springiness increased significantly with increasing soymilk concentration. This may be due to the lower moisture content of cheeses and larger amounts of proteins (Gunasekaran and Mehmet 2003; Zisu *et al.* 2005; Hassan 2008). Increasing the concentration of WPC reduced springiness significantly, while the addition of MPC had no significant effect on

it. By increasing casein concentration in the cheese matrix, the number of intra- and inter-strand linkages are increased and finally the matrix become more elastic(Guinee and Kilcawley2004). Increasing of WPC reduced casein concentration and caused loss of elasticity of cheeses.

**Gumminess**

The results showed that the linear effects of MPC, WPC and Soymilk levels on gumminess were significant (P <0.05). In addition, an interaction effect between MPC and WPC was found significant (P <0.05). Fig. 5. shows the effect of MPC and WPC on gumminess (when fixed soymilk at 10% and margarine at 5%).

According to this figure, the gumminess of the analogue cheese was significantly increased by increasing of MPC and WPC contents so that the highest gumminess was found at levels of 10% MPC and 3% WPC. This is due to the increase in protein concentration and the decrease of water content in cheese matrix. Romeih *et al.* (2002) also observed that with increasing protein to fat and water ratios in low-fat cheeses, the gumminess of cheese increased. The increase in soymilk concentration also increased the gumminess of analogue cheese which may have attributed to an increase in the content of protein (result not shown).

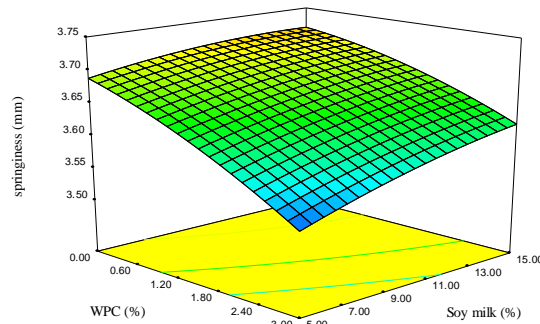


**Fig.4. The response surface for springiness of cheese as function of Soy milk and WPC concentrations in TPA test.**

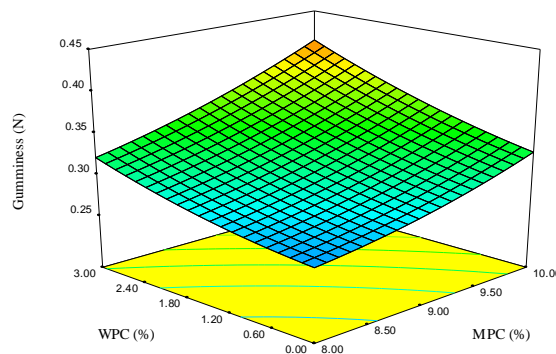


**Fig.5. The response surface for gumminess of cheese as function of MPC and WPC concentrations in TPA test.**

**Optimization**

The final objective of this study was to optimize the experimental variables in such a way that the sum of responses could be received the highest scores. The results showed that the optimum ingredient

combination for producing cheese with suitable hardness and cohesiveness and lowest adhesiveness was: 9.13% MPC, 3% WPC, 15% soymilk and 7.65% margarine. Hardness, cohesiveness, adhesiveness, springiness and gumminess of an analogue cheese based on the

optimized formula were estimated to be approximately 1.26 N, 0.3, -0.38 Ns, 3.62 mm and 0.38 N, respectively. A trial cheese was manufactured by using the optimized formula to validate these estimations. Hardness, cohesiveness, adhesiveness, springiness and gumminess of trial cheese were 1.09 N, 0.28, -

0.44 Ns, 3.42 mm and 0.30 N, respectively. According to the results obtained, no significant differences between adhesiveness and springiness of optimized and trial cheeses were observed, however, hardness, cohesiveness, and gumminess of cheeses were significantly different ( $P < 0.05$ ) (Fig. 6.).

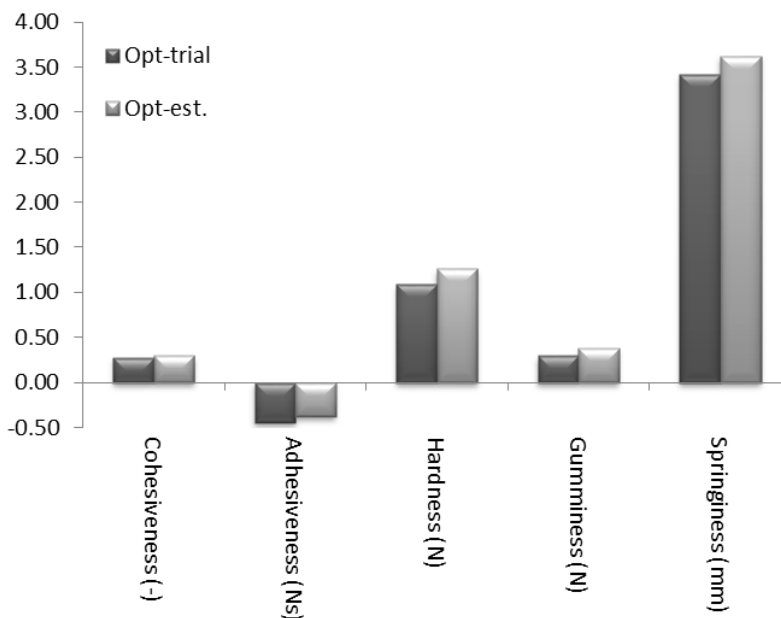


**Fig.6.** Comparison of textural properties estimated in the optimization and obtained in a trial cheese that was produced according to the optimized formula (Opt-est.: Estimated value in the optimization, Opt-trial: Trial cheese).

One approach to evaluate responses simultaneously is the study of the overlaid contour plot of responses. The contour plot for hardness, cohesiveness, adhesiveness and springiness based on corresponding models were plotted and overlaid into a single diagram (Fig. 7.). The best conditions were obtained at 9.13% MPC, 3% WPC, 15% soymilk and 7.65% margarine.

### Conclusions

The production of analogue cheese encountered to some technological problems and use of non-dairy components, such as soy flours or its isolates, may also have negative effects on functional or sensory properties of analogue cheeses, but, it is possible to minimize these problems by modifications of

formulations and process conditions and to produce products, which have unique characteristics and meet consumers' expectations. In this study, the optimum ingredient combination for producing cheese was: 9.13% MPC, 3% WPC, 15% soymilk and 7.65% margarine. This combination resulted in the suitable hardness and cohesiveness and the lowest adhesiveness. However, hardness, cohesiveness and gumminess of optimized and trial cheeses had significant differences, but no significant differences were observed between their adhesiveness and springiness. It should be noted that, in the previous study (Gholamhosseinpour *et al.* 2014), the sensory and chemical parameters of optimized and trial cheeses had no significant differences.

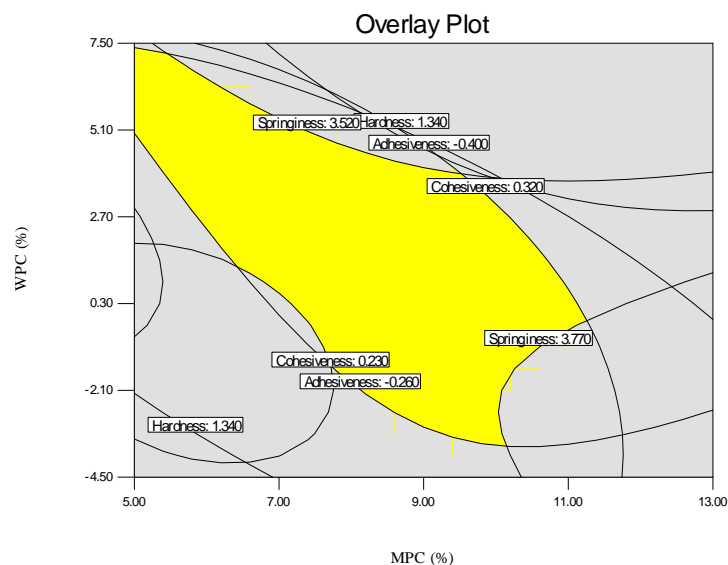


**Fig.7. Overlaid contour plot for hardness, cohesiveness, adhesiveness and springiness at different levels of MPC and WPC and constant values of soymilk and margarine.**

## References

- Abou El Nour A, Scheurer G J and Buchheim W (1998) Use of rennet casein and milk protein concentrate in the production of spread-type processed cheese analogue. *Milchwissenschaft* 53 686-690.
- Ahmed N S, Hassan F A M, Salama F M M and Enb A K M (1995) Utilization of plant proteins in the manufacture of cheese analogs. *Egyptian Journal of Food Science* 23 37-45.
- Bryant A, Ustunol Z and SteVe J (1995) Texture of cheddar cheese as influenced by fat reduction. *Journal of Food Science* 60 1216-1219.
- Bylund G (1995) *Dairy Processing Handbook*, pp 300. Lund, Sweden: Tetra Pak Processing Systems AB.
- Chavan R S and Jana A (2007) Cheese Substitutes: An Alternative to Natural Cheese- A Review. *International Journal of Food Science, Technology & Nutrition* 2 25-39.
- Cunha C R, Dias A I and Viotto W H (2010) Microstructure, texture, colour and sensory evaluation of a spreadable processed cheese analogue made with vegetable fat. *Food Research International* 43 723-729.
- Cunha C R, Grimaldi R, Alcântara M R and Viotto W H (2013) Effect of the type of fat on rheology, functional properties and sensory acceptance of spreadable cheese analogue. *International Journal of Dairy Technology* 66 54-62.
- Day L, Xu M, Hoobin P, Burgar I and Augustin M A (2007) Characterisation of fish oil emulsions stabilised by sodium caseinate. *Food Chemistry* 105 469-479.
- EI-Neshawy AA, Farahat S M and Wahbah H A (1988) Production of Processed Cheese Food Enriched with Vegetable and Whey Proteins. *Food Chemistry* 28 245-255.
- Fox P F (2011). Cheese: Overview. In *Encyclopedia of dairy sciences, Vol 3*, pp 534-543. Fuquay J W, Fox P F and McSweeney P L H, eds. San Diego, CA, USA: Academic Press.
- Fox P F, Guinee T P, Cogan T M and McSweeney P L H (2000) *Fundamentals of cheese science*, pp 1, 351 and 381. Gaithersburg, MD, USA: Aspen Publishers, Inc.
- Gholamhosseinpour A, Mazaheri Tehrani M, Razavi S M A and Rashidi H (2014) Evaluation and optimization of chemical and sensory properties of various formulations of recombined UF-Feta

- cheese analogues using response surface methodology. *Iranian Food Science and Technology Research Journal* 10 107-121.
- Guinee T P (2007) Cheese problems solved. In *Cheese-like products*, pp 384-385. Mc Sweeney P L H, ed. Florida: CRC Press.
- Guinee T P and Kilcawley K N (2004) Cheese as an ingredient. In *Cheese: Chemistry, Physics and Microbiology*, Vol. 2, pp 395-428. Fox P F, McSweeney P L H, Cogan T M, Guinee T P, eds. Amsterdam: Elsevier Academic Press.
- Guinee T P, Carić M and Kaláb M (2004) Pasteurized processed cheese and substitute/imitation cheese products. In *Cheese: Chemistry, Physics and Microbiology*, Vol. 2, pp 349-394. Fox P F, McSweeney P L H, Cogan T M, Guinee T P, eds. Amsterdam: Elsevier Academic Press.
- Gunasekaran S and Ak M M (2003) *Cheese Rheology and Texture*, pp 12, 281-284, 288-294. Boca Raton, FL: CRC Press.
- Harper W J (1991) Functional properties of whey protein concentrates and their relationship to ultrafiltration. *IDF Special Issue* 9201 77-108.
- Hassan A N (2008) ADSA Foundation Scholar Award: Possibilities and Challenges of Exopolysaccharide-Producing Lactic Cultures in Dairy Foods. *Journal of Dairy Science* 91 1282-1298.
- Hennelly P J, Dunne P G, O'Sullivan M and O'Riordan D (2005) Increasing the moisture content of imitation cheese: effects on texture, rheology and microstructure. *European Food Research and Technology* 220 415-420.
- IDF (1991) *Rheological and fracture properties of cheese*, Bulletin 268. Brussels, Belgium: International Dairy Federation.
- Iran Standard, ISIRI (2010) *Fresh cheese with vegetable oil (analog fresh cheese), Specification and test methods*, Iran Standard No. 12736. National Standards Authority of Iran, Tehran, Iran.
- Iran Standard, ISIRI (2015) *Milk and milk products -Fresh cheese, Specification and test methods*, Iran Standard No. 6629. National Standards Authority of Iran, Tehran, Iran.
- Isam A M A, Elfadil E B and Nobuhiro M (2010) pH stability and influence of salts on activity of a milk-clotting enzyme from *Solanum tuberosum* seeds and its enzymatic action on bovine caseins. *LWT - Food Science and Technology* 43 759-764.
- Lobato-Calleros C, Vernon-Carter E J, Guerrero-Legarreta I, Soriano-Santos J and Escalona-Beundia H (1997) Use of fat blends in cheese analogs: Influence on sensory and instrumental textural characteristics. *Journal of Texture Studies* 28 619-632.
- Metwalli N H, Shalabi S I, Zahran A S and Demerdash O E (1982) The use of soybean milk in soft-cheese making: I. Effect of soybean milk on rennet coagulation property of milk. *International Journal of Food Science & Technology* 17 71-77.
- Metzger L E and Mistry V V (1995) A new approach using homogenization of cream in the manufacture of reduced fat cheddar cheese. 2. Microstructure, fat globule distribution and free oil. *Journal of Dairy Science* 78 1883-1895.
- Miočinović J, Puđa P, Radulović Z, Pavlović V, Miloradović Z, Radovanović M and Paunović D (2011) Development of low fat UF cheese technology *Mljekarstvo* 61 33-44.
- Mounsey J S and O'Riordan E D (2001) Characteristics of imitation cheese containing native starches. *Journal of Food Science* 66 586-591.
- Özer B H, Robinson R K and Grandison A S (2003) Textural and microstructural properties of urfa cheese (a white-brined Turkish cheese). *International Journal of Dairy Technology* 56 171-176.
- Romeih E A, Michaelidou A, Biliaderis C G and Zerfiridis G K (2002) Low-fat white-brined cheese made from bovine milk and two commercial fat mimetics: Chemical, physical and sensory attributes. *International Dairy Journal* 12 525-540.
- Shakeel-Ur-Rehman, Farkye N Y and Drake M (2003) Reduced-fat Cheddar cheese from a mixture of cream and liquid milk protein concentrate. *International Journal of Dairy Technology* 56 94-

98.

Toufeili I and Özer B (2006) Brined Cheeses from the Middle East and Turkey. *In Brined Cheeses*, pp188-210. Tamime A Y, ed. Iowa, USA: Blackwell Publishing Ltd.

Watkinson P J, Crawford R A and Dodds C C (2002) Effect of moisture on instrumentally measured textured properties of model cheese. *Australian Journal of Dairy Technology* 57 153.

Zisu B and Shah N P (2005) Textural and functional changes in low-fat Mozzarella cheeses in relation to proteolysis and microstructure as influenced by the use of fat replacers, pre-acidification and EPS starter. *International Dairy Journal* 15 957-972.

## بهینه‌سازی ویژگی‌های بافتی پنیر فتای فراپالایش آنالوگ تولید شده از ترکیبات لبنی و غیرلبنی

علی اکبر غلامحسین پور<sup>1</sup> - مصطفی مظاهری تهرانی<sup>2\*</sup> - سید محمدعلی رضوی<sup>2</sup>

تاریخ دریافت: 1395/07/14

تاریخ پذیرش: 1396/04/13

### چکیده

در این پژوهش از مخلوط کنسانتره پروتئینی شیر، کنسانتره پروتئینی آب‌پنیر، شیر خشک پس‌چرخ، شیرسویا، مارگارین، کره و آب برای تولید پنیر فتای فراپالایش بازساخته استفاده شد. متغیرها عبارت بودند از کنسانتره پروتئینی شیر در سه سطح 8، 9 و 10 درصد، کنسانتره پروتئینی آب‌پنیر در سه سطح صفر، 1/5 و 3 درصد، شیرسویا در سه سطح 5، 10 و 15 درصد و مارگارین در سه سطح صفر، 5 و 10 درصد. نمونه‌ها از نظر ویژگی‌های بافتی پس از روز سوم تولید، آنالیز شدند. نتایج در قالب طرح مرکب مرکزی بررسی و به روش سطح پاسخ مدل‌سازی و تجزیه و تحلیل شدند. ضریب تبیین مدل‌های رگرسیون برازش شده برای صفات مختلف بین 89/59 تا 97/80 متغیر بوده و فاکتور عدم برازش تمامی صفات در سطح اطمینان 95 درصد معنی‌دار نبود، از این رو صحت مدل برای برازش اطلاعات تایید گردید. با توجه به نتایج، شرایط بهینه به دست آمده برای تولید پنیری که سختی و پیوستگی مناسبی داشته و از کمترین مقدار چسبندگی برخوردار باشد عبارت بود از: 9/13 درصد کنسانتره پروتئینی شیر، 3 درصد کنسانتره پروتئینی آب‌پنیر، 15 درصد شیرسویا و 7/65 درصد مارگارین.

**واژه‌های کلیدی:** کنسانتره پروتئینی شیر، کنسانتره پروتئینی آب‌پنیر، شیرسویا، مارگارین، پنیر آنالوگ، پروفیل بافت.

1- استادیار، گروه علوم و صنایع غذایی، دانشکده کشاورزی، دانشگاه چهرم، چهرم، ایران.  
2- استاد، گروه علوم و مهندسی صنایع غذایی، دانشکده کشاورزی، دانشگاه فردوسی مشهد  
(\* - نویسنده مسئول: Email: mmtehrani@um.ac.ir)

## Effect of pulsation period and microwave power on paddy drying

H. Jafari<sup>1</sup>, D. Kalantari<sup>2\*</sup>, M. Azadbakht<sup>3</sup>

Received: 2017.05.04

Accepted: 2017.09.25

### Abstract

In this study, the influence of different microwave powers (90, 270, and 450 W) and pulsation periods, i.e., On/Off times (30/60 and 30/120 ss<sup>-1</sup>) on drying rate and seed breakage of "Nemat" and "Hashemi" paddy varieties" was investigated. According to the results, the Midilli et al.'s model showed the best prediction accuracy for drying rate of the "Nemat" variety in the pulsation period of 30/60. Furthermore, the two-term model was found as the best model for "Hashemi" variety in the pulsation periods of 30/60 and 30/120 and for "Nemat" variety in the pulsation period of 30/120. The 270 W microwave power and 30/120 pulsation period can be recommended as a final conclusion of this study for drying "Hashemi" paddy variety. The breakage percentage at this condition was 19.1%. Breakage percent of the Nemat variety was more than 40% at all of the conducted measurements, indicating that this variety is not suitable for microwave drying. The final concluding message of this study is that a pre-test should be conducted before applying the microwave for paddy drying.

**Keywords:** Microwave drying, breakage percent, Moisture ratio, thin layer, drying models.

### Introduction

Rice (*Oryza sativa L.*) is a valuable source of energy and nutrients, which is consumed by almost half of the world population. It has been producing in tropical and sub-tropical countries such as India, Thailand, the Philippines and several other countries. The latest data shows that world paddy production in 2016 was 745.5 million tons (495.2 million tons milled rice), FAO (2016).

In Iran, rice is an ancient crop which is widely grown on areas of about 615000 ha with an annual production of about 3 million tons. Main areas of rice cultivation in Iran are located in the Northern provinces, Guilan and Mazandaran, producing 75% of the total cultivated rice crop in this country (Alizade et al. 2006).

Agricultural crops commonly contain a

high level of moisture and microorganisms at the harvest time. After harvesting, the moisture content of rice paddy is in the range of 25% - 28% (wet basis) and even higher during the rainy season. For this reason, immediate drying is a requirement in postharvest processing to avoid quality losses of these perishable agricultural products (Balbay *et al.* 2012, Al-Harashsheh *et al.* 2009, Soysal 2004). Drying is one of the most widespread methods for post-harvest protection of agricultural products such as paddies for allowing quick preservation (Dadali *et al.* 2008, Doymaz and Kocaygit 2011, Discala *et al.* 2013). Rice paddy is typically dried to reduce the moisture content to 11% or lower for a safe storage before a milling process. However, if the moisture content in paddy is too low, the grain will be brittle in the milling process. This can lead to a higher fraction of broken kernels. Keeping the rice paddy at optimized moisture content can prolong storage time and prevent mould growth (Cheenkachorn 2007).

Several drying approaches are used in the drying of foodstuff. The use of microwave technique in the drying of products has recently become common due to the quick and effective heat distribution in the product (Li *et al.* 2009, Alibas 2010, Dong *et al.* 2011). In this regard, many mathematical models have

1 and 2. MSc student and Assistant Professor, Department of bio-system Engineering, Sari Agricultural Sciences and Natural Resources University (SANRU), Sari, Iran.

3. Assistant prof of Biosystems engineering, Department of bio-system Engineering, Gorgan University of Agricultural Sciences and Natural Resources, Gorgan, Iran.

\*Corresponding author (dkalantari2000@yahoo.com)

DOI: 10.22067/ifstrj.v1396i13.64195

been formulated in order to describe the thin layer drying process (Kardum *et al.* 2011). Thin layer models can be categorized as theoretical, semi-empirical and empirical models (McMinn 2006, Alibas 2014).

The aims of this study were: I) to investigate the kinetics of thin layer microwave drying of two more conventional paddy varieties in Iran, i.e., Nemat and Hashemi, II) derivation of the semi-empirical models for the moisture ratio and seed breakage percentage as a function of drying power and time, III) evaluation of the conventional thin layer drying models in application of the microwave drying conditions, which have not been examined before.

### Materials and Methods

The paddy grain used in this study was obtained from Rice Research Institute located in the Sari Agricultural Sciences and Natural Resources University, Iran. The evaluated paddy varieties (Nemat and Hashemi) are common varieties of paddy in the north of Iran (Zareiforush *et al.* 2009). Initial moisture content (MC) of the paddy was determined by drying the samples in a laboratory oven at 103°C for 48 hr (Sacilik *et al.* 2003). Initial moisture content of "Nemat" and "Hashemi" were 20.48% and 24.5% w.b, respectively. Microwave drying experiments were performed in a domestic digital microwave oven (MW-F304ADY-S.Media, China). The microwave oven had 5 different microwave generation power stages between 90 and 900 W. The inside area of the device was 520mm×467mm×335mm with a rotation plate of a 300mm in diameter at the base of the oven. Microwave drying tests were carried out at three different microwave generation powers of 90, 270, and 450 W. The mass of each paddy sample was 30 g. Moisture loss was determined by weighting the samples using a digital balance with 0.01 precision. For a pulsed mode, the magnetron was alternately turned on and off corresponding to the specified pulsation periods. Paddy was hulled with a laboratory husker. Rice kernels with

lengths smaller than 75% of that of whole kernels were chosen as broken rice (Kalantari and Eshtevad, 2013). The whole experimental period including several 30/60 or 30/120 ss<sup>-1</sup> On/Off pulsation periods was 450 s in all of the conducted experiments in this study.

### Mathematical formulation

Moisture ratio of the samples after drying was calculated using the following equation (Manikantun *et al.* 2012):

$$MR = \frac{(M - M_e)}{(M_o - M_e)} \quad (1)$$

where MR is dimensionless moisture ratio, M is moisture content at time t, M<sub>o</sub> is initial moisture content, and M<sub>e</sub> is equilibrium moisture content on the wet basis.

In this study, the regression coefficient (R<sup>2</sup>) was considered as the main criterion for choosing the most appropriate model for describing the microwave drying curves. This correlation factor can be used to examine the linear relationship between the measured and the estimated values, which can be calculated using the following expression (Alibas 2014):

$$R^2 = \frac{\sum_{i=1}^N (M_{R_{exp,i}} - M_{R_{pre,i}})^2 - (M_{R_{pre,i}} - M_{R_{exp,i}})^2}{\sum_{i=1}^N (M_{R_{exp,i}} - M_{R_{pre,i}})^2} \quad (2)$$

where R<sup>2</sup> is the coefficient of correlation, M<sub>R<sub>exp,i</sub></sub> is experimental moisture ratio obtained by the measurements, M<sub>R<sub>pre,i</sub></sub> is estimated moisture ratio, and N is total number of observations.

The standard error of estimate (SEE) indicates information on the long-term performance of the actual deviation between predicted and measured values term by term. The ideal value of SSE is "zero". The SEE is given as Equation 3 (Alibas 2014):

$$SEE = \sqrt{\frac{\sum_{i=1}^N (M_{R_{exp,i}} - M_{R_{pre,i}})^2}{N - n_i}} \quad (3)$$

Where n<sub>i</sub> is the number of constants.

Root mean square error (RMSE) provides information on the short-term performance which can be computed from the following equation (Alibas 2014):

$$RMSE = \sqrt{\frac{\left[ \sum_{i=1}^N (M_{R_{exp,i}}) - \sum_{i=1}^N (M_{R_{pre,i}}) \right]^2}{N}} \quad (4)$$

To choose an appropriate model for describing the drying kinetics of the examined paddies, ten empirical and semi-empirical thin-layer drying models were evaluated (Table 1). However, some of the proposed models presented in this table have been constructed based on the previous models with some minor modifications. In this research, MATLAB 2013 has been used for model analyzing.

## Result and Discussion

### Effect of different powers and drying time on moisture ratio

The simultaneous influence of different powers and drying time on the moisture ratio (MR) in two varieties of "Nemat" and "Hashemi" and two pulsation periods of 30/60 and 30/120 are shown in Fig.1 (a) to (d). According to the results presented in Fig.1 (a) to (d), the moisture ratio was decreased simultaneously with the power increment and drying time. Initially, moisture ratio was decreased with a high rate due to the high moisture content of the paddy. Meanwhile, moisture ratio in the 30/60 pulsation period was decreased with a larger slope in comparison with that of 30/120 pulsation period. A prior investigation conducted by Cheepsathit and Pattala (2005) indicated that the product temperature at the pulsation period of 30/60 was higher than that of 30/120. Higher microwave powers led to higher temperature gradients inside the grain allowing water to faster evaporate during the power-on time, also increasing diffusion of water during the power-off time. In contrast, longer off times resulted in temperature decrease due to evaporative cooling, convection and radiation heat losses from paddy external surfaces. These latter results obtained in this study were similar to the previous observations on paddy

drying (Yongsawasdigul and Gunasekaran 1996, Cheenkachorn 2007).

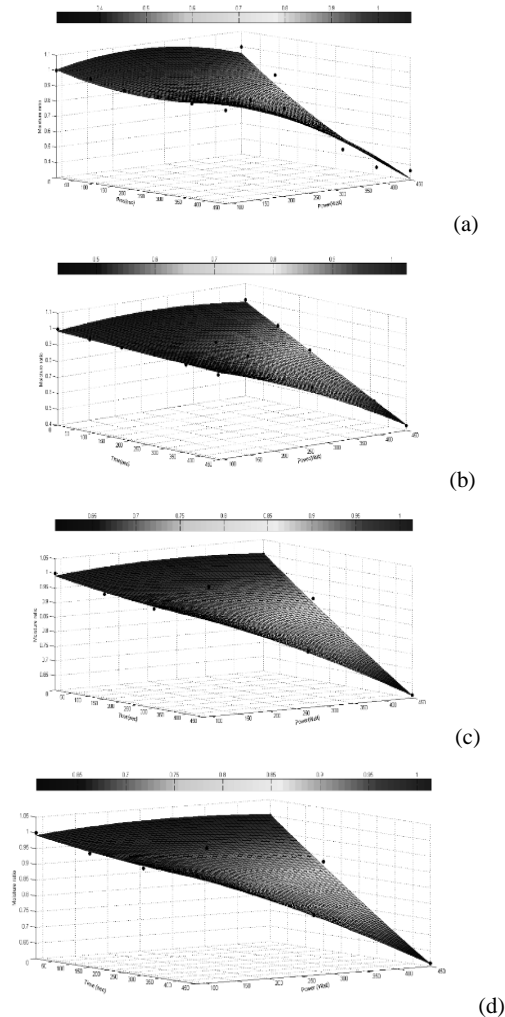


**Fig.1. Effect of different powers and drying time on moisture ratio in "Nemat" and "Hashemi" variety at 30/60(ss<sup>-1</sup>) and 30/120(ss<sup>-1</sup>) pulsation periods, (a); (b); (c); (d), respectively.**

### Evaluating the existing drying models

Evaluation of the 10 different well-known thin-layer drying models (summarized in Table 1) is presented in Table 2 and 3 for "Nemat" and "Hashemi" varieties respectively at three different microwave powers. In these tables, the values of the standard error of estimate (SEE), coefficient of correlation (R<sup>2</sup>), and root mean square error (RMSE) are presented for two examined thin-layer drying models (i.e., Midili et al.'s model and two-term

model). The best drying model was selected in this study based on the R<sup>2</sup>, RMSE and SEE values for the microwave drying powers of 90,

270, and 450 W and for the 30/60 and 30/120 pulsation periods (Doungporn *et al.*, 2012).

**Table 1. The most conventional mathematical thin-layer drying models.**

Model No.	Model name	Model equation	Eq No.
1	Lewis (Doymaz and Ismail 2011)	$MR = \exp(-kt)$	(5)
2	Page (Jangam <i>et al.</i> 2008)	$MR = \exp(-kt^n)$	(6)
3	Henderson and Pabis (Pehlivan and Toğrul 2004)	$MR = a \exp(-kt)$	(7)
4	Logarithmic (Kingsly <i>et al.</i> 2007)	$MR = \exp(-kt) + c$	(8)
5	Two-term (Demirhan and Ozbek 2011)	$MR = a \exp(-k_0 t) + b \exp(-k_1 t)$	(9)
6	Wang and Singh (Demirhan and Ozbek 2011)	$MR = 1 + at + bt^2$	(10)
7	Midilli <i>et al.</i> (Midilli <i>et al.</i> 2002)	$MR = a \exp(-kt^n) + bt$	(11)
8	Weibull distribution (Babalis 2006)	$MR = a - b \exp[-(kt^n)]$	(12)
9	Aghlasho <i>et al.</i> (Aghlasho <i>et al.</i> 2009)	$MR = \frac{\exp(-k_1 t)}{1 + k_2 t}$	(13)
10	Logistic (Alibas 2014)	$MR = \frac{a_0}{(1 + a \exp(kt))}$	(14)

MR is moisture ratio, *k*, *k*<sub>0</sub>, *k*<sub>1</sub>, *k*<sub>2</sub>, *a*, *a*<sub>0</sub>, *b*, *c* are drying constant and *t* is drying time.

Regarding the results summarized in Table 2 for (R<sup>2</sup>), (RMSE) and (SEE) values, the model proposed by Midilli *et al* had a better prediction for the Nemat variety at 30/60 pulsation period, whereas the two-term model indicated a better estimation at 30/120 pulsation period. The average of the standard error of estimate (SEE), the coefficient of correlation (R<sup>2</sup>), and root mean square error

(RMSE) for the model of Midilli *et al* at 30/60 pulsation period were equal to 0.00053854, 0.9840, and 0.013130667, respectively. For two-term model at 30/120 pulsation period, the average of the standard error of estimate (SEE), the coefficient of correlation (R<sup>2</sup>), and root mean square error (RMSE) were equal to 0.000940283, 0.9783, and 0.03847, respectively.

Table 2. Statistical results obtained from thin-layer drying model for different microwave power and pulsation period

	450 Watt		
	R <sup>2</sup>	RMSE	SEE
	0.9672	0.04918	0.01209
	0.9028	0.0707	0.01499
	0.9688	0.05475	0.01199
	0.9701	0.07414	0.01099
	0.968	0.05416	0.01173
	0.9123	0.08581	0.01473
	0.968	0.05354	0.01146
	0.9119	0.08605	0.01481
	0.968	0.06253	0.01173
	0.8702	0.09004	0.008108
	<b>0.9703</b>	<b>0.004823</b>	<b>4.652e-05</b>
	0.8797	0.005786	0.01079
	0.9671	0.04479	0.008025
	0.9791	0.06327	0.008005
	0.9681	0.07306	0.01068
	<b>0.999</b>	<b>0.07974</b>	<b>0.002632</b>
	0.9716	0.01303	0.0003397
	0.7213	0.02347	0.0348
	0.9679	0.05452	0.01189
	0.002593	0.05981	0.007155
			0.9466

Table 3. Statistical results obtained from different thin-layer drying model for different microwave power and pulsation

270 Watt			450 Watt			90 Watt					
R <sup>2</sup>	SEE	RMSE	R <sup>2</sup>	SEE	RMSE	Pulsation period (ss <sup>-1</sup> )	SEE	RMSE	R <sup>2</sup>	SEE	RMSE
0.9625	0.002926	0.02419	0.9872			30/60	0.0005258	0.01025	0.917	0.001606	0.01792
0.9761	0.0008906	0.01723	0.99			30/120	0.0001734	0.007602	0.9471	0.00413	0.0371
0.9701	0.0002675	0.008178	0.9988			30/60	0.0002465	0.00785	0.9611	0.00153	0.01956
0.9883	0.000249	0.01116	0.9972			30/120	9.314e-05	0.006824	0.9716	0.00127	0.0252
0.965	0.002255	0.02374	0.9901			30/60	0.0004428	0.01052	0.9301	0.00157	0.01981
0.9805	0.0007251	0.01904	0.9918			30/120	0.0001438	0.008479	0.9561	0.003726	0.04316
0.9649	0.002404	0.02451	0.9895			30/60	0.0004431	0.01052	0.93	0.00157	0.01981
0.9804	0.0007367	0.01919	0.9917			30/120	0.0001438	0.00848	0.9561	0.003744	0.04326
0.9566	0.0001252	0.006459	0.9995			30/60	0.0002834	0.00972	0.9552	0.00157	0.01981
0.5174	0.000353	0.01879	0.996			30/120	0.0001438	0.01199	0.9561	0.005515	0.07426
0.9683	0.0001214	0.00636	0.9995			<b>30/60</b>	<b>0.0001161</b>	<b>0.007619</b>	<b>0.9817</b>	<b>0.001453</b>	<b>0.02695</b>
0.9899	0.0001263	0.00674	0.9999			30/120	0.0001231	0.01109	0.9624	0.005109	0.03784
0.9689	0.0001335	0.005778	0.9994			30/60	0.0001455	0.00603	0.977	0.00161	0.02006
0.9843	0.0004263	0.0146	0.9952			30/120	0.0001316	0.008111	0.9598	0.0008895	0.02109
<b>0.9706</b>	<b>0.0001331</b>	<b>0.008157</b>	<b>0.9994</b>			30/60	0.0001387	0.008327	0.9781	0.001565	0.02797
<b>0.9935</b>	<b>0.0001046</b>	<b>0.008153</b>	<b>0.9988</b>			<b>30/120</b>	<b>0.0001454</b>	<b>0.01206</b>	<b>0.9556</b>	<b>4.345e-05</b>	<b>0.02234</b>
0.971	0.0002291	0.0107	0.999			30/60	0.0005748	0.01695	0.9092	0.001393	0.02639
0.9999	0.002435	0.0124	0.9726			30/120	0.0004971	0.01789	0.8482	0.01184	0.02879
0.9689	0.0001221	0.005524	0.9995			30/60	0.000175	0.006614	0.9724	0.001573	0.01983
0.984	0.0004099	0.01432	0.9954			30/120	0.0001169	0.007646	0.9643	0.002593	0.0294

90 Watt						
Model	Pulsation period(ss <sup>-1</sup> )	SEE	RMSE	R <sup>2</sup>	SEE	RMSE
Lewis	30/60	0.0001775	0.005958	0.9395	0.00175	0.01871
	30/120	0.0005103	0.01304	0.7874	0.0006481	0.0147
Page	30/60	0.0001774	0.006659	0.9395	0.001398	0.0187
	30/120	4.54e-05	0.004764	0.9811	0.0003167	0.01258
Henderson and Pabis	30/60	0.0001722	0.006561	0.9413	0.001637	0.02023
	30/120	0.0003834	0.01385	0.8403	0.0005284	0.01625
Logarithmic	30/60	0.0001722	0.00656	0.9413	0.001639	0.02024
	30/120	0.0003835	0.01385	0.8402	0.0005299	0.01628
Logistic	30/60	0.0001953	0.008068	0.9334	0.002026	0.02599
	30/120	0.0002667	0.01633	0.8889	0.01307	0.1143
Midilli et al	30/60	0.0001786	0.007716	0.9391	0.001484	0.02224
	30/120	0.0001786	0.007751	0.9999	0.0002746	0.02238
Wang and Singh	30/60	0.0001709	0.006537	0.9417	0.001454	0.01907
	30/120	0.00011	0.006547	0.9999	0.0004263	0.0146
<b>Two Term</b>	<b>30/60</b>	<b>0.0001536</b>	<b>0.008762</b>	<b>0.9477</b>	<b>0.001373</b>	<b>0.02621</b>
	<b>30/120</b>	<b>0.0001547</b>	<b>0.008774</b>	<b>0.9999</b>	<b>0.0001764</b>	<b>0.0261</b>
Weibull distribution	30/60	0.0001706	0.009236	0.9418	0.001354	0.02602
	30/120	0.0003553	0.009365	0.852	1.27E-08	0.02453
Aghlashedo et al	30/60	0.0001698	0.006514	0.9421	0.001453	0.01906
	30/120	0.0002637	0.01148	0.8901	0.0004337	0.01473

In the meantime by considering the information given in Table 3, the average of standard error of estimate (SEE), coefficient of correlation ( $R^2$ ), and root mean square error (RMSE) for the “Two-term model” at 30/60 pulsation period were equal to 0.000553233, 0.9726, and 0.014376333, respectively. For two-term model at 30/120 pulsation period, the average of the standard error of estimate (SEE), the coefficient of correlation ( $R^2$ ), and root mean square error (RMSE) were equal to 0.000145233, 0.9974, and 0.014342333, respectively.

Drying constant and coefficient values for the Midilli et al.'s and “Two-term model” have been computed using the Matlab software. The

obtained data for the parameters existing in their models including  $k$ ,  $k_0$ ,  $k_1$ ,  $n$ ,  $a$ , and  $b$  are given in Table 4 for the Nemat and Hashemi varieties.

Variation of the moisture ratio (MR) as a function of time ( $t$ ) was given in Fig.2 (a) to (d) for two examined paddy grains. Prediction of the Midilli et al.'s model for “Nemat” variety at 30/60(ss<sup>-1</sup>) pulsation periods is presented in Fig 2(a). The results presented in this figure indicate a good prediction of this model at the lower power-off time, whereas the “Two-term model” proposed by Demirhan and Ozbek (2011) had a better prediction for the longer off-times, i.e., 120 s off-time. It is interesting that the “Two-term model” showed the best

prediction at 120 s off-time for all of the microwave powers for both "Nemat" and "Hashemi" varieties. The latter results can be observed in Fig.2 (b) to (d). The average coefficient of correlation ( $R^2$ ) for the "Two-term model" was the highest amount within the 10 examined models, (Table 2). For "Two-term model", the value of the coefficient of correlation ( $R^2$ ) was very close to "1", meaning that the estimated data corresponded well with the experimental data.

Considering the results presented in Fig.2(a) to (d), moisture ratio decreased with increasing the power and drying time. This result has a good agreement with the previous observations on drying of paddy, (Yongsawasdigul and Gunasekaran 1996, Cheenkachorn 2007, Cheepsathit and Pattala 2005, Zarein *et al.*, 2013 and Chungcharoen *et*

*al.*, 2015).

Based on the results obtained in this study, moisture ratio in the 30/60 pulsation period was decreased with a higher rate in comparison with the 30/120 pulsation period only at higher power rates, i.e., 450 W. At lower powers rate (90 and 270 W), influence of the 30/60 and 30/120 pulsation periods was not significant, (Table 5). This result is also presented in Fig 3(a) to (d), indicating that moisture transfer inside the paddy occurs faster at the higher microwave powers and lower microwave power off-times. This phenomenon can be explained by the more continuously heat generation within the paddy at higher microwave powers, yielding a larger vapor pressure difference between the center and surface of the grain.

**Table 4. Statistical results and coefficients obtained from thin-layer drying models for the different microwave power and pulsation period for "Nemat" and "Hashemi" varieties.**

Model	Pulsation period (s/s)	Power (Watt)	SEE	RMSE	$R^2$	a	b	K	n	$K_0$	$K_1$	
Nemat variety	Midilli et al	30/60	0.0001161	0.007619	0.9817	1.001	0.0007988	0.0007667	1.089	-	-	
		30/120	-	-	-	-	-	-	-	-	-	
		30/60	0.001453	0.02695	0.9703	1	0.0004766	0.003973	0.4201	-	-	
	Two-Term	30/120	450	4.652e-05	0.004823	0.9999	0.9998	0.000719	0.0001509	1.639	-	-
		30/60	90	-	-	-	-	-	-	-	-	-
		30/120	90	0.0001454	0.0001454	0.9556	0.0161	0.9839	-	-	0.1186	0.0001408
		30/60	-	-	-	-	-	-	-	-	-	-
		30/120	270	4.345e-05	0.02234	0.999	1.081e-16	0.9975	-	-	0.07664	0.0004286
		30/60	-	-	-	-	-	-	-	-	-	-
		30/120	450	0.002632	0.07974	0.9803	5.729e-17	0.9817	-	-	0.07922	0.0008697
Hashemi variety	Two-Term	30/60	0.0001536	0.008762	0.9477	-1.484	2.48	-	-	0.0006935	0.0004564	
		30/120	0.0001547	0.008774	0.9999	0.7071	0.2929	-	-	0.0009077	0.001051	
		30/60	0.001373	0.02621	0.9706	-	1.057	-	-	0.007436	0.0007637	
		30/120	0.0001764	0.0261	0.9935	1.038	-0.03759	-	-	0.0006226	0.1161	
		30/60	0.0001331	0.008157	0.9994	-3.372	4.373	-	-	1.447e-07	0.0003113	
		30/120	0.0001046	0.008153	0.9988	1.055	-0.05509	-	-	0.001236	0.112	

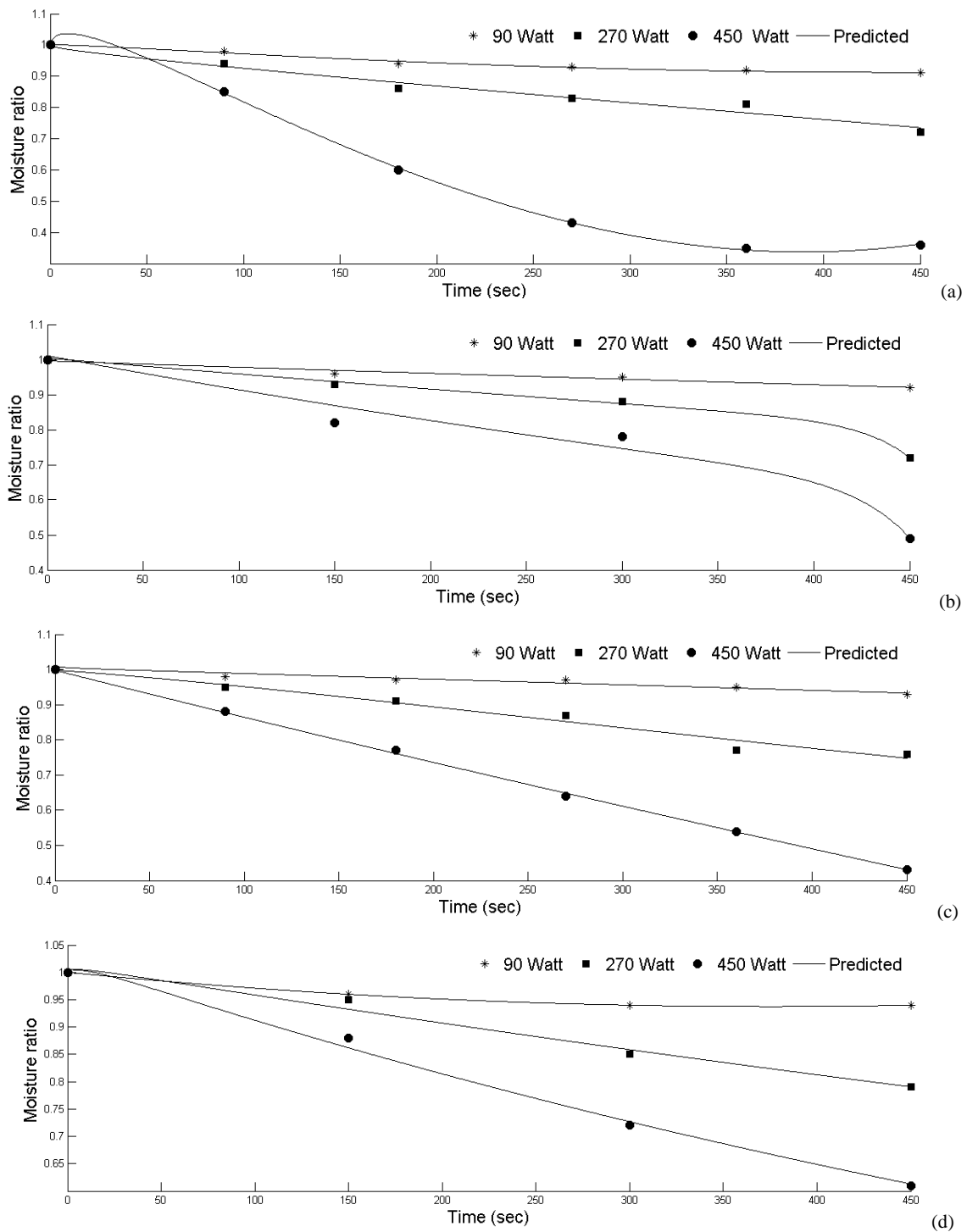


**Fig.2. Moisture ratio versus drying time, comparing prediction curves (—) with the experimental data (single points): a) Model of Midilli et al for the "Nemat" variety and 30/60(ss<sup>-1</sup>) pulsation periods; b) Two-term model for the "Nemat" variety and 30/120(ss<sup>-1</sup>) pulsation periods; c) Two-term model for the "Hashemi" variety and 30/120(ss<sup>-1</sup>) pulsation periods; and d) Two-term model for the "Hashemi" variety and 30/60(ss<sup>-1</sup>) pulsation periods.**

**Table 5. Moisture ratio at the end of drying time for all powers and variety**

Variety	Pulsation period (s s <sup>-1</sup> )	Power (Watt)		
		90	270	450
Nemat	30/60	0.91	0.72	0.36
	30/120	0.92	0.72	0.49
Hashemi	30/60	0.93	0.76	0.73
	30/120	0.94	0.79	0.61

### Effect of different powers and drying time on seed breakage percentage

Simultaneous influence of different powers and drying time on the seed breakage in two "Nemat" and "Hashemi" varieties and two pulsation periods of 30/60 and 30/120 are shown in Fig.3 (a) to (d).

According to Fig.3 (a) to (d), the seed breakage was increased simultaneously with increasing the microwave power and drying time. The experimental data showed that both microwave power and pulsation period affect the broken fractions. For the pulsation period of 30/60, the higher broken fraction was observed at higher microwave powers, e.g., 450 W. These results might due to the higher energy absorption of the paddy grains which led to a rapid increase in the grain temperature. However, a rapid increase of grain temperature resulted in the higher rate of water removal. Excessively high moisture content removal most likely causes a high fraction of broken kernels. The results were similar to those of previous studies conducted by Soponronarit et al. (1996), Taweerattanpanich et al. (1999) and Cheenkachorn (2007). The obtained empirical expressions for the seed breakage percentage (SB %) as a function of microwave power and drying time together with the moisture ratio (MR) are given in Table 6. These expressions have been derived using MATLAB software

### Conclusion

In this investigation, the influence of different microwave powers and pulsation periods on the moisture ratio and seed breakage of two paddy varieties was investigated. According to the obtained results in this study, the following conclusions can be summarized.

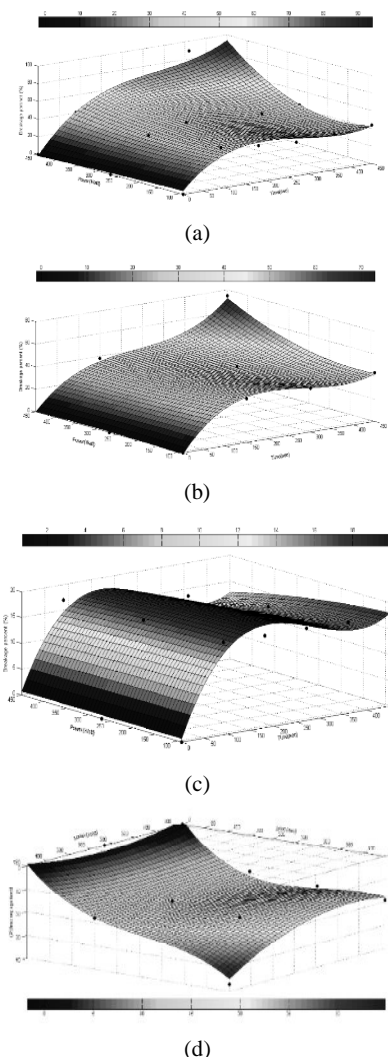


**Fig.3. Effect of different powers and drying time on seed breakage percent in "Nemat" variety and "Hashemi" variety at 30/60(ss<sup>-1</sup>) and 30/120(ss<sup>-1</sup>) pulsation periods, (a); (b); (c); (d), respectively.**

**Table 6. Fitted equation for moisture ratio and seed breakage according to power and drying time in different variety and pulsation period**

R <sup>2</sup>	SEE	RMSE
0.9621	0.03114	0.05094
0.9572	0.01065	0.04214
0.9923	0.00371	0.01758
0.9931	0.00116	0.01395
0.9655	0.03688	0.06402
0.9872	0.00699	0.0483
0.9449	0.00391	0.02086
0.9453	0.00707	0.04857

- The minimum moisture ratio and the maximum seed breakage percentage were observed at the microwave power of 450 W and pulsation period of 30/60. This can be explained by the higher heat generation inside the grain and consequently higher evaporation rate at the grain surfaces, yielding larger pressures and thermal gradients inside the grain.
- The maximum moisture ratio and the minimum seed breakage percentage were obtained at the microwave power of 90 W and pulsation period of 30/120.
- At all of the examined microwave powers (90, 270 and 450 W), the "Midilli et al.'s model" and "Two-term model" have been found to be the best model for the "Nemat" variety in the 30/60 and 30/120 pulsation periods, respectively.
- For all of the examined microwave powers, the "Two-term model" has been found to be the best model for the "Hashemi" variety in the 30/60 and 30/120 pulsation periods. This model has been selected using the statistical information including R<sup>2</sup>, SEE, and RMSE and simultaneously comparing with the experimental data.
- Moisture ratio in the 30/60 pulsation period was decreased with a higher rate in comparison with 30/120 pulsation period at higher microwave power, i.e., 450 W for both examined varieties. This result is in agreement with the prior investigation carried out by Cheepsathit and Pattala (2005).
- The Nemat variety is not recommended for a microwave drying based on the results obtained in this study for all of the examined microwave powers and test conditions. The minimum breakage percentage was obtained about 40% at 90 W and 270 W microwave powers and 30/120 pulsation period.
- For the Hashemi variety, the minimum breakage percentage was obtained equal to 17.6% at 90 W and 30/120 pulsation period. The breakage percentage at 270 W and 30/60 and 30/120 pulsation periods were obtained equal to 20% and 19.1%, respectively. Therefore overall and simultaneously considering the breakage percentage and the drying rate (Figs.3 (a) to (d)), the 270 W microwave power and 30/120 pulsation period can be recommended as a final concluding results of this study. The 270 W microwave power with 30/60 pulsation period is not recommended due to the larger energy consumption and no significant drying rate increment and breakage percentage decrement in comparison with 270 W and 30/120 pulsation period.

## Reference

Aghbashlo, M., Kianmehr, M.H., Khani, S. & Ghasemi, M. 2009. Mathematical modeling of carrot thin-layer drying using new mode. *International Agrophysics* 23: 313-317.

- Al-Harashseh, M., Al-Muhtaseb, A. H. & Magee T.R.A.2009. Microwave drying kinetics of tomato pomace: Effect of osmotic dehydration. *Chemical Engineering and Processing* 48: 524-531.
- Alibas, I. 2010. Correlation of drying parameters, ascorbic acid and color characteristics of nettle leaves during microwave-, air- and combined microwave-air-drying. *Journal of Food Process Engineering* 33(2): 213-233.
- Alibas, I. 2014. Mathematical modeling of microwave dried celery leaves and determination of the effective moisture diffusivities and activation energy. *Journal of food Science and Technology* 34 (2): 394-401.
- Alibas, I.2014. Microwave, Air and Combined Microwave-Air Drying of Grape Leaves (*Vitis vinifera* L.) and the Determination of Some Quality Parameters. *International Journal of Food Engineering* 10(1): 69-88.
- Balbay, A., Kaya, Y. & Sahin, O. 2012. Drying of black cumin (*Nigella sativa*) in a microwave assisted drying system and modeling using extreme learning machine. *Energy* 44: 352-357.
- Cheenkachorn, K. 2007. Drying of rice paddy using a microwave-vacuum dryer. In: *Proceedings of European Congress of Chemical Engineering (ECCE-6)*. Copenhagen 16-20 September.
- Cheepsathit, A. & Pattala, E.2005. Microwave-vacuum drying of paddy. *Biosystem Engineering Thesis*. King Mongkut's Inst. Tech. Norht Bangkok, Thailand.
- Chungcharoen, T., Prachayawarakorn, S., Tungtrakul, P. & Soponronnarit, S. 2015. Effect of germination time and drying temperature on drying characteristics and quality of germinated paddy. *Food and Bioproducts Processing* 94:707-716.
- Dadali, G., Demirhan, E. & Özbek, B. 2007. Effect of drying conditions on rehydration kinetics of microwave dried spinach. *Food and Bio-products processing* 86: 235-241.
- Demirhan, E. & Ozbek, B. 2011. Thin-layer drying characteristics and modeling of celery leaves undergoing microwave treatment. *Chemical Engineering Communications* 7 (198): 957-975.
- Discala, K., Meschino, G., Vega-Galvez, A., Lemus-Mondaca, R., Roura, S. & Mascheroni, R. 2013. An artificial neural network model for prediction of quality characteristics of apples during convective dehydration. *Food Science and Technology* 33(3): 411-416.
- Dong, J., Ma, X., Fu, Z. & Guo, Y. 2011. Effects of microwave drying on the contents of functional constituents of *Eucommia ulmoides* flower tea. *Industrial Crops and Products* 34: 1102-1110.
- Doungporn, S., Poomsa-ad, N. & Wiset, L. 2012. Drying equations of Thai Hom Mali paddy by using hot air, carbon dioxide and nitrogen gases as drying media. *Food and Bioproducts Processing*. 90: 187-198.
- Doymaz, Í. & Kocayigit, F. 2011. Drying and Rehydration Behaviors of Convection Drying of Green Peas. *Drying Technology* 29: 1273- 1282.
- FAO STAT. 2016. Rice market monitor. Available at: [www.fao.org/fileadmin/templates/est/COMM\\_MARKETS\\_MONITORING/](http://www.fao.org/fileadmin/templates/est/COMM_MARKETS_MONITORING/).
- Jangam, S.V., Joshi, V.S., Mujumdar, A.S. & Thorat, B.N. 2008. Studies of dehydration of *sapota* (*Achras zapota*). *Drying Technology* 26: 369-377.
- Kalantari, D. & Eshtevad, R. 2013. Influence of different of tempering period and vacuum conditions on the rice grain breakage in thin layer dryer. *Cercetări Agronomice în Moldova* 47(4): 5-12.
- Kardum, J. P., Sander, A. & Skansi, D. 2011. Comparison of convective, vacuum, and microwave drying chlorpropamide. *Drying Technology* 19(1):167-183.
- Kingsly, R.P., Goyal, R.K., Manikantan, M.R. & Ilyas, S.M. 2007. Effects of pretreatment and drying air temperature on drying behavior of peach slice. *International journal of Food Science and Technology* 42: 65-69.
- Li, Z., Raghavan, G.S.V., Wang, N. & Garipey, Y. 2009. Real-time, volatile-detection-assisted control for microwave drying. *Computers and Electronics in Agriculture* 69: 177-184.
- Manikantun, M.R., Barnwalr, P. & Goyal, R.K. 2012. Modeling the drying kinetics of paddy in an

- integrated paddy dryer. *I.K. International Publishing House Pvt.Ltd.New. Delhi, Bangalore* 103-110.
- McMinn, W.A.M. 2006. Thin-layer modelling of the convective, microwave, microwave-convective and microwave-vacuum drying of lactose powder. *Journal of Food Engineering* 72: 113-123
- Midilli, A., Kucuk, H. & Yapar, Z. 2002. A new model for single layer drying. *Drying Technology* 20(7): 1503-1513.
- Pehlivan, D. & Togrul, I.T. 2004. Modeling of thin layer drying kinetics of some fruits under open-air sun drying process. *Journal of food Engineering* 65(3): 413-425.
- Sacilik, K., Ozturk, R. & Keskin, R. 2003. Some physical properties of hempseed. *Biosystem Engineering* 86(2): 191-198.
- Soysal, Y. 2004. Microwave drying characteristics of parsley. *Biosystems Engineering* 89(2): 167-173.
- Taweerattanapanish, A., Soponronarit, S., Wetchakama, S., Kongseri, N. & Wongpiyachon, S. 1999. Effects of Drying on Head Rice Yield using Fluidization Technique. *Drying Technology* 17: 345-353.
- Yongsawasdigul, J. & Gunasekaran, S. 1996. Microwave-vacuum drying of cranberries: Part I. Energy use and efficiency. *Journal of Food Processing and Preservation* 20: 121-143.
- Zareiforush, H., Komarizadeh, M.H. & Alizadeh, M.R. 2009. Effect of moisture content on some physical properties of paddy grains. *Research Journal of Applied Science Engineering and Technology* 13: 132-139.
- Zarein, M., Samadi, S.H., & Ghobadian, B. 2013. Investigation of microwave dryer effect on energy efficiency during drying of apple slices. *Journal of the Saudi Society of Agricultural Sciences* 14 (1): 41-47.

## اثر دوره تابش و توان مایکروویو در خشک کردن برنج

حسن جعفری<sup>1</sup> - داوود کلانتری<sup>2\*</sup> - محسن آزادبخت<sup>3</sup>

تاریخ دریافت: 1396/02/14

تاریخ پذیرش: 1396/07/03

### چکیده

در این تحقیق اثر توان‌های مختلف (90، 270 و 450 وات) و دوره تابش یعنی زمان‌های روشن - خاموش (30/60 و 30/120 ثانیه / ثانیه) بر روی نسبت خشک شدن و صدمه دانه در خشک کردن به روش مایکروویو در دو رقم نعمت و هاشمی مورد بررسی قرار گرفت. طبق نتایج به دست آمده، مدل میدیلی و همکاران بهترین پیش بینی را برای خشک کردن رقم نعمت در دوره 30/60 نشان داد. علاوه بر این مدل Two-term برای رقم هاشمی در دوره‌های 30/60 و 30/120 و برای رقم نعمت در دوره 30/120 بهترین پیش بینی را داشت. طبق نتایج این تحقیق برای رقم هاشمی توان 270 وات و دوره 30/120 توصیه می‌شود. در این شرایط شکست دانه 19/1 درصد بود. در تمام حالات درصد شکست در رقم نعمت بالای 40 درصد بود و این نشان می‌دهد این رقم مناسب خشک کردن با مایکروویو نیست. توصیه می‌شود یک پیش آزمایش قبل از انجام آزمایش‌های مایکروویو انجام شود.

**واژه‌های کلیدی:** خشک کن مایکروویو، درصد شکست، نسبت رطوبت، لایه نازک، مدل خشک‌کنی

1 و 2 - به ترتیب دانشجوی کارشناسی ارشد و استادیار، گروه مهندسی بیوسیستم، دانشگاه علوم کشاورزی و منابع طبیعی ساری، ساری، ایران.  
3 - استادیار، گروه مهندسی بیوسیستم، دانشگاه علوم کشاورزی و منابع طبیعی گرگان، گرگان، ایران.  
\* - نویسنده مسئول: (Email: dkalantari2000@yahoo.com)

## Changes in the surface tension and viscosity of fish oil nanoemulsions developed by sonication during storage

M. Nejadmansouri<sup>1</sup>, S. M. H. Hosseini<sup>\*2</sup>, M. Niakosari<sup>3</sup>, Gh. H. Yousefi<sup>4</sup>, M. T. Golmakani<sup>5</sup>

Received: 2017.03.14

Accepted: 2017.09.11

### Abstract

Adequate consumption of  $\omega$ -3 essential fatty acids (EFAs) has a positive impact on human health. EFAs-enriched functional foods may be used for this purpose. Nanoemulsion is a promising delivery system for incorporating EFAs into a variety of foods and beverages. In this work, fish oil nanoemulsions developed by sonication method were subjected to various analyses as a function of hydrophilic lipophilic balance (HLB) and surfactant to oil ratio (SOR). Analyses were performed upon production and during 1-month storage at two temperatures (4 and 25 °C) in the presence (100 ppm) or absence of  $\alpha$ -tocopherol. Increasing in HLB and SOR decreased the particle size and surface tension; while, increased the refractive index and viscosity. During storage, the particle size of  $\alpha$ -tocopherol-loaded nanoemulsions decreased; whereas, that of  $\alpha$ -tocopherol-free nanoemulsions increased in a temperature-dependent manner. Irrespective of the storage temperature, surface tension values of antioxidant-loaded nanoemulsions remained constant. However, their viscosity values increased. Antioxidant incorporation fairly increased the nanoemulsions stability likely due to partitioning at the interface. TEM micrographs confirmed the results obtained by static light scattering. The results of this study may help the rational design of functional foods using nanoemulsion-based delivery systems.

**Keywords:** Fish Oil, High Intensity Ultrasound, Viscosity, Surface Tension, Nanoemulsion

### Introduction

Recently, nanoemulsions, as a sub-group of emulsion-based systems, have gained particular attention due to simple fabrication method, high kinetic stability and bioavailability (McClements, 2011; Walker *et al.*, 2015). The droplet radii of nanoemulsions (<100 nm) results in the formation of semi-turbid or even optically transparent systems particularly at sufficiently small particle sizes (<50 nm) (Mason *et al.*, 2006; Tadros *et al.*, 2004). High- or low-energy methods can be used to fabricate nanoemulsions. In high-energy approaches, mechanical devices such as microfluidizer, high pressure valve homogenizer and high intensity horn sonicator are usually applied to create fine droplets

(McClements, 2011; McClements & Rao, 2011). These methods do not have any limitations on the types of the oils and surfactants. Moreover, low surfactant to oil ratio (SOR) is typically needed. As determined in previous works (Nejadmansouri *et al.*, 2016; Kumar Dey *et al.*, 2012; Ghosh *et al.*, 2013), the application of sonication for the formation of nanoemulsions may lead to promising results without any requirement for coarse emulsion.

The increasing awareness about the biological roles of  $\omega$ -3 polyunsaturated fatty acids (PUFAs) in human health has prompted significant researches to find appropriate methods for incorporating fish oil (or its essential fatty acids) into functional foods and beverages, while preventing them from oxidation and off-flavor development. Natural antioxidants, such as  $\alpha$ -tocopherol, are used for this purpose. They act as chain-breaking electron-donor antioxidants (Shimajiri *et al.*, 2013). The antioxidant activity depends on the chemical structure of antioxidant molecules and interactions in the emulsions. The “polar paradox” theory describes that lipophilic

1, 2, 3 and 5. PhD student, Assistant Professor, Professor and Associate Professor, Department of Food Science and Technology, Shiraz University

4. Associate professor, Department of Pharmaceutics, Shiraz University of Medical Sciences

\*Corresponding author email: (hosseini@shirazu.ac.ir)

DOI: 10.22067/iftstr.v1396i13.63073

antioxidants are more effective than hydrophilic ones to retard the oxidation in O/W emulsions (Porter, 1993). This hypothesis cannot be extended to all antioxidant molecules. Therefore, the application of antioxidants in real food emulsions generally leads to unpredictable results (Shahidi & Zhong, 2011; Asnaashari *et al.*, 2014).

In this work, we studied the effects of hydrophilic lipophilic balance (HLB), surfactant to oil ratio (SOR) and  $\alpha$ -tocopherol incorporation on the particle size, dynamic viscosity and surface tension of nanoemulsions during storage. Research in this area is important to find appropriate strategies for incorporating lipophilic active ingredients into aqueous-based foods or beverages (such as fortified waters, soft drinks and sauces) using emulsion-based delivery systems.

#### Materials and methods

Fish oil (containing 25% EPA+DHA of total fatty acids) was purchased from Pars Kilka Co. (Babolsar, Iran). Tween 80 (HLB $\approx$ 15), and Span 80 (HLB $\approx$ 4.3) were purchased from Merck Co. (Darmstadt, Germany).  $\alpha$ -tocopherol was purchased from Sigma-Aldrich (St. Louis, MO, USA). Double distilled water (DDW) was utilized to prepare all emulsions.

#### Nanoemulsion preparation

O/W nanoemulsions containing 5 wt% dispersed phase were prepared using a mixture of non-ionic surfactants at various SORs (0.5-1.5) and HLBs (9-15). Briefly, the dispersed phase containing the required amount of Span 80 was gradually added into the aqueous phase (containing Tween 80) under magnetic stirring (700 rpm for 15 min) at room temperature. After that, a coarse emulsion was prepared by a disperser/homogenizer (Heidolph Silent Crusher, Schwabach, Germany) at 20000 rpm (715 xg) for 5 min. The coarse emulsion was then treated (amplitude 80%, cycle 0.7 s, duration 10 min) by a horn sonicator (Hielscher, UP 200H, Teltow, Germany) to develop nanoemulsions. Sonication was

performed in a glass beaker placed in an ice bath. The temperature did not exceed 25-30 °C during the process. In some batches,  $\alpha$ -tocopherol (100 ppm) was incorporated into the dispersed phase prior to emulsification.

#### Calculation of HLB

The required amounts of non-ionic surfactants to obtain a given HLB (denoted as HLB<sub>x</sub>) were calculated using the Pearson's square:

$$(A)\% = \left( \frac{HLB_x - HLB_B}{HLB_A - HLB_B} \right) \times 100 \quad (1)$$

$$(B)\% = 100 - (A) \quad (2)$$

where, HLB<sub>A</sub> and HLB<sub>B</sub> are the HLB values of Tween 80 and Span 80, respectively. (A) and (B)% represent the required amounts of surfactants in the emulsifier mixture (Peshkovsky *et al.*, 2013). The final weight of the surfactant mixture was determined based on the required SOR.

#### Particle size measurement

The volume-weighted mean droplet size ( $D_{4,3}$ ) and Span of 10-times diluted nanoemulsions were determined using static light scattering (SLS, laser diffraction, SALD-2101, Shimadzu, Japan) at room temperature (Gulotta *et al.*, 2014).

#### Refractive index measurement

The refractive indices of nanoemulsion, fish oil and aqueous phase were measured at 20 °C using a refractometer (RX7000 $\alpha$ ; Atago, Japan) (Rao *et al.*, 2013).

#### Surface tension measurement

The surface tension (mN m<sup>-1</sup>) of nanoemulsions was measured at 20 °C using a tensiometer (Sigma 703D; KSV, USA) equipped with a Du Nouy ring (Joe *et al.*, 2012). The dimensions of ring and wire were 9.545 and 0.185 mm, respectively.

#### Viscosity measurement

The viscosity of nanoemulsions was

measured using a U-tube capillary viscometer (type 51810, Schott Geräte, Germany) at  $25 \pm 0.1^\circ\text{C}$ . Dynamic viscosity was calculated

$$\text{Dynamic Viscosity (mpa.s)} = \text{Density (kg/m}^3\text{)} \times \text{Kinematic Viscosity (mm}^2\text{/s)} \times 0.001 \quad (3)$$

### Density measurement

The density of some selected samples was measured using a 25-ml pycnometer at  $25^\circ\text{C}$  (Qian *et al.*, 2011).

### Storage stability

$\alpha$ -tocopherol-free and  $\alpha$ -tocopherol-incorporated (100 ppm) nanoemulsions (HLB 12, SOR 1.5) were subjected to various physical stability tests (namely changes in droplet size, viscosity and surface tension) during storage at 4 and/or  $25^\circ\text{C}$  for 1 month. The experiments were carried out in 7-day intervals (Li *et al.*, 2013).

### Droplet morphology

Morphological studies were performed using transmission electron microscopy (TEM). A nanoemulsion drop was placed on a carbon-coated copper grid followed by staining with uranyl acetate. After 2 min, the grid was dried by forced air and then imaged by CM10 transmission electron microscope (Philips, Netherlands) (Salvia-Trujillo *et al.*, 2013).

### Statistical Analysis

A completely randomized design was used in this study. All experiments were performed at least three times. The results were reported as mean  $\pm$  standard deviation (SD). Data were analyzed using one-way analysis of variance (ANOVA) with Duncan's multiple comparison post hoc tests at a significance level of 0.05. The analysis was conducted using SPSS software (version 21, IBM Corp. USA) (Chang *et al.*, 2013).

## Results and discussion

### Effects of SOR and HLB on the particle size and Span

As a preliminary experiment, coarse emulsions were subjected to various sonication

according to the following equation (Secco *et al.*, 2014):

times. The smallest droplet size (82 nm) was obtained after 10-min sonication. Particle size reached a plateau at higher sonication times. The average particle size and Span values of nanoemulsions prepared at various SOR and HLB values are reported in Table 1.

The main reason for choosing Span 80 was to obtain different HLB values. Using various combinations of Span 80 and Tween 80. HLB is an important factor during the release process. An increase in HLB value increases the lag time in the jejunum and decreases the rate of lipolysis and hence the bioaccessibility of FFAs in the small intestine (Walker *et al.*, 2015). Mixed-emulsifier systems are more effective than a single-type emulsifier in retarding the particle aggregation (McClements *et al.*, 2011). Simultaneous application of lipophilic and hydrophilic surfactants may facilitate the formation of small particles using high-energy approaches. Both emulsifiers used in this study have an oleic acid residue which may facilitate the bending of surfactant molecule. Previous studies have also shown that the presence of double bonds (unsaturation) along the non-polar chains of non-ionic surfactants favors the formation of nanoemulsions with smaller droplet sizes (Wang *et al.*, 2009). At the same SOR, the effects of HLB values (from 11 to 14) on the particle size were not significant; confirming that the hydrophilicity of the emulsifier mixture was adequate to develop nanoemulsions. Molecular geometry and HLB value of surfactant molecules are of paramount importance (Wang *et al.*, 2009). The effects of HLB value on the particle size can be explained in terms of partition coefficient of surfactant molecules in lipid and aqueous phases. In addition, deposition of surfactant molecules onto the interfacial layer has an important role on particle size (i.e., heterogeneous emulsifier molecules present

within an emulsifier mixture show a preference to be arranged beside the molecules

of their own type to decrease the free surface energy) (Nejadmansouri *et al.*, 2016).

**Table 1. Effect of SOR and HLB on particle size (nm) and refractive index of nanoemulsions**

HLB	SOR	Particle size (nm)	Span	Refractive index
9	0.5	460±3 <sup>b</sup>	0.403±0.016 <sup>b</sup>	1.3441±0.0004 <sup>d</sup>
	1	489±37 <sup>a</sup>	0.472±0.073 <sup>b</sup>	1.3469±0.0011 <sup>c</sup>
	1.5	461±1 <sup>b</sup>	0.412±0.006 <sup>b</sup>	1.3499±0.0007 <sup>b</sup>
10	0.5	468±9 <sup>ab</sup>	0.440±0.016 <sup>b</sup>	1.3442±0.0001 <sup>d</sup>
	1	472±11 <sup>ab</sup>	0.445±0.026 <sup>b</sup>	1.3471±0.0010 <sup>c</sup>
	1.5	87±2 <sup>c</sup>	0.678±0.011 <sup>a</sup>	1.3504±0.0003 <sup>ab</sup>
11	0.5	469±8 <sup>ab</sup>	0.437±0.020 <sup>b</sup>	1.3440±0.0002 <sup>d</sup>
	1	91±2 <sup>c</sup>	0.673±0.015 <sup>a</sup>	1.3472±0.0006 <sup>c</sup>
	1.5	88±5 <sup>c</sup>	0.677±0.006 <sup>a</sup>	1.3513±0.0000 <sup>a</sup>
12	0.5	474±1 <sup>ab</sup>	0.451±0.002 <sup>b</sup>	1.3442±0.0000 <sup>d</sup>
	1	87±1 <sup>c</sup>	0.688±0.002 <sup>a</sup>	1.3473±0.0001 <sup>c</sup>
	1.5	90±3 <sup>c</sup>	0.666±0.004 <sup>a</sup>	1.3508±0.0001 <sup>ab</sup>
12.5	0.5	474±1 <sup>ab</sup>	0.452±0.000 <sup>b</sup>	1.3440±0.0004 <sup>de</sup>
	1	88±2 <sup>c</sup>	0.667±0.016 <sup>a</sup>	1.3474±0.0001 <sup>c</sup>
	1.5	93±2 <sup>c</sup>	0.687±0.034 <sup>a</sup>	1.3510±0.0003 <sup>a</sup>
13	0.5	469±8 <sup>ab</sup>	0.438±0.020 <sup>b</sup>	1.3440±0.0001 <sup>de</sup>
	1	89±2 <sup>c</sup>	0.672±0.008 <sup>a</sup>	1.3471±0.0001 <sup>c</sup>
	1.5	94±5 <sup>c</sup>	0.715±0.095 <sup>a</sup>	1.3509±0.0009 <sup>ab</sup>
14	0.5	472±10 <sup>ab</sup>	0.447±0.026 <sup>b</sup>	1.3436±0.0001 <sup>de</sup>
	1	91±0 <sup>c</sup>	0.657±0.002 <sup>a</sup>	1.3472±0.0004 <sup>c</sup>
	1.5	94±3 <sup>c</sup>	0.710±0.052 <sup>a</sup>	1.3512±0.0002 <sup>a</sup>
15	0.5	75±6 <sup>c</sup>	0.712±0.072 <sup>a</sup>	1.3429±0.0004 <sup>e</sup>
	1	82±14 <sup>c</sup>	0.686±0.017 <sup>a</sup>	1.3474±0.0004 <sup>c</sup>
	1.5	72±1 <sup>c</sup>	0.696±0.002 <sup>a</sup>	1.3506±0.0001 <sup>ab</sup>

HLB: hydrophilic lipophilic balance; SOR: surfactant to oil ratio. Means in each column with different superscript letters are significantly different ( $p<0.05$ ).

Irrespective of the SOR, the largest particle sizes were obtained at HLB 9; which means that the final particle size is dependent on the hydrophobicity of emulsifier mixture. In other words, nanodroplets cannot be developed within an O/W emulsion where the hydrophobic characteristics of surfactant molecules exceed a certain level. An increase in the SOR generally decreased the particle size. Tween 80 is derived from polyethoxylated sorbitan and oleic acid. Span 80 is sorbitane monooleate. Both molecules have an oleic acid residue. A decrease in the HLB value led to higher concentrations of Span 80 (as an emulsifier with low affinity toward water) in the mixed emulsifier system. An increase in the surface area to volume ratio and hence higher surfactant concentrations were required to obtain lower particle sizes. At higher HLB

values, the dependence of particle size on the amount of SOR was more than lower HLBs. To obtain lower particle sizes, surfactant molecules should be easily placed at the interface; however, lipophilic molecules of Span 80 were not able to, mainly because of the presence of water as the continuous medium. Therefore, the particle size was independent from low SOR values at low HLBs. Particle size decreased at a SOR value (1.5) higher than a critical SOR (1) likely due to the increased concentration of surfactant molecules in the emulsion. At higher HLB values, the hydrophilic head groups of Tween 80 could be readily positioned at the interface and hence particle size decreased by increasing the surfactant concentration or SOR. In other words, higher concentrations of surfactant molecules could provide adequate interfacial layers for effective coating of newly developed

nanodroplets (i.e., increased specific surface area). An increase in the surfactant concentration can decrease the particle size through various mechanisms (Lamaallam et al., 2005). First, higher amounts of surfactant molecules would result in a higher decrease in the interfacial tension and hence increasing the mobility of the oil–water interfaces, where oil droplets are formed. Second, higher concentration gradient results in more flux of surfactant molecules from the lipid phase into the aqueous phase upon contact and hence enhances the formation of finer droplets at the oil–water boundary. Third, higher surfactant concentrations may lead to favorable rearrangements within the system. Our results are in good agreement with those reported by Li and colleagues (2013). These researchers prepared nanoemulsions of D-limonene using a catastrophic phase inversion method. An increase in the surfactant concentration led to a decrease in the mean particle diameter. Gulotta and colleagues (2014) prepared a mixture of fish and lemon oils nanoemulsions using a spontaneous method and Tween 80 as the emulsifier. The mean particle diameter was large ( $>1000$  nm) at relatively low surfactant levels ( $SOR < 0.75$ ); whereas, small ( $<200$  nm) particle sizes were obtained at higher levels ( $SOR \geq 0.75$ ).

As shown in Table 1, a significant ( $p < 0.05$ ) increase in the Span values was observed by increasing the SOR. The amounts of emulsifiers used to stabilize emulsions are generally larger than the actual amounts required to be loaded at the interfaces. Therefore, a substantial fraction of the emulsifier molecules remains un-adsorbed. This fraction may be partitioned between oil and water phases and hence develops surfactant micelles (Berton-Carabin et al., 2014). The presence of un-adsorbed surfactant molecules may lead to broadening the particle size distribution.

#### **Effect of SOR value and HLB factor on refractive index**

The effect of surfactant concentration on the refractive index of nanoemulsions is

reported in Table 1. The refractive index of nanoemulsions increased significantly ( $p < 0.05$ ) by increasing the SOR. The ratio of the refractive index of oil ( $n_1$ ) to that of aqueous phase ( $n_2$ ) has a vital role on the optical properties of the resultant emulsion. As an example, for HLB 15, the refractive index of the oil was 1.477. An upward trend in  $n_2$  (from 1.336 to 1.343) was observed by increasing the amount of Tween 80. At higher SORs, when  $n_1:n_2$  ratio moved toward unity, the emulsions became less opaque. The light detection mechanisms in turbidity and reflectance measurements are different. In turbidity, the propagated light through an emulsion is measured. As the scattering efficiency of the dispersed droplets increases above a certain level, the fraction of the light waves that can transmit through the emulsions falls below a detectable level (i.e., increased turbidity). Reflectance measurement relies on the light that has been reflected from the emulsions. At high droplet concentrations, reflectance occurs more than transmittance (Chantrapornchai et al., 2001). An increase in SOR resulted in increasing the number of smaller droplets and hence the amount of reflected light (i.e., increased refractive index). There is a direct relationship between the particle size and turbidity up to a defined particle size (around 75 nm), above which turbidity increases more rapidly. Kumar Dey et al (2012) reported that the refractive index of fish oil nanoemulsion was slightly higher than that of fish oil emulsion. Rao and McClements (2013) found that incorporating high levels of polar cosolvents into the aqueous phase prior to homogenization led to formation of optically transparent lemon oil nanoemulsions. This observation was due to the fact that cosolvent reduced the refractive index contrast, rather than reducing the particle size.

#### **Effect of SOR and HLB on surface tension**

Particle size reduction under the effect of increased SOR could be explained by the fact that a larger amount of emulsifier resulted in reducing the surface tension and eventually

creating smaller droplets. There was not any significant difference between the surface tension of nanoemulsions obtained at SOR values of 1 and 1.5 (Table 2). However, a decreasing trend could be detected by increasing the SOR. The surface tension of water and oil were 71.43 and 31.2 mN/m, respectively. During this study we did not measure the effects of a wide range of surfactant concentrations on the reduction of surface tension. It is obvious that the presence of surfactant molecules results in a decrease in the surface tension by disrupting the cohesive forces between water molecules. At higher surfactant concentrations, the adhesive forces between polar head groups of surfactant molecules and continuous medium (water) may compensate the decreased cohesive forces. Therefore, above a certain level, surface tension might be relatively independent from the concentration of surfactant molecules. The ability of emulsifiers to reduce the surface tension was dependent on the total amount as well as the ratio of emulsifiers (HLB). This dependency on HLB was more obvious at SOR of 0.5. An increase in the HLB increased the surface tension. Indeed, the increase in the proportion of the polar head groups of the emulsifiers resulted in

extensive hydrogen bonding with water molecules and surface tension increased for this reason. Previous studies have shown that smaller droplets can be formed when the disperse-to-continuous phases viscosity ratio ( $\eta_D/\eta_C$ ) is close to unity and when the disperse-to-continuous phases interfacial tension is reduced (Wooster *et al.*, 2008; Qian & McClements., 2011). The diffusion of surfactant molecules from the bulk phase onto the droplet surface reduces the interfacial density fluctuations at the thin liquid films. Since the rate of diffusion increases with surfactant concentration, the average droplet diameter is lowered. Joe and colleagues (2012) reported a decrease in the surface tension using a variety of oils by reducing the particle size. Yang and McClements (2013) reported a decrease in the interfacial tension of the aqueous phase and also the particle size by increasing glycerol concentration. Moreover, a decrease in vitamin E concentration resulted in increasing the interfacial tension of the organic phase and hence increasing the particle size. The tensiometer used in this study had a manual movement of the ring. We could not precisely determined the location of the ring at the interface of water and oil and interfacial tension was not measured for this reason.

**Table 2. Effect of SOR and HLB on the surface tension (mN/m), density (Kg/m<sup>3</sup>) and dynamic viscosity (mPa.s) of nanoemulsions**

HLB	SOR	Surface tension (mN/m)	Density (kg/m <sup>3</sup> )	Dynamic viscosity (mPa.s)
9	0.5	31.05±0.18 <sup>bc</sup>	1008.36±0.10 <sup>i</sup>	1.16±0.001 <sup>h</sup>
	1	30.68±0.25 <sup>bc</sup>	1009.16±0.10 <sup>f</sup>	1.31±0.001 <sup>g</sup>
	1.5	30.89±0.19 <sup>bc</sup>	1011.48±0.09 <sup>c</sup>	1.78±0.004 <sup>a</sup>
10	0.5	31.33±0.08 <sup>b</sup>	1007.44±0.11 <sup>k</sup>	1.16±0.001 <sup>h</sup>
	1	30.49±0.15 <sup>c</sup>	1008.40±0.10 <sup>h</sup>	1.34±0.001 <sup>f</sup>
	1.5	30.86±0.25 <sup>bc</sup>	1011.20±0.08 <sup>d</sup>	1.61±0.001 <sup>b</sup>
11	0.5	32.67±0.30 <sup>a</sup>	1008.16±0.10 <sup>j</sup>	1.14±0.002 <sup>i</sup>
	1	30.94±0.29 <sup>bc</sup>	1010.56±0.11 <sup>e</sup>	1.36±0.003 <sup>e</sup>
	1.5	31.18±0.11 <sup>bc</sup>	1013.24±0.10 <sup>a</sup>	1.53±0.002 <sup>d</sup>
12	0.5	32.29±0.05 <sup>a</sup>	1007.36±0.10 <sup>l</sup>	1.16±0.001 <sup>h</sup>
	1	31.24±0.17 <sup>bc</sup>	1008.72±0.08 <sup>g</sup>	1.34±0.001 <sup>f</sup>
	1.5	31.41±0.29 <sup>b</sup>	1012.52±0.11 <sup>b</sup>	1.54±0.003 <sup>c</sup>

HLB: hydrophilic lipophilic balance; SOR: surfactant to oil ratio. Means in each column with different superscript letters are significantly different ( $p < 0.05$ ).

#### Effect of SOR and HLB on viscosity and density

An increase in the surfactant concentration increased the amounts of viscosity and density of nanoemulsions (Table. 2). Similar results

have been reported by Ghosh *et al* (2013) for the viscosity of basil oil nanoemulsion prepared by different amounts of Tween 80.

There are several factors which influence the emulsion viscosity namely, the volume fraction of the dispersed phase, the rheology of component phases, droplet size, colloidal (inter-particle) interactions and droplet charge (McClements, 2005; Pal, 2011). Emulsions of various viscosities can be obtained at different droplet concentrations. Flocculation may appreciably increase the emulsion viscosity. Moreover, incorporation of thickening agents into aqueous phase may have similar effect (McClements, 2002). The viscosity of a nanoemulsion may be significantly greater than that of a macroemulsion at the same lipid concentration, particularly when it contains a thick or charged interfacial layer (Tadros et al., 2004; Weiss & McClements., 2000). Increasing the emulsifier concentration may

change the characteristics of the interfacial layers surrounding the oil droplets. After formation of interfacial layers of limited thickness, the non-adsorbed fraction of surfactant molecules might be responsible for increasing the viscosity and density of the continuous phase.

#### Storage stability of fish oil nanoemulsions at different temperatures

$\alpha$ -Tocopherol-free and -loaded fish oil nanoemulsions prepared at SOR 1.5 and HLB 12 were used for the stability tests. During the shelf life of a product, minimum changes in particle size distribution are required. Changes in the droplet size of nanoemulsions during 1-month storage at 4 and 25°C are shown in Table. 3.

**Table 3. Effect of temperature (4 and 25 °C) on particle size, viscosity and surface tension of nanoemulsions as a function of time**

Day	Sample/ Temperature (°C)	Particle size (nm)	Dynamic viscosity (mPa.s)	Surface tension (mN/m)
1	TS 4 °C	102±1.80 <sup>h</sup>	1.68±0.002 <sup>a</sup>	31.97±0.10 <sup>a</sup>
	TS 25 °C	60±1.42 <sup>p</sup>	1.58±0.001 <sup>c</sup>	30.70±0.35 <sup>b</sup>
	TS $\alpha$ 4 °C	88±1.23 <sup>k</sup>	1.55±0.001 <sup>b</sup>	31.92±0.15 <sup>a</sup>
7	TS $\alpha$ 25 °C	78±1.28 <sup>m</sup>	1.56±0.001 <sup>d</sup>	31.80±0.40 <sup>a</sup>
	TS 4 °C	119±1.73 <sup>g</sup>	1.50±0.001 <sup>c</sup>	31.81±0.29 <sup>ab</sup>
	TS 25 °C	71±1.01 <sup>no</sup>	1.53±0.003 <sup>e</sup>	32.08±0.31 <sup>a</sup>
	TS $\alpha$ 4 °C	81±1.44 <sup>l</sup>	1.45±0.001 <sup>e</sup>	31.88±0.22 <sup>a</sup>
14	TS $\alpha$ 25 °C	95±1.02 <sup>j</sup>	1.57±0.002 <sup>c</sup>	31.93±0.20 <sup>a</sup>
	TS 4 °C	130±1.43 <sup>f</sup>	1.43±0.004 <sup>e</sup>	31.42±0.19 <sup>b</sup>
	TS 25 °C	70±1.22 <sup>o</sup>	1.60±0.001 <sup>b</sup>	32.53±0.15 <sup>a</sup>
	TS $\alpha$ 4 °C	78±1.56 <sup>m</sup>	1.47±0.002 <sup>d</sup>	32.19±0.41 <sup>a</sup>
21	TS $\alpha$ 25 °C	72±1.38 <sup>n</sup>	1.58±0.001 <sup>b</sup>	32.07±0.48 <sup>a</sup>
	TS 4 °C	156±1.33 <sup>e</sup>	1.54±0.001 <sup>b</sup>	31.49±0.39 <sup>ab</sup>
	TS 25 °C	467±1.12 <sup>b</sup>	1.55±0.002 <sup>d</sup>	32.22±0.49 <sup>a</sup>
	TS $\alpha$ 4 °C	70±1.45 <sup>o</sup>	1.54±0.002 <sup>c</sup>	32±0.83 <sup>a</sup>
28	TS $\alpha$ 25 °C	466±1.87 <sup>b</sup>	1.58±0.003 <sup>b</sup>	32.57±0.48 <sup>a</sup>
	TS 4 °C	209±1.28 <sup>d</sup>	1.46±0.002 <sup>d</sup>	31.71±0.26 <sup>ab</sup>
	TS 25 °C	464±1.66 <sup>c</sup>	1.62±0.002 <sup>a</sup>	32.25±0.62 <sup>a</sup>
	TS $\alpha$ 4 °C	98±1.29 <sup>i</sup>	1.57±0.002 <sup>a</sup>	31.89±0.29 <sup>a</sup>
	TS $\alpha$ 25 °C	483±1.57 <sup>a</sup>	1.61±0.003 <sup>a</sup>	32.52±0.46 <sup>a</sup>

Means in each column with different superscript letters are significantly different ( $p < 0.05$ ). TS: antioxidant-free samples; TS $\alpha$ : samples incorporated with 100 ppm  $\alpha$ -tocopherol.

The increase in the droplet size of  $\alpha$ -tocopherol-loaded nanoemulsions kept at 4°C was less than that of  $\alpha$ -tocopherol-free ones. At 25°C, the particle size was relatively constant during first 14 days; however, an abrupt increase was observed at longer storage times (>21 days). The increase in the particle

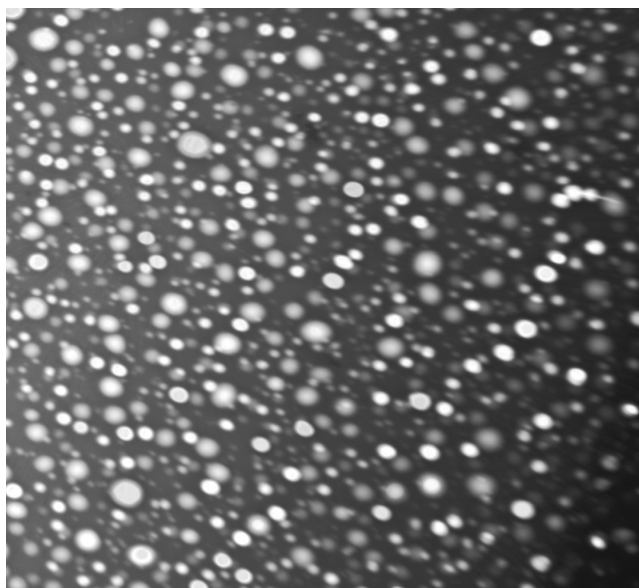
size can be explained in terms of droplet collisions within the aqueous phase. Temperature has an enhancing effect on the Brownian motion of nanoparticles. The higher stability of antioxidant-incorporated nanoemulsions was attributed to the presence of antioxidant at interface. Generally, the

viscosity of nanoemulsions increased significantly ( $p < 0.05$ ) as a function of time (Table 3). As already mentioned, the viscosity of nanoemulsions is considerably larger than that of conventional emulsions at same oil content. Different destabilization mechanisms may occur during storage of nanoemulsions including flocculation, coalescence and Ostwald ripening. During flocculation, the continuous phase is entrapped within flocculated particles and viscosity increases for this reason. In other words, emulsion viscosity may increase appreciably if the droplets are flocculated because of the continuous phase entrapment (McClements *et al.*, 2010). Therefore, the viscosity of emulsions is a function of both particle size and the amount of flocculated particles. Particle size reduction (via increasing the surface area to volume ratio) and flocculation (through entrapment of continuous phase) have an enhancing effect on the emulsion viscosity. The final viscosity is a consequence of these two parameters. The viscosity of antioxidant-free nanoemulsions stored at 4 °C revealed an opposite trend (i.e., a slight decrease in the viscosity was observed during storage). Surface tension of antioxidant-free

nanoemulsions increased as a result of increased particle size; whereas, it remained relatively constant in antioxidant containing system at two studied temperatures (Table 3). The arrangement of surfactant molecules near each other may have an important role in the observed surface tension. Indeed, the interfacial layer is not a homogeneous shell around the oil droplet core and consists of various molecules with specific structures, organizations and interactions (Lam & Nickerson., 2013). Teixeira *et al* (2016) reported that the viscosity of  $\alpha$ -tocopherol-loaded nanoemulsions was higher than that of antioxidant-free ones; however, the surface tension of nanoemulsions without antioxidant was higher than those with antioxidant.

#### The morphology of droplets

Nanoemulsions, prepared at HLB 12 and SOR 1.5, were subjected to morphological studies using TEM (Fig. 1). A mean diameter of less than 100 nm could be observed. Based on TEM observation, we can conclude that the dispersed phase of emulsion was in nanometer range confirming the results of laser diffraction technique.



700 nm  
Fig 1. TEM image of nanoemulsions

## Conclusion

In this work, a high energy approach was used to develop fish oil nanoemulsion. The characteristics of nanoemulsions were studied under the influence of SOR, HLB and storage temperature. A decrease in the particle size and surface tension as well as an increase in the refractive index and viscosity was observed by increasing the SOR and HLB. During storage, incorporating  $\alpha$ -tocopherol into nanoemulsions fairly increased the stability of nanoemulsion. The results reported in this study may have implications for the

design and utilization of nanoemulsions as delivery systems for food fortification particularly after optimization of formulation using off-flavors masking agents. In future studies, it would be informative to examine the lipid digestion, bioavailability and body intake.

## Acknowledgment

The authors are thankful to Shiraz University for financial support (Grant number 93GRD3M194065).

## References

- Asnaashari, M., Farhoosh, R., & Sharif, A. (2014). Antioxidant activity of gallic acid and methyl gallate in triacylglycerols of Kilka fish oil and its oil-in-water emulsion. *Food chemistry*, *159*, 439-444.
- Berton-Carabin, C. C., Ropers, M. H., & Genot, C. (2014). Lipid Oxidation in Oil-in-Water Emulsions: Involvement of the Interfacial Layer. *Comprehensive Reviews in Food Science and Food Safety*, *13*, 945-977.
- Chang, Y., McLandsborough, L., & McClements, D. J. (2013). Physicochemical properties and antimicrobial efficacy of carvacrol nanoemulsions formed by spontaneous emulsification. *Journal of agricultural and food chemistry*, *61*, 8906-8913.
- Chantrapornchai, W., Clydesdale, F., & McClements, D. (2001). Influence of relative refractive index on optical properties of emulsions. *Food research international*, *34*, 827-835.
- Ghosh, V., Mukherjee, A., & Chandrasekaran, N. (2013). Ultrasonic emulsification of food-grade nanoemulsion formulation and evaluation of its bactericidal activity. *Ultrasonics sonochemistry*, *20*, 338-344.
- Gulotta, A., Saberi, A. H., Nicoli, M. C., & McClements, D. J. (2014). Nanoemulsion-based delivery systems for polyunsaturated ( $\omega$ -3) oils: formation using a spontaneous emulsification method. *Journal of agricultural and food chemistry*, *62*, 1720-1725.
- Joe, M. M., Bradeeba, K., Parthasarathi, R., Sivakumaar, P. K., Chauhan, P. S., Tipayno, S., Benson, A., & Sa, T. (2012). Development of surfactin based nanoemulsion formulation from selected cooking oils: Evaluation for antimicrobial activity against selected food associated microorganisms. *Journal of the Taiwan Institute of Chemical Engineers*, *43*, 172-180.
- kumar Dey, T., Ghosh, S., Ghosh, M., Koley, H., & Dhar, P. (2012). Comparative study of gastrointestinal absorption of EPA & DHA rich fish oil from nano and conventional emulsion formulation in rats. *Food research international*, *49*, 72-79.
- Lam, R. S., & Nickerson, M. T. (2013). Food proteins: a review on their emulsifying properties using a structure–function approach. *Food chemistry*, *141*, 975-984.
- Lamaallam, S., Bataller, H., Dicharry, C., & Lachaise, J. (2005). Formation and stability of miniemulsions produced by dispersion of water/oil/surfactants concentrates in a large amount of water. *Colloids and Surfaces A: Physicochemical and Engineering Aspects*, *270*, 44-51.
- Li, Y., Zhang, Z., Yuan, Q., Liang, H., & Vriesekoop, F. (2013). Process optimization and stability of D-limonene nanoemulsions prepared by catastrophic phase inversion method. *Journal of Food*

- Engineering*, 119, 419-424.
- Mason, T. G., Wilking, J., Meleson, K., Chang, C., & Graves, S. (2006). Nanoemulsions: formation, structure, and physical properties. *Journal of Physics: Condensed Matter*, 18, 635.
- McClements, D. J. (2002). Theoretical prediction of emulsion color. *Advances in colloid and interface science*, 97, 63-89.
- McClements, D. J. (2005). Theoretical analysis of factors affecting the formation and stability of multilayered colloidal dispersions. *Langmuir*, 21, 9777-9785.
- McClements, D. J. (2011). Edible nanoemulsions: fabrication, properties, and functional performance. *Soft Matter*, 7, 2297-2316.
- McClements, D. J., & Li, Y. (2010). Structured emulsion-based delivery systems: Controlling the digestion and release of lipophilic food components. *Advances in colloid and interface science*, 159, 213-228.
- McClements, D. J., & Rao, J. (2011). Food-grade nanoemulsions: formulation, fabrication, properties, performance, biological fate, and potential toxicity. *Critical reviews in food science and nutrition*, 51, 285-330.
- Nejadmansouri, M., Hosseini, S. M. H., Niakosari, M., Yousefi, G. H., & Golmakani, M. T. (2016). Physicochemical properties and oxidative stability of fish oil nanoemulsions as affected by hydrophilic lipophilic balance, surfactant to oil ratio and storage temperature. *Colloids and Surfaces A: Physicochemical and Engineering Aspects*, 506, 821-832.
- Pal, R. (2011). Rheology of simple and multiple emulsions. *Current opinion in colloid & interface science*, 16, 41-60.
- Peshkovsky, A. S., Peshkovsky, S. L., & Bystryak, S. (2013). Scalable high-power ultrasonic technology for the production of translucent nanoemulsions. *Chemical Engineering and Processing: Process Intensification*, 69, 77-82.
- Porter, W. L. (1993). Paradoxical behavior of antioxidants in food and biological systems. *Toxicology and Industrial Health*, 9, 93.
- Qian, C., & McClements, D. J. (2011). Formation of nanoemulsions stabilized by model food-grade emulsifiers using high-pressure homogenization: factors affecting particle size. *Food Hydrocolloids*, 25, 1000-1008.
- Rao, J., & McClements, D. J. (2013). Optimization of lipid nanoparticle formation for beverage applications: Influence of oil type, cosolvents, and cosurfactants on nanoemulsion properties. *Journal of Food Engineering*, 118, 198-204.
- Salvia-Trujillo, L., Rojas-Graü, M. A., Soliva-Fortuny, R., & Martín-Belloso, O. (2013). Effect of processing parameters on physicochemical characteristics of microfluidized lemongrass essential oil-alginate nanoemulsions. *Food Hydrocolloids*, 30, 401-407.
- Secco, R. A., Kostic, M., & deBruyn, J. R. (2014). Fluid Viscosity Measurement. In *Measurement, Instrumentation, and Sensors Handbook, Second Edition: Spatial, Mechanical, Thermal, and Radiation Measurement* (pp. 46-1). CRC Press.
- Shahidi, F., & Zhong, Y. (2011). Revisiting the polar paradox theory: a critical overview. *Journal of agricultural and food chemistry*, 59, 3499-3504.
- Shimajiri, J., Shiota, M., Hosokawa, M., & Miyashita, K. (2013). Synergistic antioxidant activity of milk sphingomyeline and its sphingoid base with  $\alpha$ -tocopherol on fish oil triacylglycerol. *Journal of agricultural and food chemistry*, 61, 7969-7975.
- Tadros, T., Izquierdo, P., Esquena, J., & Solans, C. (2004). Formation and stability of nanoemulsions. *Advances in colloid and interface science*, 108, 303-318.
- Teixeira, M. C., Severino, P., Andreani, T., Boonme, P., Santini, A., Silva, A. M., & Souto, E. B. (2016). D- $\alpha$ -tocopherol nanoemulsions: Size properties, rheological behavior, surface tension, osmolarity and cytotoxicity. *Saudi Pharmaceutical Journal*, in press; Doi:10.1016/j.jsps.2016.06.004.

- Walker, R. M., Decker, E. A., & McClements, D. J. (2015). Physical and oxidative stability of fish oil nanoemulsions produced by spontaneous emulsification: effect of surfactant concentration and particle size. *Journal of Food Engineering*, *164*, 10-20.
- Wang, L., Dong, J., Chen, J., Eastoe, J., & Li, X. (2009). Design and optimization of a new self-nanoemulsifying drug delivery system. *Journal of colloid and interface science*, *330*, 443-448.
- Weiss, J., & McClements, D. (2000). Influence of Ostwald ripening on rheology of oil-in-water emulsions containing electrostatically stabilized droplets. *Langmuir*, *16*, 2145-2150.
- Wooster, T. J., Golding, M., & Sanguansri, P. (2008). Impact of oil type on nanoemulsion formation and Ostwald ripening stability. *Langmuir*, *24*, 12758-12765.
- Yang, Y., & McClements, D. J. (2013). Encapsulation of vitamin E in edible emulsions fabricated using a natural surfactant. *Food Hydrocolloids*, *30*, 712-720.

## تغییرات کشش سطحی و گرانیروی نانوامولسیون روغن ماهی تولید شده با روش فراصوت طی انبارمانی

مریم نژادمنصوری<sup>1</sup> - سید محمدهاشم حسینی<sup>2\*</sup> - مهرداد نیاکوثری<sup>3</sup> - غلامحسین یوسفی<sup>4</sup> - محمدتقی گل‌مکانی<sup>5</sup>

تاریخ دریافت: 1395/12/14

تاریخ پذیرش: 1396/06/20

### چکیده

مصرف کافی از اسیدهای چرب ضروری امگا 3 تأثیری مثبت بر سلامت انسان دارد. برای دستیابی به این هدف از مواد غذایی فراسودمند غنی شده با اسیدهای چرب ضروری می‌توان بهره برد. نانوامولسیون‌ها می‌توانند به‌عنوان یک سیستم تحویل اسیدهای چرب ضروری در مواد غذایی مختلف و نوشیدنیها مورد استفاده قرار گیرند. در این مطالعه، نانوامولسیون روغن ماهی تولید شده با روش فراصوت در نسبت‌های مختلف HLB و SOR طی نگهداری در دو دمای 4 و 25 درجه سانتی‌گراد برای مدت 1 ماه تحت آزمون‌های مختلفی قرار گرفتند. در نیمی از نمونه‌ها از آلفاتوکوفرول با غلظت 100 پی‌پی‌ام استفاده گردید. با افزایش میزان HLB و SOR، اندازه ذره و کشش سطحی کاهش ولی گرانیروی و ضریب شکست افزایش یافتند. طی انبارمانی، اندازه ذرات نانوامولسیون حاوی آنتی‌اکسیدان آلفاتوکوفرول کاهش یافت اما اندازه ذرات نانوامولسیون‌های بدون آلفا توکوفرول (طی روندی وابسته به دمای نگهداری) افزایش یافت. صرف نظر از دمای نگهداری، کشش سطحی نانوامولسیون‌های حاوی آنتی‌اکسیدان آلفا توکوفرول ثابت باقی ماند، هرچند که ویسکوزیته آنها افزایش یافت. پایداری شیمیایی نمونه‌های حاوی آنتی‌اکسیدان به دلیل قرار گرفتن آنها در فضای بین سطحی نسبتاً افزایش یافت. تصاویر میکروسکوپ الکترونی عبوری وجود ذرات در مقیاس نانومتر را تایید نمودند. نتایج این تحقیق ممکن است به طراحی غذاهای فراسودمند با استفاده از سیستم‌های تحویل بر پایه نانوامولسیون کمک نماید.

**واژه‌های کلیدی:** روغن ماهی، فراصوت با شدت بالا، ویسکوزیته، کشش سطحی، نانوامولسیون

1، 2، 3 و 5- به ترتیب دانشجوی دکتری، استادیار، استاد و دانشیار، گروه علوم و صنایع غذایی، دانشگاه شیراز، شیراز، ایران.  
4- دانشیار، دانشکده داروسازی، دانشگاه علوم پزشکی شیراز، شیراز، ایران.  
(\* - نویسنده مسئول: Email: hhosseini@shirazu.ac.ir)

## Effect of ultrasound bath and probe combined to brine and brine-polyphosphate solutions on the qualitative and textural properties of beef meat

M. H Naeli<sup>1</sup>, R. Esmailzadeh Kenari<sup>2\*</sup>

Received: 2017.09.16

Accepted: 2017.12.13

### Abstract

Various mechanical, enzymatic and chemical techniques are used to improve the quality levels of meat. Such techniques have disadvantages such as being time-consuming and damaging to the meat quality indicators. Ultrasound is used as an effective method to modify technological properties and tenderize the meat. The meat samples (Flank area) were put into brine solution or a mixture of the phosphate-brine solution under the ultrasound bath (at a frequency of 37 kHz) and probes (20 kHz) in 20, 25 and 30 minutes at 30, 40 and 50°C. The changes in the technological and textural properties of meat samples were then investigated. The results showed an increase in pH (from 5.55 for control up to 7.14), water-holding capacity (from 20.00 % for control up to 38.15 %), water-binding capacity (from 12.63 % for control up to 31.65 %) and a reduction in the drip loss (from 12.50 % for control up to 3.21 %), cooking loss (from 36.70 % for control up to 16.46 %), hardness and chewiness, whereas showed an increase in tenderness. In general, ultrasound treatment probe in a solution of mixed polyphosphate-brine was more efficient. It is concluded that ultrasound is an effective technique to improve the meat quality.

**Keywords:** Beef meat, Technological properties, Tenderize, Textural properties, Ultrasound

### Introduction:

The quality of meat is evaluated by the parameters such as chemical composition, physical properties, organoleptic properties and appearance. Organoleptic properties and the overall quality of meat are mainly affected by the tenderness, flavor and water-holding capacity (WHC). In general, the functional and technological properties of meat such as WHC, water-binding capacity (WBC) and emulsifying properties are affected by the myofibrillar proteins. Tenderness is affected by the myofibrils protein composition and structure of the skeletal muscle. Many factors cause the loss of technological quality and palatability of meat. For example, it has been found that with increasing age of the animal, the covalent cross-links between collagen building blocks (tropocollagen) increased and result in decreased collagen solubility. Such a

problem directly reduces the technological quality of meat. So, in such cases the use of various mechanical, enzymatic and chemical methods is necessary to improve the meat quality. Some techniques have disadvantages such as being time-consuming or damage to the meat quality indicators. In such cases, it is required to use new technologies with minimal damage to the product (Xiong *et al.*, 2012).

Ultrasound is an innovative technology with applications in food industry. In this technique, the sound waves are applied to the frequencies higher than those of which the human ears are capable of hearing (20 kHz) (Alarcon-Rojo *et al.*, 2015). This process causes condensation and expansion of the particles in the environment and thereby creating of voids or bubbles. These voids grow during ultrasound cycles and eventually become unstable and shatter and release high temperature and pressure. The bubble shattering affects biological materials in micro and macro scales (Alarcon-Rojo *et al.*, 2015).

In the meat industry, the ultrasound technology is currently applied as a fast alternative technique, relatively inexpensive, simple, and reliable to improve meat quality

1 and 2. PhD student and Associate Professor, Department of Food Science and Technology, Sari Agricultural Sciences and Natural Resources University, Sari, Iran.

(\*-Corresponding Author: reza\_kenari@yahoo.com)

DOI: 10.22067/ifst.v1396i13.63782

criteria, such as tenderness, extraction of proteins and gelatin. It can also help to create the texture in the meat products, reduce the salt, and enhance the curing process (Turantaş *et al.*, 2015).

Brining is an old preserving and processing method of meat in which meat was cut out into pieces and put in a salt solution. This process improved durability, flavor, juiciness and tenderness of meat products. The salt release occurred slowly in the meat matrices, but can be improved by injection. However, in these circumstances, the products have lower quality. It is observed that permeability of muscle texture increases with ultrasound, thereby it can be used to enhance the penetration of salt used in brining process (Leal-Ramos *et al.*, 2011).

Studies have been published on the use of low-frequency ultrasound in order to tenderize meat. Jayasooriya *et al.* (2007) investigated the effects of ultrasonic treatment (24 kHz, Wcm-2 12 and a maximum of 4 minutes) on the qualitative properties of beef muscle in the brine. Based on their results, ultrasound leads to a reduced hardness and an increased brittleness and pH of the meat. Ultrasound treatment had no effect on color parameters (L\*, a\*, b\*, Chroma, hue); however it increases the cooking loss and also the total loss. Siró *et al.* (2009) examined three brining methods of static conduction, under vacuum conduction and low-frequency ultrasound (20 kHz and extremely Wcm<sup>-2</sup> 2-4) to the curing process of pork lower back muscles with salt (at 5 °C). They reported that WBC parameter and textural characteristics are more improved by ultrasound in comparison with the other two treatments. The chewiness reduces based on the results of the ultrasound treatment and consequently the brittleness increases. In general, the lower sound intensities were more effective. The Ultrasound treatment significantly results in increased penetration index of salt compared to the brining under static conditions. It was also shown that the penetration rate increases randomly with increasing the ultrasound intensity.

Several studies indicated the significant and

profound impact of polyphosphate in small amounts on the juiciness and tenderness of the meat. A reduction in the curing quality loss was also reported which leads to extensive use of polyphosphate (often combined with salt) in the processed meat production and minced meat products such as burgers and sausages (Sheard *et al.*, 1999).

This study aiming at determining the effects of ultrasound bath (at a frequency of 37 kHz) and probes (20 kHz) combined with brine solution (40 gr/L of water) and polyphosphate (20 gr/L of water) for 20, 25 and 30 minutes at 30, 40 and 50°C on the qualitative characteristics of meat was conducted. To the best of our knowledge, no study on using ultrasound combined to polyphosphates for meat products has been conducted.

## Materials and Methods

### Meat production and preparation of samples

Beef meat (Flank area) was purchased from the local market (Sari, Iran) (48 hours after slaughter). Three meat samples with the weight of 50 grams were prepared from the central parts of the flank muscle (preferably without fat) in the same shape and dimensions (length, width and thickness of 50, 30 and 10 mm, respectively) with the help of a sharp knife. The samples were covered with waterproof coatings and kept at 4°C until the time of testing (Ozuna *et al.*, 2013).

### Prepare salt water solution and a solution containing salt and polyphosphate

A solution of brine was prepared by dissolving 40 grams of salt in one liter of distilled water. Also, the solution mixture of brine-polyphosphate was prepared by dissolving 20 grams of NaCl and 20 grams of polyphosphate in one liter of distilled water. The ratio of meat to the solutions for all mixtures was 10 : 1 (w/w) (Siró *et al.*, 2009).

### Ultrasound treatment

The meat samples were subjected to ultrasound and placed in the brine based on two methods of bath and probe for 20, 25 and

30 minutes at 30, 40 and 50°C. In the probe method, an ultrasound cell disruptor (Model KS-250F, China, Ningbo Zhejiang) was used with a frequency of 20 kHz, amplitude of 45% and a power of 250 watts. For bath method Elma Ultrasonic cleaning device (model S 30 H, Germany) was used with a frequency of 37 kHz and a power of 280 watts. Untreated meat sample was considered as a control. After the ultrasound, the pieces of meat were wrapped in a filter paper, dried and packed until analyses at 4 °C (Chang *et al.*, 2012).

#### Measuring pH:

PH of the samples was measured with the digital pH meter electrode penetration PB 11 (Sartorius, Germany).

#### Water-holding capacity (WHC)

WHC was measured based on pressing the filter paper method for 24 hours after the treatment. For this purpose, small pieces of meat (2 g) were cut from the samples and were pressed on a filter paper (Whatman No. 1) with the means of a 2 kg lifting weight for 5 minutes. Then, WHC percentage was calculated by the following equation (1):

$$\%WHC = \frac{W_{ap}}{W_{bp}} \times 100 \quad (1)$$

Where  $W_{ap}$  is the sample weight after pressing and  $W_{bp}$  is the sample weight before pressing (Savadkoohi *et al.*, 2014).

#### Water binding capacity (WBC)

WBC for 50 g of the samples was calculated immediately after soaking them in brine by the following equation (2):

$$\%WBC = \frac{m_{brine} - m_{brine0}}{m_{brine0}} \times 100 \quad (2)$$

Where  $m_{brine0}$  is the initial brine solution weight and  $m_{brine}$  is the brine solution weight after treatment (Siró *et al.*, 2009). The control sample of WBC was calculated according to the above formula based on static brining at 30°C and 20 minutes.

#### Drip loss

The drip loss of meat sample was determined 7 days after ultrasound treatment (stored at -18°C). For this purpose, after removing the samples from inside of the package, thawing process was performed at a temperature of 20°C, then the samples were dried completely with filter paper and drip loss percentage was calculated by the equation 3 (Xiong *et al.*, 2012):

$$\%Drip\ loss = \frac{Initial\ weight - Drip\ weight}{Initial\ weight} \times 100 \quad (3)$$

#### Cooking loss (curing loss)

To determine the amount of cooking loss, the samples were thawed in a warm water bath (Ben Murray) to perform the baking operation at 80 °C. The cooking operations continued for 30 minutes, and the surface of the cooked meat was then well dried with filter paper and weighed. Cooking loss percentage was calculated according to the following equation (Xiong *et al.*, 2012):

$$\%Cook\ loss = \frac{Drip\ weight - Cook\ weight}{Drip\ weight} \times 100 \quad (4)$$

#### Texture profile analysis (TPA)

To study the changes resulting from the ultrasound on the textural characteristics of the samples, texture profile analysis (TPA) was conducted by Brookfield CT3 Texture Analyzer (Brookfield Engineering Laboratories, USA) during the compression cycle of the cylindrical probe (diameter 10 mm) to 40% of the original thickness. The pre-test speed, speed test and returning speed was 1 mm/minute, 2 mm and 100 mm/minute, respectively. The texture qualitative characteristics were evaluated as Hardness; Resilience; Cohesiveness; Adhesiveness, Springiness; Chewiness (Jayasooriya *et al.*, 2007).

#### Statistical analysis

All experiments were carried out in triplicate and presented as a mean  $\pm$  standard deviation. Analysis of variance (ANOVA) of samples followed by Duncan test was carried out at the significant level of  $p < 0.05$  by SAS

software (version 9, SAS Institute).

## Results and Discussion

### The effects of ultrasound treatment on pH

pH as the most important quality parameters of meat, has a direct impact on many technological properties such as WHC, WBC and the meat quality (tenderness). For example, the amount of water within the muscle tissue is dependent on the available space between actin fibers, which depends on pH. In general, higher and lower pH value of the isoelectric point would greatly increase WHC of meat. However, the role of pH levels above the isoelectric point is more considerable. A decrease in the pH value of the isoelectric point causes a WHC decrease in the meat.

At the complex actomyosin isoelectric point (with a pH value of 2.5) most groups of COOH are in form of COO<sup>-</sup> anions and most groups of NH<sup>2</sup> are in form of NH<sup>3+</sup>. In this case, the positive and negative ions attract each other and a tightly bound protein molecule will be created with a net charge of zero. As a result, only a very small amount of water can be attached to the protein. The increase of both positive and negative charged groups in the protein molecule by creating more space between protein molecules leads to an increase in the WHC. When the negative charge is higher than the positive charge, pH values will also be higher than the isoelectric point of the protein; therefore WHC increased (Feiner, 2006).

Fig. 1, shows the effects of different temperatures and times of ultrasound treatment on the pH of beef in a brine solution (Fig. 1a) and brine and polyphosphate solution (Fig. 1b).

As can be seen in Fig. 1, generally, with increasing temperature and ultrasound treatment time, a significant increase in the pH was observed ( $p < 0.05$ ). Meat pH increase as a result of the ultrasound treatment can vary because of several different mechanisms. The main mechanisms can be the damage of cell structure, the release of ions into the cytosol, and the covering of the hidden acidic group by

the protein strands. As a result of heat and high pressure in the cavitation, meat proteins are partially denatured, which lead to hiding acid groups in the field of protein and consequently an increase in the pH. With increasing temperature caused by converting ultrasound energy to heat, an increase in pH was observed (Jayasooriya *et al.*, 2007). Jayasooriya *et al.* (2007) also reported that ultrasound treatment with increasing of time from 25 to 250 seconds (24 kHz, Wcm-2 12 and room temperature) was able to increase the pH of beef. Ma & Ledward (2004) evaluated the effects of high pressure (200-800 MPa) at different temperatures (20–70°C) for 20 min on post-rigor beef. They reported an increase in the pH of beef muscle, which may be related to heat and pressure generated by the ultrasound cavitation phenomenon. They also reported that with increasing temperature to 40, 60 and 80 °C, pH value increases to 0.60, 0.11 and 0.14, respectively.

Some studies reported no significant change in meat pH as a result of ultrasound treatment which is different from the present results. It can be explained by different ultrasound treatment conditions (Dolatowski *et al.*, 2007). Dolatowski & Stadnik (2007) demonstrated no significant difference between beef meat treated with ultrasound (frequency 45 kHz, power 2 W/cm<sup>2</sup>, 120 seconds at 4 °C) and the meat stored for 72 and 96 hours. They reported no significant difference between the pH of beef meat treated with ultrasound 24, 72 and 96 hours after rigor mortis. This is most likely due to different ultrasound conditions applied such as frequency, power and especially the temperature.

As can be seen in Fig. 1, generally, with increasing temperature and ultrasound treatment time, a significant increase in the pH was observed ( $p < 0.05$ ). Meat pH increase as a result of the ultrasound treatment can vary because of several different mechanisms. The main mechanisms can be the damage of cell structure, the release of ions into the cytosol, and the covering of the hidden acidic group by the protein strands. As a result of heat and high pressure in the cavitation, meat proteins are

partially denatured, which lead to hiding acid groups in the field of protein and consequently an increase in the pH. With increasing temperature caused by converting ultrasound energy to heat, an increase in pH was observed (Jayasooriya *et al.*, 2007). Jayasooriya *et al.* (2007) also reported that ultrasound treatment with increasing of time from 25 to 250 seconds (24 kHz, Wcm-2 12 and room temperature) was able to increase the pH of beef. Ma & Ledward (2004) evaluated the effects of high pressure (200-800 MPa) at different temperatures (20–70°C) for 20 min on post-rigor beef. They reported an increase in the pH of beef muscle, which may be related to heat and pressure generated by the ultrasound cavitation phenomenon. They also reported that with increasing temperature to 40, 60 and 80 °C, pH value increases to 0.60, 0.11 and 0.14, respectively.

Some studies reported no significant change in meat pH as a result of ultrasound treatment which is different from the present results. It can be explained by different ultrasound treatment conditions (Dolatowski *et al.*, 2007). Dolatowski & Stadnik (2007) demonstrated no significant difference between beef meat treated with ultrasound (frequency 45 kHz, power 2 W/cm<sup>2</sup>, 120 seconds at 4 °C) and the meat stored for 72 and 96 hours. They reported no significant difference between the pH of beef meat treated with ultrasound 24, 72 and 96 hours after rigor mortis. This is most likely due to different ultrasound conditions applied such as frequency, power and especially the temperature.

As can be seen in Fig. 1, generally, with increasing temperature and ultrasound treatment time, a significant increase in the pH was observed ( $p < 0.05$ ). Meat pH increase as a result of the ultrasound treatment can vary because of several different mechanisms. The main mechanisms can be the damage of cell structure, the release of ions into the cytosol, and the covering of the hidden acidic group by the protein strands. As a result of heat and high pressure in the cavitation, meat proteins are

partially denatured, which lead to hiding acid groups in the field of protein and consequently an increase in the pH. With increasing temperature caused by converting ultrasound energy to heat, an increase in pH was observed (Jayasooriya *et al.*, 2007). Jayasooriya *et al.* (2007) also reported that ultrasound treatment with increasing of time from 25 to 250 seconds (24 kHz, Wcm-2 12 and room temperature) was able to increase the pH of beef. Ma & Ledward (2004) evaluated the effects of high pressure (200-800 MPa) at different temperatures (20–70°C) for 20 min on post-rigor beef. They reported an increase in the pH of beef muscle, which may be related to heat and pressure generated by the ultrasound cavitation phenomenon. They also reported that with increasing temperature to 40, 60 and 80 °C, pH value increases to 0.60, 0.11 and 0.14, respectively.

Some studies reported no significant change in meat pH as a result of ultrasound treatment which is different from the present results. It can be explained by different ultrasound treatment conditions (Dolatowski *et al.*, 2007). Dolatowski & Stadnik (2007) demonstrated no significant difference between beef meat treated with ultrasound (frequency 45 kHz, power 2 W/cm<sup>2</sup>, 120 seconds at 4 °C) and the meat stored for 72 and 96 hours. They reported no significant difference between the pH of beef meat treated with ultrasound 24, 72 and 96 hours after rigor mortis. This is most likely due to different ultrasound conditions applied such as frequency, power and especially the temperature.

As can be seen in Fig. 1, generally, the treated samples with a brine-polyphosphate solution has a higher pH than those of brine solution ( $p < 0.05$ ). Almost all kinds of phosphates and phosphate mixtures used in the meat industry (alkaline and alkaline phosphatase) leads to an increase the pH value in meat. The increase of pH causes an increase of electrostatic repulsion between actin and myosin and therefore WHC and WBC increased (Feiner, 2006).

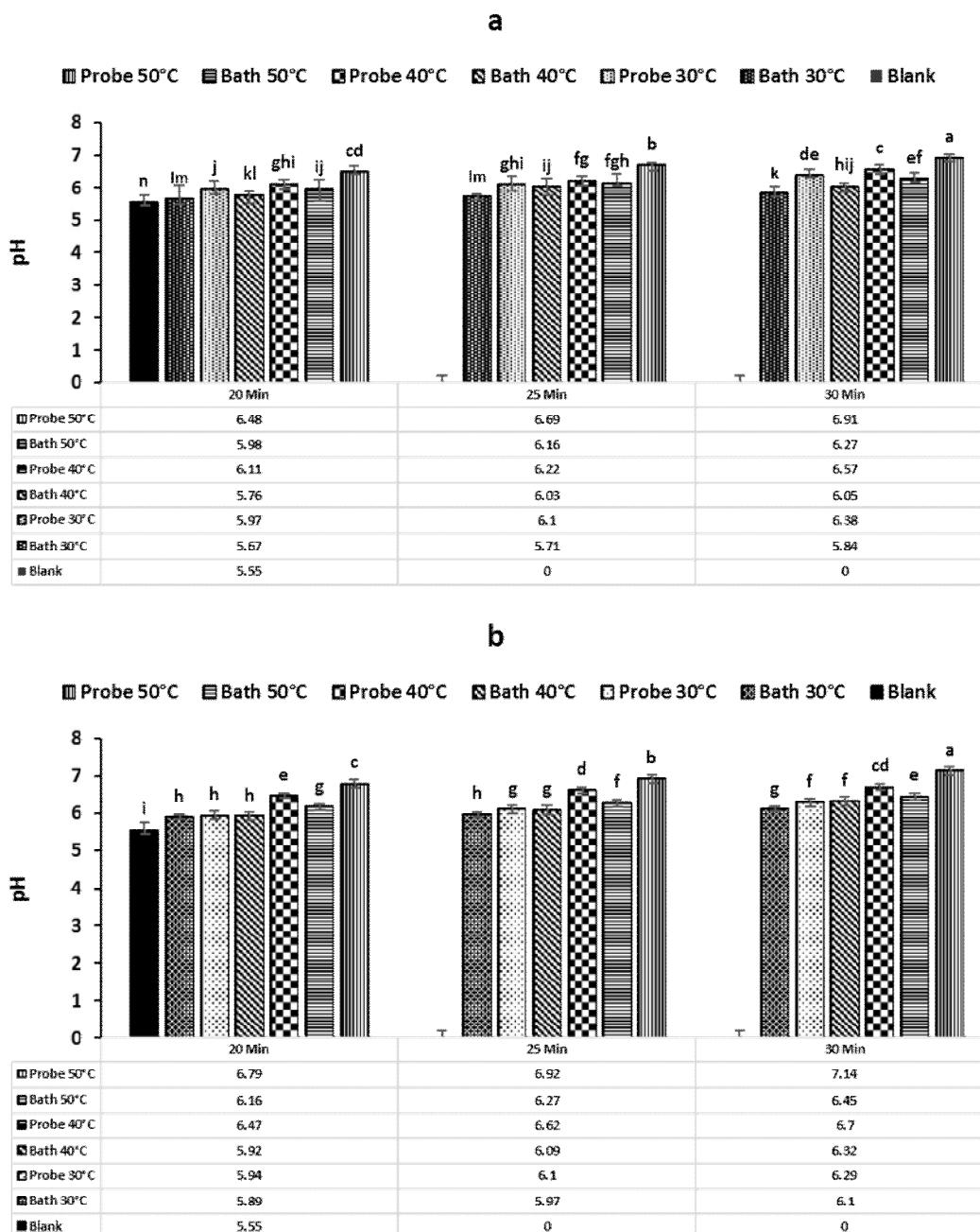


Fig. 1. The effect of ultrasound on the pH of beef meat treated in a solution of brine (a) treated with a mixed solution of brine and polyphosphate (b).

Sheard *et al.* (1999) injected an aqueous solution of polyphosphate (3 and 5%) into pork. The results showed that injection of an aqueous solution of polyphosphate leads to significant increase in meat pH. They also stated that pH increased proportionally by

increasing polyphosphates in meat.

The increase in meat pH as a result of ultrasound can have important potential implications in meat tenderness. The optimal pH of the protease-cathepsin system is relatively acidic. Hence, it can be expected

that the ultrasound treatment with an increase in pH and thus an increase in the activity of protease calpain system, will enhance meat tenderization (Jayasooriya *et al.*, 2007).

#### The effects of ultrasound treatment on water holding capacity (WHC) and water binding capacity (WBC) of meat

WHC is a term used to describe the ability of a muscle to hold water within a set of conditions (such as cutting, pressing, packing, baking, heat treatment, etc.). WHC is relevant to some sensory characteristics of meat, such as juiciness, texture and flavor. In general, it has been proven that the forces led to retention of free water in the structure of the muscle or meat products are a kind of surface tension (Siró *et al.*, 2009; Cheng & Sun, 2008).

WHC increases after rigor mortis and relative decomposition of Actomyosin proteins. Meat sonication after slaughter or during rigor mortis can be a useful technique to modify water-protein interactions (Ahmed *et al.*, 2009).

Tables 1 and 2 showed the WHC amounts of the control samples and the treated meat with ultrasound in a brine solution and brine-polyphosphate solution, respectively. The amount of WHC in control was found to be 22.00%. In general, ultrasound treatment caused a significant increase in WHC compared to the control ( $p < 0.05$ ). The WHC amount of treated samples with ultrasound was in the range of 13.27 to 38.15 % (Tables 1 and 2). As can be seen in Tables 1 and 2, with the temperature increase of ultrasound from 30 to 50 °C, WHC significantly declines. WHC of the treatments conducted at 50°C was lower than that of the control ( $p < 0.05$ ). Also, at all experiment conditions, with increasing ultrasound treatment time, WHC decreased significantly ( $p < 0.05$ ). The reason for these results is related to meat protein denaturation in higher ultrasound time and also an increased temperature which can reduce the ability of meat to hold water.

**Table 1. Water holding capacity (WHC), water binding capacity (WBC), drip loss and cooking loss of beef meat treated with ultrasound in a solution of brine**

Type ultrasound	WHC (%)	WBC (%)	Drip Loss (%)	Cooking Loos (%)	
Bath	20 min, 30 °C	28.11±1.22 <sup>c</sup>	16.84±1.42 <sup>b</sup>	4.96±0.24 <sup>q</sup>	19.24±1.18 <sup>o</sup>
	20 min, 40 °C	26.04±2.35 <sup>g</sup>	10.96±0.60 <sup>i</sup>	7.25±0.35 <sup>m</sup>	20.58±0.32 <sup>k</sup>
	20 min, 50 °C	23.26±2.17 <sup>j</sup>	8.72±1.23 <sup>m</sup>	8.22±0.17 <sup>k</sup>	21.68±1.23 <sup>i</sup>
	25 min, 30 °C	27.96±2.11 <sup>d</sup>	12.80±1.31 <sup>g</sup>	6.52±0.42 <sup>n</sup>	20.45±0.99 <sup>l</sup>
	25 min, 40 °C	24.33±1.24 <sup>i</sup>	9.66±0.22 <sup>k</sup>	9.13±0.08 <sup>h</sup>	21.86±0.35 <sup>h</sup>
	25 min, 50 °C	18.97±1.31 <sup>m</sup>	7.89±0.85 <sup>n</sup>	10.18±0.10 <sup>f</sup>	22.90±0.65 <sup>f</sup>
	30 min, 30 °C	26.77±1.33 <sup>e</sup>	11.47±0.52 <sup>h</sup>	8.75±0.51 <sup>j</sup>	21.88±0.34 <sup>h</sup>
	30 min, 40 °C	22.40±0.62 <sup>k</sup>	9.07±1.40 <sup>l</sup>	10.95±0.47 <sup>d</sup>	23.25±0.26 <sup>e</sup>
30 min, 50 °C	16.76±1.40 <sup>o</sup>	6.15±1.50 <sup>q</sup>	11.27±1.32 <sup>c</sup>	24.85±0.63 <sup>c</sup>	
Probe	20 min, 30 °C	31.97±1.42 <sup>a</sup>	20.37±2.12 <sup>a</sup>	3.88±0.50 <sup>r</sup>	18.15±0.11 <sup>p</sup>
	20 min, 40 °C	26.42±2.20 <sup>f</sup>	14.41±1.62 <sup>d</sup>	5.84±0.33 <sup>o</sup>	19.52±0.24 <sup>m</sup>
	20 min, 50 °C	22.16±1.42 <sup>l</sup>	7.22±0.13 <sup>o</sup>	8.93±0.17 <sup>i</sup>	22.82±1.19 <sup>f</sup>
	25 min, 30 °C	29.27±2.16 <sup>b</sup>	16.56±0.71 <sup>c</sup>	5.45±0.16 <sup>p</sup>	19.33±0.40 <sup>n</sup>
	25 min, 40 °C	25.04±2.15 <sup>h</sup>	12.89±0.46 <sup>f</sup>	7.71±0.51 <sup>l</sup>	20.74±0.53 <sup>j</sup>
	25 min, 50 °C	17.62±1.33 <sup>n</sup>	6.48±0.33 <sup>p</sup>	10.82±1.30 <sup>e</sup>	24.00±0.60 <sup>d</sup>
	30 min, 30 °C	26.47±1.21 <sup>f</sup>	14.11±1.23 <sup>e</sup>	7.66±0.23 <sup>l</sup>	20.76±1.21 <sup>k</sup>
	30 min, 40 °C	23.35±1.16 <sup>j</sup>	10.62±1.34 <sup>i</sup>	9.46±0.25 <sup>g</sup>	22.15±0.44 <sup>g</sup>
30 min, 50 °C	13.27±0.51 <sup>p</sup>	5.73±0.50 <sup>r</sup>	12.03±1.13 <sup>b</sup>	25.32±0.21 <sup>b</sup>	
Untreated samples	20.00±1.70 <sup>l</sup>	12.63±1.53 <sup>g</sup>	12.50±1.42 <sup>a</sup>	26.70±1.02 <sup>a</sup>	

Average values (n= ±3) standard deviation, Different letters indicate significant differences in each column ( $p < 0.05$ ).

**Table 2. Water holding capacity (WHC), water binding capacity (WBC), drip loss and cooking loss of beef meat treated with ultrasound in a mixture solution of brine-polyphosphate**

Type ultrasound	WHC (%)	WBC (%)	Drip Loss (%)	Cooking Loos (%)	
Bath	20 min, 30 °C	35.02±0.33 <sup>b</sup>	24.97±1.71 <sup>e</sup>	4.02±0.31 <sup>p</sup>	17.57±0.24 <sup>l</sup>
	20 min, 40 °C	32.65±0.20 <sup>e</sup>	19.23±1.20 <sup>k</sup>	6.24±0.25 <sup>l</sup>	19.04±0.32 <sup>i</sup>
	20 min, 50 °C	26.10±0.15 <sup>m</sup>	13.48±1.22 <sup>o</sup>	7.12±0.27 <sup>i</sup>	19.96±0.30 <sup>h</sup>
	25 min, 30 °C	33.32±0.26 <sup>d</sup>	23.15±2.10 <sup>g</sup>	5.60±0.40 <sup>m</sup>	18.84±1.19 <sup>j</sup>
	25 min, 40 °C	29.79±0.16 <sup>i</sup>	17.08±1.30 <sup>l</sup>	7.77±0.19 <sup>h</sup>	20.31±0.05 <sup>g</sup>
	25 min, 50 °C	32.87±0.19 <sup>o</sup>	11.20±0.15 <sup>q</sup>	8.89±0.15 <sup>f</sup>	21.35±1.17 <sup>f</sup>
	30 min, 30 °C	32.15±0.33 <sup>f</sup>	21.32±1.23 <sup>i</sup>	7.83±0.32 <sup>h</sup>	20.33±1.14 <sup>g</sup>
	30 min, 40 °C	26.97±0.21 <sup>k</sup>	15.19±0.44 <sup>n</sup>	10.03±0.26 <sup>d</sup>	21.84±0.34 <sup>p</sup>
	30 min, 50 °C	19.89±0.53 <sup>f</sup>	9.70±1.22 <sup>r</sup>	10.16±0.30 <sup>c</sup>	22.06±2.19 <sup>d</sup>
Probe	20 min, 30 °C	38.15±0.11 <sup>a</sup>	31.65±1.35 <sup>a</sup>	3.21±0.20 <sup>q</sup>	16.46±0.31 <sup>m</sup>
	20 min, 40 °C	31.77±0.09 <sup>g</sup>	26.84±1.40 <sup>c</sup>	5.18±0.13 <sup>n</sup>	17.82±1.13 <sup>k</sup>
	20 min, 50 °C	26.64±0.23 <sup>n</sup>	20.61±1.23 <sup>j</sup>	8.23±0.31 <sup>g</sup>	21.22±0.88 <sup>f</sup>
	25 min, 30 °C	33.70±0.36 <sup>c</sup>	27.24±2.64 <sup>b</sup>	4.78±0.26 <sup>o</sup>	17.69±0.52 <sup>jl</sup>
	25 min, 40 °C	28.75±0.15 <sup>j</sup>	23.77±1.55 <sup>f</sup>	6.83±0.41 <sup>k</sup>	19.12±1.20 <sup>i</sup>
	25 min, 50 °C	20.83±0.19 <sup>p</sup>	17.05±1.30 <sup>l</sup>	10.05±0.10 <sup>d</sup>	22.44±0.20 <sup>c</sup>
	30 min, 30 °C	31.24±0.21 <sup>h</sup>	25.76±1.28 <sup>d</sup>	6.95±0.25 <sup>k</sup>	19.03±1.23 <sup>i</sup>
	30 min, 40 °C	26.20±0.18 <sup>l</sup>	22.08±1.15 <sup>h</sup>	9.13±0.14 <sup>e</sup>	20.38±0.14 <sup>g</sup>
	30 min, 50 °C	16.55±0.20 <sup>s</sup>	15.35±1.16 <sup>m</sup>	11.31±0.23 <sup>b</sup>	23.95±0.80 <sup>b</sup>
Untreated samples	20.00±1.70 <sup>q</sup>	12.63±1.53 <sup>p</sup>	12.50±1.42 <sup>a</sup>	26.70±1.02 <sup>a</sup>	

Average values (n= ±3) standard deviation, Different letters indicate significant differences in each column (p<0.05).

In the meantime, the treated samples by ultrasound probe at 30 and 40°C have greater WHC in comparison with samples treated with ultrasound bath (p<0.05). However, samples treated by ultrasound probe at 50°C, have less WHC than samples treated with ultrasonic bath (at the same temperature and time). This finding could be related to the more damaging impact of ultrasound probes on meat protein and also more denaturation compared to ultrasonic bath treatment at 50°C. In general, it can be stated that maximum WHC was obtained during 20 minutes at 30°C by the ultrasound probe (38.15 %). Diluted brine solution (up to 5 % salt) leads to improvement of water absorption and swelling of the meat proteins by increasing similar loads in myofibrillar proteins. This phenomenon is called salting-in (Feiner, 2006). Data indicate that ultrasound treatment can lead to an increase the distribution of salt and thus accelerating the process of brining and the uniform distribution of salt in meat which also helps to increase the WHC and WBC of the meat (Siró *et al.*, 2009). Recently, Inguglia *et al.* (2017) investigated the effect of geometric parameters of the ultrasound instrument during

meat salting in order to enhance salt diffusion and salt distribution in pork meat on a lab scale. They investigated the effects of probe size (Ø 2.5 and 1.3 cm) and of different distances between the transducer and the meat sample (0.3, 0.5, and 0.8 cm) on NaCl diffusion. Their results showed that 0.3 cm was the most efficient distance between the probe and the sample to ensure a higher salt diffusion rate. A distance of 0.5 cm was considered as trade-off distance to ensure salt diffusion and maintenance of meat quality parameters. The enhancement of salt diffusion by ultrasound was observed to be decreased with increasing horizontal distance from the probe.

Polyphosphate has a wide applications in the meat industry. The polyphosphate disturbs the actin and myosin complex through a decrease in electrostatic force, which leads to an increase the solubility and water absorption of meat. The separation of actin and myosin is due to the connection of negative charged phosphate ions with the positive ions of Mg<sup>+2</sup> and Ca<sup>+2</sup>, because the positive ions of Mg<sup>+2</sup> and Ca<sup>+2</sup> have a vital role in muscle contraction (Feiner, 2006).

Pohlman *et al.* (1997) reported that during the ultrasound treatment of meat with a water bath at refrigerator temperature, the ultrasound intensity increase did not cause the WHC to change. They stated that the reason for no dramatic change in WHC is connected to the lack of meat thermal denaturation due to low temperature applied in the experiment.

Siró *et al.* (2009) reported that with respect to WHC, there is no significant difference between the static brining and brining treated with ultrasound (20 kHz, 2-2 Wcm<sup>-2</sup>, 30 to 180 minutes and at a temperature of 4°C). They also reported that the intensity and ultrasound treatment did not affect the WHC; which can be attributed to the low temperature used in this research.

WBC is one of the very important quality parameters during the production of meat. Indeed, WBC represents the ability of connection and absorption of water. It is known that soluble proteins in salt like actin and myosin have better emulsifying properties and have higher WBC than water-soluble proteins. The importance of increasing WBC in meat products is because of the improvement in the sensory quality of the final product in addition to creating more affordable products (Feiner, 2006).

The WBC of control sample during the static brining was 12.63 % for 20 minutes at a temperature of 30 °C. The WBC of treated meat with ultrasound can be seen in Tables 1 and 2 for brine and a mixture of brine-polyphosphate solutions, respectively. In general, it can be stated that the effect of ultrasound treatment on WBC was similar to that of WHC. Ultrasound treatment significantly increased WBC compared to the control sample ( $p < 0.05$ ). The WBC amounts of treated samples with ultrasound were in the range of 5.73 to 31.65 % (Tables 1 and 2). Similar to the result reported for WHC, by increasing the ultrasound treatment temperature from 30 to 50°C, WBC was significantly decreased. However, the WBC of all treatments was more than the control sample ( $p < 0.05$ ).

With increasing the time of ultrasound

treatment in all test conditions, WBC significantly reduced ( $p < 0.05$ ), as reported for WHC. The decrease of WBC with increasing temperature and time can be attributed to meat protein denaturation. The denaturation of proteins leads to the opening of proteins and increasing of the surface of hydrophobic groups and therefore reducing WBC of meat (Feiner, 2006).

At 30 to 40°C and the same treating time, the treated samples by probe ultrasound had greater WBC than those samples treated with bath ultrasound ( $p < 0.05$ ). However, samples treated by probe ultrasound at 50°C, have less WBC than those of bath ultrasound (at the same treating time). In fact, the ultrasound probe due to exert higher power than the bath ultrasound can be more effective on the meat texture and consequently the salt and polyphosphate penetrate more greatly into meat. However, the ultrasound probe at higher temperatures intensifies the effects of heat on meat protein denaturation and thus decreasing the WBC. As reported for WHC, the highest amount of WBC was found to be 31.65 % for probe ultrasound (20 minutes at 30°C).

Siró *et al.* (2009) reported that brining under ultrasound treatment leads to more effectively improve WBC and increase penetration coefficient of sodium chloride, than static brining and soaking into the brine solution. They reported that ultrasound treatment is able to increase the distance between the fibers because of charging of membrane myofibril proteins.

#### **The effects of ultrasound treatment on drip loss and cooking loss of meat:**

The amount of drip and cooking loss of control and ultrasound treated samples in brine and brine-polyphosphate are shown in Tables 1 and 2, respectively. Drip and cooking loss of control samples were 12.5 and 26.70 %, respectively. Drip and cooking loss of samples treated with ultrasound was in the range of 3.21-12.03 % and 16.46-25.32 %, respectively. There is a close relationship between WHC and WBC results with drip and cooking loss in such a way that the higher WHC and WBC of

samples showed lower drip and cooking loss. As can be seen in Tables 1 and 2, generally, applying ultrasound reduces drip and cooking loss ( $p < 0.05$ ). With increasing time and temperature of ultrasound treatment, an increase in drip and cooking loss were observed. The reason for this phenomenon could be explained by denaturation the meat myofibrillar proteins which led to a reduction in the meat WHC and WBC.

Ojha *et al.* (2016) investigated the effect of a combined sonication (at power levels of 9.0 and 54.9 W cm<sup>-2</sup> for 120 min) and 5 % NaCl on the cooking loss of pork meat. They reported a reduction in cooking losses with an increase in brining time. They also reported that samples treated with ultrasound had lower cook loss than the control sample which might be due to an increase in the sodium content in pork samples.

#### The effects of ultrasound treatment on the meat texture

The texture is one of the most important organoleptic characteristics of meat which is related to brittleness and mouthfeel. Meat textures depend on factors such as tenderness, WHC or the juiciness as well as the level of meat ripeness and animal age (amount and

quality of the connective texture). Texture profile analysis (TPA) is a very important indicator for determining the changes in meat texture (Xiong *et al.*, 2012; Chang *et al.*, 2012).

TPA parameters (hardness, resilience, adhesion, cohesion, springiness and potential for chewing) of the control sample and meat treated with ultrasound in brine and a brine-polyphosphate solution are mentioned in Tables 3 and 4, respectively.

Hardness represents the amount of force necessary to achieve the desired deformation in the sample. The hardness of control samples, the samples treated with ultrasound in brine and a mixture of brine-polyphosphate solution were in the range of 77.93 N, 18.24-48.87 N and 12.37-42.49 N, respectively (Tables 3 and 4). Ultrasound treatment at higher temperatures leads to reduce the meat hardness ( $p < 0.05$ ). This most likely due to the more meat proteins denaturation at further temperatures and times. Siró *et al.* (2009) reported that higher intensity of ultrasound treatment led to denaturation of proteins and consequently a reduction in the WHC and hardness of meat.

**Table 3. Parameters of texture samples treated with ultrasound in a solution of brine**

Type ultrasound	TPA parameters						
	Hardness (N)	Resilience	Adhesiveness (mJ)	Cohesiveness	Springiness (mm)	Chewiness (mJ)	
Bath	20 min, 30 °C	20.98±4.33 <sup>p</sup>	0.20±0.01 <sup>bc</sup>	0.90±0.11 <sup>c</sup>	0.51±0.12 <sup>bcd</sup>	5.78±0.32 <sup>g</sup>	61.60±6.24 <sup>m</sup>
	20 min, 40 °C	29.90±3.20 <sup>h</sup>	0.22±0.06 <sup>b</sup>	1.10±0.25 <sup>b</sup>	0.50±0.03 <sup>bcd</sup>	5.06±0.23 <sup>k</sup>	75.20±7.32 <sup>j</sup>
	20 min, 50 °C	45.05±5.15 <sup>d</sup>	0.18±0.04 <sup>bcd</sup>	0.40±0.17 <sup>c</sup>	0.48±0.02 <sup>bcd</sup>	5.48±0.27 <sup>i</sup>	119.30±4.31 <sup>e</sup>
	25 min, 30 °C	22.62±1.26 <sup>l</sup>	0.23±0.05 <sup>b</sup>	0.20±0.06 <sup>f</sup>	0.54±0.10 <sup>bc</sup>	6.68±0.44 <sup>a</sup>	81.60±5.19 <sup>h</sup>
	25 min, 40 °C	33.04±2.16 <sup>f</sup>	0.23±0.04 <sup>b</sup>	1.00±0.19 <sup>bc</sup>	0.56±0.30 <sup>ab</sup>	6.03±0.19 <sup>f</sup>	111.70±6.05 <sup>f</sup>
	25 min, 50 °C	48.32±5.19 <sup>c</sup>	0.23±0.06 <sup>b</sup>	0.10±0.15 <sup>fg</sup>	0.48±0.15 <sup>bcd</sup>	6.28±0.17 <sup>cd</sup>	145.80±2.18 <sup>e</sup>
	30 min, 30 °C	28.79±2.33 <sup>i</sup>	0.18±0.03 <sup>bcd</sup>	0.90±0.22 <sup>c</sup>	0.42±0.23 <sup>def</sup>	6.44±0.30 <sup>b</sup>	77.30±5.14 <sup>i</sup>
	30 min, 40 °C	42.49±1.21 <sup>e</sup>	0.32±0.04 <sup>a</sup>	0.01±0.01 <sup>g</sup>	0.65±0.34 <sup>a</sup>	6.66±0.26 <sup>a</sup>	111.72±5.34 <sup>f</sup>
30 min, 50 °C	48.87±3.53 <sup>b</sup>	0.19±0.02 <sup>bcd</sup>	0.70±0.20 <sup>d</sup>	0.48±0.22 <sup>bcd</sup>	6.22±0.31 <sup>de</sup>	145.20±3.19 <sup>d</sup>	
Probe	20 min, 30 °C	18.24±1.11 <sup>q</sup>	0.23±0.04 <sup>b</sup>	0.20±0.20 <sup>f</sup>	0.47±0.15 <sup>bcd</sup>	5.66±0.23 <sup>h</sup>	48.60±3.31 <sup>p</sup>
	20 min, 40 °C	22.49±2.09 <sup>m</sup>	0.14±0.20 <sup>d</sup>	1.00±0.85 <sup>bc</sup>	0.36±0.06 <sup>ef</sup>	5.57±0.13 <sup>hi</sup>	45.00±2.13 <sup>q</sup>
	20 min, 50 °C	30.15±3.23 <sup>g</sup>	0.18±0.09 <sup>bcd</sup>	0.90±0.37 <sup>c</sup>	0.43±0.13 <sup>cdef</sup>	5.14±0.32 <sup>k</sup>	66.00±1.28 <sup>l</sup>
	25 min, 30 °C	20.67±1.36 <sup>p</sup>	0.15±0.10 <sup>cd</sup>	0.40±0.10 <sup>e</sup>	0.45±0.12 <sup>bcd</sup>	5.30±0.36 <sup>g</sup>	49.40±2.52 <sup>jo</sup>
	25 min, 40 °C	26.90±2.15 <sup>k</sup>	0.21±0.04 <sup>b</sup>	1.10±0.29 <sup>b</sup>	0.49±0.15 <sup>bcd</sup>	6.37±0.41 <sup>bc</sup>	84.10±2.20 <sup>g</sup>
	25 min, 50 °C	33.04±4.19 <sup>f</sup>	0.23±0.05 <sup>b</sup>	1.00±0.25 <sup>bc</sup>	0.56±0.30 <sup>ab</sup>	6.03±0.19 <sup>f</sup>	111.70±3.20 <sup>f</sup>
	30 min, 30 °C	21.96±1.21 <sup>n</sup>	0.23±0.03 <sup>b</sup>	0.40±0.32 <sup>e</sup>	0.43±0.28 <sup>cdef</sup>	6.15±0.25 <sup>e</sup>	57.60±1.23 <sup>n</sup>
	30 min, 40 °C	28.05±3.18 <sup>m</sup>	0.21±0.04 <sup>b</sup>	0.40±0.26 <sup>e</sup>	0.48±0.15 <sup>bcd</sup>	5.17±0.17 <sup>k</sup>	69.40±2.14 <sup>k</sup>
30 min, 50 °C	42.49±3.20 <sup>e</sup>	0.32±0.08 <sup>a</sup>	0.01±0.01 <sup>g</sup>	0.65±0.16 <sup>bcd</sup>	6.66±0.23 <sup>a</sup>	182.70±4.80 <sup>a</sup>	
Untreated samples	77.93±4.85 <sup>a</sup>	0.15±0.02 <sup>cd</sup>	1.60±0.27 <sup>a</sup>	0.33±0.02 <sup>f</sup>	6.48±0.67 <sup>b</sup>	164.70±3.06 <sup>b</sup>	

Average values (n= ±3) standard deviation, Different letters indicate significant differences in each column ( $p < 0.05$ ).

**Table 4. Parameters of texture samples treated with ultrasound in a mixture solution of brine-polyphosphate**

Type ultrasound		TPA parameters					
		Hardness (N)	Resilience	Adhesiveness (mJ)	Cohesiveness	Springiness (mm)	Chewiness (mJ)
Bath	20 min, 30 °C	16.75±0.32 <sup>p</sup>	0.19±0.01 <sup>cd</sup>	0.50±0.31 <sup>d</sup>	0.44±0.07 <sup>f</sup>	5.53±0.21 <sup>j</sup>	41.10±2.24 <sup>k</sup>
	20 min, 40 °C	20.99±0.27 <sup>l</sup>	0.20±0.03 <sup>cd</sup>	0.90±0.26 <sup>c</sup>	0.42±0.20 <sup>f</sup>	5.64±0.25 <sup>h</sup>	49.80±2.32 <sup>i</sup>
	20 min, 50 °C	28.95±0.15 <sup>e</sup>	0.22±0.02 <sup>cd</sup>	0.10±0.37 <sup>gh</sup>	0.50±0.22 <sup>def</sup>	9.79±0.67 <sup>a</sup>	143.00±5.30 <sup>k</sup>
	25 min, 30 °C	19.37±0.46 <sup>m</sup>	0.18±0.04 <sup>cd</sup>	0.10±0.42 <sup>sh</sup>	0.49±0.11 <sup>def</sup>	5.38±0.40 <sup>k</sup>	51.60±3.19 <sup>j</sup>
	25 min, 40 °C	24.24±0.56 <sup>h</sup>	0.17±0.05 <sup>d</sup>	0.20±0.19 <sup>fg</sup>	0.49±0.10 <sup>def</sup>	6.82±0.29 <sup>c</sup>	80.90±3.05 <sup>de</sup>
	25 min, 50 °C	30.15±0.19 <sup>c</sup>	0.18±0.05 <sup>cd</sup>	0.90±0.15 <sup>c</sup>	0.43±0.15 <sup>f</sup>	5.14±0.25 <sup>l</sup>	66.00±4.17 <sup>g</sup>
	30 min, 30 °C	22.21±0.13 <sup>j</sup>	0.33±0.03 <sup>a</sup>	0.10±0.32 <sup>sh</sup>	0.65±0.23 <sup>ab</sup>	5.72±0.42 <sup>h</sup>	82.40±2.14 <sup>d</sup>
	30 min, 40 °C	28.79±0.21 <sup>f</sup>	0.18±0.14 <sup>cd</sup>	0.90±0.20 <sup>c</sup>	0.42±0.34 <sup>fg</sup>	6.44±0.26 <sup>e</sup>	77.30±1.34 <sup>c</sup>
	30 min, 50 °C	42.49±0.53 <sup>b</sup>	0.32±0.05 <sup>ab</sup>	0.00±0.00 <sup>h</sup>	0.65±0.28 <sup>ab</sup>	6.66±0.34 <sup>d</sup>	182.70±2.19 <sup>a</sup>
	Probe	20 min, 30 °C	12.37±0.18 <sup>r</sup>	0.20±0.03 <sup>cd</sup>	0.30±0.31 <sup>ef</sup>	0.46±0.35 <sup>ef</sup>	7.97±0.20 <sup>b</sup>
20 min, 40 °C		17.38±0.09 <sup>n</sup>	0.28±0.03 <sup>abc</sup>	0.40±0.25 <sup>de</sup>	0.71±0.40 <sup>a</sup>	6.27±0.48 <sup>f</sup>	82.60±2.13 <sup>d</sup>
20 min, 50 °C		23.35±0.13 <sup>i</sup>	0.18±0.07 <sup>cd</sup>	0.20±0.27 <sup>fg</sup>	0.51±0.25 <sup>def</sup>	5.51±0.11 <sup>g</sup>	72.90±3.28 <sup>f</sup>
25 min, 30 °C		14.29±0.26 <sup>q</sup>	0.22±0.04 <sup>cd</sup>	0.10±0.40 <sup>sh</sup>	0.55±0.44 <sup>cde</sup>	6.09±0.26 <sup>g</sup>	48.00±2.52 <sup>ij</sup>
25 min, 40 °C		21.71±0.15 <sup>k</sup>	0.17±0.04 <sup>d</sup>	0.10±0.19 <sup>sh</sup>	0.47±0.25 <sup>def</sup>	5.63±0.47 <sup>hi</sup>	58.00±1.20 <sup>h</sup>
25 min, 50 °C		25.45±0.16 <sup>g</sup>	0.20±0.05 <sup>cd</sup>	0.50±0.15 <sup>d</sup>	0.51±0.30 <sup>def</sup>	5.00±0.16 <sup>m</sup>	64.60±4.00 <sup>g</sup>
30 min, 30 °C		16.97±0.21 <sup>o</sup>	0.17±0.03 <sup>d</sup>	0.40±0.32 <sup>de</sup>	0.44±0.29 <sup>f</sup>	4.36±0.25 <sup>k</sup>	32.60±2.23 <sup>l</sup>
30 min, 40 °C		23.35±0.19 <sup>i</sup>	0.18±0.04 <sup>cd</sup>	0.20±0.26 <sup>fg</sup>	0.57±0.15 <sup>bsd</sup>	5.51±0.24 <sup>g</sup>	72.90±4.14 <sup>f</sup>
30 min, 50 °C	29.81±0.22 <sup>d</sup>	0.23±0.02 <sup>cd</sup>	1.80±0.30 <sup>a</sup>	0.61±0.16 <sup>abc</sup>	6.89±0.33 <sup>c</sup>	125.40±6.80 <sup>c</sup>	
Untreated samples	77.93±4.85 <sup>a</sup>	0.15±0.02 <sup>d</sup>	1.60±0.27 <sup>b</sup>	0.33±0.02 <sup>g</sup>	6.48±0.67 <sup>e</sup>	164.70±3.06 <sup>b</sup>	

Average values (n= ±3) standard deviation, Different letters indicate significant differences in each column (p<0.05).

In general, samples treated with a brine-polyphosphate solution had a lower hardness in comparison with those of brine solution only. This is related to higher WHC and WBC of samples because the amounts of water attached to the meat make it softer (Cheng & Sun, 2008). Samples treated with probe ultrasound had a lower hardness than those of ultrasound bath, which attributed to the extremely damaging effect of the ultrasound probe on meat texture.

Resilience represents the capacity of a substance to store energy caused by stress in the linear elastic range. Higher resilience means that the substance has a higher resistance to permanent deformation (Chang *et al.*, 2012). According to Tables 3 and 4, the resilience of samples treated with ultrasound, in most cases was significantly increased compared to that of control samples (p<0.05). However, in some cases the increase was not significant.

Adhesion is a parameter to describe food sticking to the teeth by chewing. The amount of adhesion was noticeably reduced by ultrasound treatment (p<0.05).

Coherence parameter helps to have a comprehensive understanding of the viscoelastic properties, such as material tensile

strength. As can be seen in Tables 3 and 4, generally, the coherence of samples treated with ultrasound was increased significantly (except for a few examples) (p<0.05). This indicates that the cohesion of samples was a little affected by ultrasound treatments and therefore samples maintained their cohesion. Zhong *et al.*, (2007) reported that increased meat cohesion is most likely due to the release of some components during the sonication.

Meat springiness is likely to be related to the degree of swelling of muscle fibers (diameter of muscle fibers). It seems that this parameter affects myosin denaturation and  $\alpha$ -actinin (Chang *et al.*, 2012). According to Tables 3 and 4, the springiness of samples was independent from the temperature, the time and the type of ultrasound treatment.

Chewiness can be used to evaluate meat tenderness, which is obtained by multiplying indicators of hardness, cohesion and springiness. There is an indirect relationship between chewiness and meat tenderness in such a way that the lower chewiness value of meat, has the more tenderness value (Siró *et al.*, 2009). As can be seen in Tables 3 and 4, ultrasound treatment in most samples leads to a significant reduction in meat chewiness compared to the control samples. It represents

an increase in meat tenderness treated with ultrasound ( $p < 0.05$ ). With increasing temperature and ultrasound treatment time, small reduction in chewiness was occurred in comparison with that of the control sample; which can be related to the denaturation of proteins at higher temperatures and longer times. The sample chewiness treated with probe ultrasound was lower than those of ultrasound bath ( $p < 0.05$ ). This indicates a greater ability of ultrasound probe to increase the meat tenderness. The chewiness of treated samples in a mixture solution of brine-polyphosphate was less than those of brine (Tables 3 and 4). It is attributed to higher WHC and WBC of this samples (Table 1 and 2), which resulted in their higher tenderness.

Similar to the present results, Siró *et al.* (2009) reported that ultrasound treatment reduces the hardness and the chewiness of meat. They also expressed that the increase in temperature and intensity of ultrasound treatment is due to denaturation of proteins that causes higher hardness and chewiness of meat compared to lower temperature and intensity of the ultrasound. Chang *et al.* (2012) showed that the use of ultrasound (40 kHz, 1500W) in beef meat for 10, 20, 30, 40, 50, and 60 minutes did not have a significant effect on color. In general, ultrasound

treatment leads to a reduction in total meat hardness. In this regard, the lowest hardness of the samples was for those of under ultrasound treatment for 10 minutes.

The most important reasons for the increase in meat tenderness with ultrasound treatment can be directly connected to the physical degradation of the skeletal muscle (especially Nebulin grids) and bonded coating on the muscles (perimysium). It could also be indirectly related to activation of calcium-dependent proteolytic enzymes (for example calpains), through the release of calcium ions and cathepsin from the sarcoplasm network and other organelles (Jayasooriya *et al.*, 2007; Xiong *et al.* 2012).

In general, the results showed that ultrasonic treatment can effectively improve meat quality such as increasing WHC and WBC and reducing drip, cooking loss, hardness, chewiness and tenderness of meat. It was also found that the probe ultrasound was more effective than ultrasound bath and a solution mixture of brine-polyphosphate is better than only brine solution. Furthermore, results showed that ultrasound treatment at lower temperatures and short times resulted in an improve in meat quality in comparison with longer ultrasound times and higher temperatures.

## References

- Ahmed, J., Ramaswamy, H. S., Kasapis, S., Boye, J. I. (2009). *Novel food processing: effects on rheological and functional properties*, CRC Press.
- Alarcon-Rojo, A., Janacua, H., Rodriguez, J., Paniwnyk, L., Mason, T. (2015). Power ultrasound in meat processing. *Meat science*, 107, 86-93.
- Chang, H.-J., Xu, X.-L., Zhou, G.-H., Li, C.-B., Huang, M. (2012). Effects of characteristics changes of collagen on meat physicochemical properties of beef semitendinosus muscle during ultrasonic processing. *Food and Bioprocess Technology*, 5, 285-297.
- Cheng, Q., Sun, D.-W. (2008). Factors affecting the water holding capacity of red meat products: A review of recent research advances. *Critical reviews in food science and nutrition*, 48, 137-159.
- Dolatowski, Z., Stadnik, J. (2007). Effect of sonication on technological properties of beef. *Вісник Дніпропетровського університету. Біологія, екологія*, 1.
- Feiner, G. (2006). *Meat Products Handbook: Practical Science and Technology*, CRC Press.
- Inguglia, E. S., Zhang, Z., Burgess, C., Kerry, J. P., & Tiwari, B. K. (2017). Influence of extrinsic operational parameters on salt diffusion during ultrasound assisted meat curing. *Ultrasonics*.
- Jayasooriya, S. D., Torley, P., D'arcy, B. R., Bhandari, B. R. (2007). Effect of high power ultrasound and aging on the physical properties of bovine Semitendinosus and Longissimus muscles. *Meat Science*, 75, 628-639.

- Leal-Ramos, M. Y., Alarcon-Rojo, A. D., Mason, T. J., Paniwnyk, L., Alarjah, M. (2011). Ultrasound-enhanced mass transfer in Halal compared with non-Halal chicken. *Journal of the Science of Food and Agriculture*, 91, 130-133.
- Ma, H.-J., Ledward, D. (2004). High pressure/thermal treatment effects on the texture of beef muscle. *Meat science*, 68, 347-355.
- Ojha, K. S., Keenan, D. F., Bright, A., Kerry, J. P., & Tiwari, B. K. (2016). Ultrasound assisted diffusion of sodium salt replacer and effect on physicochemical properties of pork meat. *International journal of food science & technology*, 51(1), 37-45.
- Ozuna, C., Puig, A., García-Perez, J. V., Mulet, A., Cárcel, J. A. (2013). Influence of high intensity ultrasound application on mass transport, microstructure and textural properties of pork meat (Longissimus dorsi) brined at different NaCl concentrations. *Journal of Food Engineering*, 119, 84-93.
- Pohlman, F., Dikeman, M., Kropf, D. (1997). Effects of high intensity ultrasound treatment, storage time and cooking method on shear, sensory, instrumental color and cooking properties of packaged and unpackaged beef pectoralis muscle. *Meat Science*, 46, 89-100.
- Savadkoochi, S., Hoogenkamp, H., Shamsi, K., Farahnaky, A. (2014). Color, sensory and textural attributes of beef frankfurter, beef ham and meat-free sausage containing tomato pomace. *Meat science*, 97, 410-418.
- Sheard, P., Nute, G., Richardson, R., Perry, A., Taylor, A. (1999). Injection of water and polyphosphate into pork to improve juiciness and tenderness after cooking. *Meat Science*, 51, 371-376.
- Siró, I., Ven, C., Balla, C., Jónás, G., Zeke, I., Friedrich, L. (2009). Application of an ultrasonic assisted curing technique for improving the diffusion of sodium chloride in porcine meat. *Journal of Food Engineering*, 91, 353-362.
- Stadnik, J., Dolatowski, Z. J. (2011). Influence of sonication on Warner-Bratzler shear force, colour and myoglobin of beef (m. semimembranosus). *European Food Research and Technology*, 233, 553-559.
- Turantaş, F., Kılıc, G. B., Kılıc, B. (2015). Ultrasound in the meat industry: General applications and decontamination efficiency. *International journal of food microbiology*, 198, 59-69.
- Xiong, G., Zhang, L., Zhang, W., Wu, J. (2012). Influence of ultrasound and proteolytic enzyme inhibitors on muscle degradation, tenderness, and cooking loss of hens during aging. *Czech J. Food Sci*, 30, 195-205.
- Zhong, S., Jiang, M., Wang, S., Dai, F., Chen, H. (2007). Effects of combined ultrasonic and calcium chloride treatment on beef quality. *Food Science*, 11, 124-146.

## اثر اولتراسوند حمام و پروب در ترکیب با محلول های آب نمک و آب نمک- پلی فسفات بر خواص کیفی و بافتی گوشت گاو

محمد حسین نائلی<sup>1</sup> - رضا اسماعیل زاده کناری<sup>2\*</sup>

تاریخ دریافت: 1396/06/25

تاریخ پذیرش: 1396/09/22

### چکیده

تکنیک‌های مختلف مکانیکی، آنزیمی و شیمیایی برای بهبود کیفیت گوشت استفاده می‌شود. چنین تکنیک‌هایی معایبی مانند زمان‌بر بودن و آسیب رساندن به شاخص‌های کیفی گوشت دارند. اولتراسوند به‌عنوان یک روش موثر برای اصلاح خواص تکنولوژیکی و ترد کردن گوشت استفاده می‌شود. نمونه‌های گوشت (از قسمت قلوه‌گاه) درون محلول نمکی یا مخلوطی از محلول آب نمک - پلی فسفات در التراسوند حمام (در فرکانس 37 کیلوهرتز) و پروب (20 کیلوهرتز) در دماهای 30، 40 و 50 درجه سانتی‌گراد به مدت 20، 25 و 30 دقیقه. تحت تیماردهی قرار گرفتند. تغییرات خواص تکنولوژیکی و بافتی نمونه‌های گوشتی مورد بررسی قرار گرفت. نتایج افزایش pH (از 5/55 برای نمونه کنترل تا 7/14)، ظرفیت نگهداری آب (WHC) (از 20/00% برای نمونه کنترل تا 38/15%)، ظرفیت اتصال آب (WBC) (از 12/63% برای نمونه کنترل تا 31/65%) و یک کاهش در افت خونابه (از 12/50% برای نمونه کنترل تا 3/21%)، افت پخت (از 36/70% برای کنترل تا 16/46%) را نشان داد. همچنین پارامترهای بافتی از جمله سختی و قابلیت جویدن کاهش، در حالی که تردی افزایش یافت. به‌طور کلی، تیمار اولتراسوند پروب درون محلول ترکیبی آب نمک - پلی فسفات کارآمدتر بود. می‌توان نتیجه گرفت که التراسوند یک روش موثر برای بهبود کیفیت گوشت می‌تواند باشد.

**واژه‌های کلیدی:** گوشت گاو، خواص تکنولوژیکی، تردی، ویژگی‌های بافتی، اولتراسوند

## Development of a chitosan-montmorillonite nanocomposite film containing *Satureja hortensis* essential oil

V. Alizadeh<sup>1</sup>, H. Barzegar<sup>2\*</sup>, B. Nasehi<sup>3</sup>, V. Samavati<sup>2</sup>

Received: 2016.01.04

Accepted: 2016.06.25

### Abstract

The present work describes the physicochemical and antimicrobial properties of active films developed by incorporating different concentrations (0.5, 1, and 2% v/v) of *Satureja hortensis* essential oil (SEO) and 3% (w/w) nanoclay into a chitosan- montmorillonite nanocomposite film. The tensile strength (TS) of the films significantly decreased and elongation at break (EAB) increased with the incorporation of SEO. The control film exhibited the lowest water vapor permeability. In addition, decreases in water solubility (WS) and transparency were observed with increasing the concentration of SEO. Thermogravimetric analysis (TGA) indicated that films incorporated with SEO exhibited a higher degradation temperature compared with the control. The structural properties and morphology of the nanocomposite films were examined by X-ray diffractometry (XRD) and Scanning electron microscopy (SEM). SEO-incorporated films were more effective against gram positive bacteria (*Staphylococcus aureus* and *Bacillus cereus*) than gram negative ones (*Salmonella typhimurium* and *Escherichia coli*). The results suggested that SEO, as a natural antibacterial agent, has the potential to be applied in antimicrobial biodegradable films.

**Keywords:** Nanocomposite film, Chitosan, *Satureja hortensis*, Essential oil, Antimicrobial.

### Introduction

Compared to plastic packaging materials, application of biopolymer-based films for shelf-life extension purposes has grown extensively in the last 20 years due to their environmental advantages. Biopolymer-based edible films and coatings can also act as a barrier to external influences such as moisture, carbon dioxide, oxygen, lipid and mechanical property modifiers, as a carrier for food additive in food systems (Gennadios, Hanna, & Kurth, 1997). Materials available for developing edible films usually based on polysaccharides, proteins and lipids (Peng, & Li, 2014). Chitosan, a deacetylated (to varying degrees) product of chitin, is the second most abundant natural biopolymer after cellulose. Compared to other polysaccharides, chitosan has several advantages, such as non-toxicity,

biodegradability, biocompatibility and biofunctionality (Abdollahi, Rezaei, & Farzi, 2012). However, weak mechanical and gas barrier properties, and poor water resistance limit its further applications, particularly in the presence of water and humid environments (Wang *et al.*, 2005; Xu, Ren, & Hanna, 2006). Nanocomposites are one of the most promising options to improve the mechanical, barrier and thermal properties of films made from biopolymers (Avella *et al.*, 2005). Development of polymer/layered silicate nanocomposites is one of the latest revolutionary steps of the polymer technology. Incorporation of nanoparticles into biopolymers in low percentages improves their mechanical strength, heat resistance, and barrier characteristics and thus can broadly be used for diverse applications, specifically packaging needs (Zolfi, Khodaiyan, Mousavi & Hashemi, 2014). Montmorillonite (MMT) is the most prevalent and important nano-clay used layered silicates because it is eco-friendly and easily accessed in large amounts with relatively low cost. Therefore, it is possible to improve the properties of chitosan films through the addition of small amounts (2–8%)

1, 2 and 3. MSc. Student, Assistant Professor and Associate Professor, Department of Food Science and Technology, Ramin Agriculture and Natural Resources University of Khuzestan, Iran.

(\*-Corresponding Author: hbarzegar@ramin.ac.ir)

DOI: 10.22067/iftstrj.v1396i13.64248

of MMT (Almasi, Ghanbarzadeh & Entezami, 2010). Another approach to improve the functional characteristics of the biopolymer-based films is to activate them with various types of additives such as antimicrobial agents to increase the shelf-life of foods. Currently, the use of natural active antimicrobials, such as plant extracts, instead of synthetic preservatives appears to be an attractive option (Atef, Rezaei, & Behrooz, 2015). Plant essential oils are major sources of phenolic compounds and have been indicated to have a wide range of antimicrobial effects (Shen & Kamdem, 2015). *Satureja hortensis* (or commonly known as Summer Savory) is a well-known medicinal plant, annual and aromatic herb belonging to the *Lamiaceae* family, which is widely cultivated in the Mediterranean region. It has shown antispasmodic, antidiarrheal, antioxidant and good antimicrobial properties (Hadian, Ebrahimi, & Salehi, 2010; Shojaee-Aliabadi *et al.*, 2013). Phenols, carvacrol and thymol as well as p-cymene, b-caryophyllene, linalool and other terpenoids are the major active constituents of *Satureja hortensis* essential oil (SEO) (Sefidkon, Abbasi, & Khaniki, 2006). The antimicrobial effect of SEO has been reported in several studies (Shojaee-Aliabadi *et al.*, 2013; Atef *et al.*, 2014; Sefidkon *et al.*, 2006). Thus, the incorporation of SEO into chitosan films offers the probability not only for imparting bioactivity (e.g. antimicrobial and antioxidant activity), but also improving the physicochemical properties of films. To the best of our knowledge, no specific study has been done on the incorporation of SEO into nanocomposite films based on chitosan and MMT. Hence, this work was carried out to evaluate SEO effects on the properties of chitosan/MMT nanocomposite films. The characterizations included the mechanical properties, water barrier ability, optical attributes, microstructural and thermal behavior as well as antimicrobial activity of the films against *S. aureus*, *B. cereus*, *E. coli* and *S. typhimurium*.

## Materials and methods

Crab shell chitosan with the deacetylation degree of 75–85% (medium molecular weight) was purchased from Sigma–Aldrich Chemical Co., USA. Unmodified natural MMT (Cloisite Na+) was purchased from Southern Clay Products (USA). Calcium chloride (analytical grade), Tween 80, Glacial acetic acid and Glycerol were supplied from Merck, Germany. Sodium chloride was obtained from Dr. Mojallai (Tehran, Iran). Mueller–Hinton agar (MHA) and Mueller–Hinton Broth (MHB) were provided from Merck Co. (Darmstadt, Germany). *Satureja hortensis* essential oil was bought from Barij Essence Pharmaceutical Co. (Kashan, Iran), and stored in a sealed dark container at 6 °C until the day of experiments.

## Bacterial strains

The bacterial strains used in the present study included *Staphylococcus aureus* (ATCC 25923), *Bacillus cereus* (PTCC 1154), *Salmonella typhimurium* (ATCC 14028) and *Escherichia coli* (PTCC 1330). All the stock cultures were provided by Persian Type Culture Collection (Tehran, Iran). Stock cultures of the studied bacteria were reserved in Brain Heart Infusion Broth (BHI) and kept at -20°C before the tests. Subculturing was conducted every 30 days to preserve bacterial viability.

## Preparation of the antimicrobial films

Chitosan solutions were prepared through the casting method proposed by Abdollahi *et al.* (2012) with some modifications. Film solution with the concentration of 2% (w/v) was prepared by dissolving crab shell chitosan in a 1% (w/v) aqueous acetic acid solution while mixing vigorously at 1250 rpm on a magnetic stirrer set at 90°C for about 20 min. After dissolution, glycerol was added as a plasticizer at 30% content based on dry chitosan film. The montmorillonite (3% w/w on solid polymer), was dispersed in 1% (v/v) aqueous acetic acid solution and vigorously stirred for 6 h. The obtained mixture was sonicated for 30 min at room temperature. The

clay dispersion was added to the aqueous acetic acid dispersion of chitosan and stirring was continued for 4 h. Tween 80 at 0.2% of SEO (v/v) was added as oil dispersant. Stirring was continued for a further 30 min at 40°C after the addition of the emulsifier. Finally, SEO was incorporated into the film forming solution at the final concentrations of 0.5, 1 and 2% (v/v) of the chitosan solution. Homogenization was performed by Ultra Turrax homogenizer (IKA T25-Digital Ultra Turrax, Staufen, Germany) at 13,500 rpm for 3 min. The filmogenic solution was then stirred slowly for 10 min to remove all air bubbles. Finally the film solution was cast on Plexiglas plate and dried for 30 h in an oven (35°C). Dried films were preconditioned in desiccators containing saturated solutions of Ca (NO<sub>3</sub>)<sub>2</sub>, 6H<sub>2</sub>O (at 25°C and 53% relative humidity) until evaluation. All samples were prepared in triplicate.

#### Film thickness measurement

Thickness of the film was measured using a manual digital micrometer (Mituto, Tokyo, Japan) having a sensitivity of 0.001 mm, at 8 random locations. The mean value was used for the calculation of tensile strength (TS) and water vapor permeability (WVP).

#### Water solubility

The film solubility in water was determined from immersion assay under constant agitation in distilled water for 6 h, according to the method suggested by Hosseini *et al.* (2009). After filtration, the undissolved film was dried at 110°C to reach a constant weight (final dry weight). The initial dry weight of the samples (1 cm × 3 cm) was determined by drying at 110°C to reach a constant weight. The difference between the initial and final dry weights was reported as solubility.

#### Water vapor permeability (WVP)

WVP tests were performed at 25°C and 75% RH gradient based on ASTM E96 gravimetric method (Shojaee-Aliabadi *et al.* 2013). Briefly, the glass permeation cups with the internal diameter of 3 cm and depth of 3.5 cm, containing anhydrous calcium chloride

(desiccant 0% RH), were sealed by the test films. The film-covered cups were stored in a desiccator containing the sodium-chloride-saturated solution. The weight gain of the test cups was recorded in 6 h intervals over a 48 h period. The difference in RH corresponding to a driving force of 1753.55 Pa, was expressed as water vapor partial pressure. The water vapor transmission rate (WVTR) of the films was measured from the slope reached by linear regression analysis (weight change vs. time) of moisture weight gain ( $\Delta m$ ) transferred through an effective film area ( $A$ ) during a certain time ( $\Delta t$ ), once the stationary state (linear) was obtained. WVTR and WVP were calculated using the following equations:

$$\text{WVP (10}^{-10} \text{ g/m s Pa)} = \frac{\text{WVTR} \times X}{P(R1 - R2)} \quad (1)$$

$$\text{WVTR} = \frac{\Delta m}{A \times \Delta t} \quad (2)$$

where  $X$  is the average film thickness (mm),  $P(R1 - R2)$  is the water vapor pressure differential across the film (Pa),  $R1$  is the relative humidity in the desiccator (75%) and  $R2$  is the relative humidity in the cup (0%). All tests were performed in three replicates.

#### Mechanical properties

Tensile strength (TS, MPa) and elongation-at-break (ELB, %) were performed at 25°C and 53% RH by a Texture Analyzer (TA-XT-plus Stable Micro Systems, Surrey, UK), according to ASTM (D882-02, 2002) standard. In order to prepare the samples, films were cut into 1 × 6 cm<sup>2</sup> strips. All tested film strips were fixed with an initial grip separation of 40 mm and stretched at a crosshead speed of 0.83 mm/s until breaking.

#### Optical properties

Color values of the film samples were determined using a CR-400 series colorimeter (Minolta, Tokyo, Japan). Measurements were expressed as lightness ( $L$ ), redness ( $a$ ) and yellowness ( $b$ ). Color measurements were done on white standard backgrounds ( $L^*=92.23$ ,  $a^*=-1.29$ , and  $b^*=1.19$ ). Prior to optical measurements, the films were conditioned in desiccators at 53% RH. At

least, three points of each film specimen were selected randomly to measure the optical properties of the chitosan films. The total color difference ( $\Delta E$ ) and the whiteness index (WI) were calculated as follows:

$$\Delta E = \sqrt{(L^* - L)^2 + (a^* - a)^2 + (b^* - b)^2} \quad (3)$$

$$WI = 100 - \sqrt{(100 - L)^2 + a^2 + b^2} \quad (4)$$

Where  $L^*$ ,  $a^*$ , and  $b^*$  are the color parameters of the standard plate and  $L$ ,  $a$ , and  $b$  are the color parameters of the sample.

#### X-ray diffraction (XRD)

XRD measurements were performed using a Philips X'Pert MPD Diffractometer (Eindhoven, Netherlands), operating at Cu  $K\alpha$  wavelength of 1.544 nm, at 40 kV and 30 mA. Nanocomposite films were scanned in the angular region ( $2\theta$ ) of 1–12°, speed of 1°min<sup>-1</sup> at room temperature.

#### Scanning electron microscopy (SEM)

SEM images of the surface and cross-section of the film samples were captured by a SEM apparatus (KYKY-EM3200, China). The film samples were fixed on the support using the double side adhesive tape and then mounted on the specimen holder. The films were coated with gold by sputter coater (Model: KYKY-SBC12, China) under vacuum condition. The samples were scanned using an accelerating beam voltage of 22 kV.

#### Thermogravimetric (TGA) analysis

Thermogravimetric analysis of the films was carried out using a Thermal Analyzer (TGA7, PerkinElmer, Norwalk, CT, USA) from 25 to 550 °C at a heating rate of 10 °Cmin<sup>-1</sup> under a nitrogen flow rate of 20 mL min<sup>-1</sup>. Weight losses of the film specimens were reported as a function of temperature (Ahmad, Benjakul, Prodpran, & Dubois, 2010).

#### Microbiological analysis

The disc-diffusion method was employed to determine the antibacterial activity of the films on bacterial strains. The film samples were cut

into discs with the diameter of 10 mm. Next, they were placed on the surface of MHA plates. The medium had been previously smeared with 0.1 ml of an overnight broth culture containing approximately 10<sup>8</sup> colony forming units (CFU) per milliliter of the test bacteria. Bacterial strains were subsequently incubated at 37°C for 24 h. The diameter of the inhibition zone was measured with a caliper to the nearest 0.02 mm and recorded in millimeters. A film without essential oil was applied as control in parallel. The clear zones surrounding the film discs were measured as the inhibition zone (annular radius) indicating the antimicrobial activity (Dashipour *et al.*, 2015).

#### Statistical analysis

Mean  $\pm$  standard deviation was obtained using the GLM procedure in SAS statistical software (Version 9.1; Statistical Analysis System Institute Inc., Cary, NC, USA). Significant differences between the means were detected by the Duncan's multiple range test at the confidence level of  $P < 0.05$ .

## Results and Discussion

#### Physical properties

The effects of incorporating SEO on the physical properties of chitosan-based nanocomposite films are reported in Table 1. Film thickness varied between 0.141 and 0.190 mm. The thickness of the control film (without essential oil) was 0.141 mm; these were increased significantly ( $P < 0.05$ ) as SEO content was increased. This increase was probably due to the entrapment of SEO microdroplets within the polymer matrix. A similar trend was observed when *Zataria multiflora* essential oil was added to carboxymethyl cellulose film (Dashipour *et al.*, 2014). The solubility of the bionanocomposite films as a function of SEO content is shown in Table 1. In this study, chitosan-based nanocomposite film showed a low solubility value (18.18 $\pm$ 0.94) after 6 h of dipping which was similar to the value (15.03 $\pm$ 0.96 %) reported by (Abdollahi *et al.*, 2012). When SEO was added, a significant

( $P < 0.05$ ) decrease was observed in water solubility. By increasing the SEO concentration from 0.5 to 2% in film solutions, WS was decreased significantly ( $P < 0.05$ ) from 18.18 to 13.10. This might attributed to the hydrophobic nature of SEO as well as the

formation of intermolecular interactions between essential oil constituents and the hydroxyl groups of chitosan matrix—(Atef *et al.*, 2014, Salarbashi *et al.*, 2013, Shojae-Aliabadi *et al.*, 2013).

**Table 1. Physical and mechanical properties of chitosan-based nanocomposite films incorporated with SEO.**

SEO (% v/v)	Thickness (mm)	Solubility in water (%)	WVP ( $\text{g s}^{-1} \text{m}^{-1} \text{Pa}^{-1} \times 10^{-10}$ )	TS (MPa)	EAB (%)
0.0	0.141 ± 0.003 <sup>d</sup>	18.18 ± 0.94 <sup>a</sup>	0.64 ± 0.04 <sup>d</sup>	27.76 ± 2.13 <sup>a</sup>	38.61 ± 1.27 <sup>c</sup>
0.5	0.153 ± 0.004 <sup>c</sup>	17.40 ± 0.72 <sup>a</sup>	0.76 ± 0.05 <sup>c</sup>	26.03 ± 1.05 <sup>a</sup>	39.29 ± 1.77 <sup>bc</sup>
1	0.166 ± 0.002 <sup>b</sup>	15.56 ± 0.32 <sup>b</sup>	0.92 ± 0.07 <sup>b</sup>	23.14 ± 0.85 <sup>b</sup>	41.90 ± 0.98 <sup>b</sup>
2	0.190 ± 0.003 <sup>a</sup>	13.10 ± 0.79 <sup>c</sup>	1.23 ± 0.05 <sup>a</sup>	16.05 ± 0.73 <sup>c</sup>	44.72 ± 1.41 <sup>a</sup>

Values within each column with different letters are significantly different ( $P < 0.05$ ).

#### Water vapor permeability

WVP values of chitosan-MMT films containing SEO at various concentrations are summarized in Table 1. The results revealed that an increase in SEO content increased the WVP value ( $P < 0.05$ ). The WVP was  $0.64 \times 10^{-10} \text{ g s}^{-1} \text{ m}^{-1} \text{ Pa}^{-1}$  for the control film (without essential oil), which was increased to  $1.23 \times 10^{-10} \text{ g s}^{-1} \text{ m}^{-1} \text{ Pa}^{-1}$  for the nano composites that contained 2% SEO. Although the presence of SEO microdroplets increase the hydrophobicity ratio of the films, it caused an increase in the moisture passing through the film as well. This can be attributed to the negative effect of SEO incorporation on the cohesion forces of the polymer matrix. Similar results have been reported by Bonilla *et al.* (2012) in chitosan based films containing basil and thyme essential oils and in quince seed mucilage based films containing oregano essential oil (Jouki, Yazdi, Mortazavi, & Koocheki, 2014). They showed that the rise in basil, thyme and oregano essential oils concentration, led to an increase in WVP values.

#### Mechanical properties

Stress-strain test is one of the most important tests in packaging materials and may contribute to the estimation and prediction of their mechanical properties in food applications (Ghasemlou, Khodaiyan, & Oromiehie, 2011). The effect of various SEO incorporations on the mechanical properties of

the film samples is presented in Table 1. The results demonstrated that SEO significantly ( $P < 0.05$ ) affected the tensile strength and extensibility of the nanocomposite films. The TS was 27.76 MPa for the control film and was decreased significantly ( $P < 0.05$ ) to 16.05 MPa for the films containing 2% SEO. The results are in agreement with the previously published literature (Sánchez-González, Gonzalez- Martinez, Chiralt, & Chafer, 2010). Conversely, EAB of the nanocomposite films was increased significantly from 38.61% to 44.72% ( $P < 0.05$ ). Since the essential oil acted as plasticizer and increased the extensibility of the polymer chains. Addition of essential oil to the film can result in the formation of a weak network structure (Atef *et al.*, 2015). A similar trend was reported by Hosseini *et al.* (2015) on fish gelatin-chitosan films incorporated with *Origanum vulgare* L. essential oil.

#### Optical properties

Optical properties are important factors in terms of general appearance and consumer acceptance (Abdollahi *et al.*, 2012). Table 2 shows the color values (L, a, b), total color difference ( $\Delta E$ ) and whiteness index (WI) of the nanocomposite films and those containing SEO. Films without SEO were clear and had a transparent appearance (higher L value). However, the films containing SEO had a slightly yellow appearance, as demonstrated by a remarkable increase in the yellow/blue (b) value and total color difference ( $\Delta E$ ).

Nevertheless, a decrease was observed in the lightness (L), red/green (a), and whiteness index (WI) values as a function of SEO content. Similar results were observed for agar-cellulose bionanocomposite films containing savory essential oil (Atef *et al.*, 2015). This phenomenon is probably due to the presence of phenolic compounds in SEO, which might have light absorbance at low wavelengths. The films incorporated with SEO

showed a markedly ( $p < 0.05$ ) greater total color difference ( $\Delta E$ ) in comparison to the control films; this could be ascribed to the decrease in brightness ( $L^*$ ) and the increase observed in the colorimetric coordinate ( $b^*$ ). Similar results were observed by Benavides *et al.* (2012) when oregano essential oil was added to the alginate film.

**Table 2. Effect of various concentrations of SEO on color parameters of chitosan-based nanocomposite films.**

SEO (% v/v)	L	a	b	$\Delta E$	WI
0.0	85.51 $\pm$ 0.13 <sup>a</sup>	-1.54 $\pm$ 0.09 <sup>a</sup>	7.70 $\pm$ 0.04 <sup>d</sup>	10.79 $\pm$ 0.13 <sup>d</sup>	83.52 $\pm$ 0.12 <sup>a</sup>
0.5	83.29 $\pm$ 0.58 <sup>b</sup>	-2.73 $\pm$ 0.03 <sup>b</sup>	12.09 $\pm$ 0.75 <sup>c</sup>	15.14 $\pm$ 0.91 <sup>c</sup>	79.19 $\pm$ 0.89 <sup>b</sup>
1	81.98 $\pm$ 1.60 <sup>b</sup>	-3.04 $\pm$ 0.14 <sup>c</sup>	14.57 $\pm$ 1.73 <sup>b</sup>	17.78 $\pm$ 2.36 <sup>b</sup>	76.62 $\pm$ 2.33 <sup>c</sup>
2	79.65 $\pm$ 0.19 <sup>c</sup>	-3.27 $\pm$ 0.29 <sup>c</sup>	17.53 $\pm$ 0.52 <sup>a</sup>	21.50 $\pm$ 0.41 <sup>a</sup>	72.94 $\pm$ 0.40 <sup>d</sup>

Values within each column with different letters are significantly different ( $P < 0.05$ ).

#### X-ray diffraction (XRD)

X-ray diffractograms of chitosan, pure nano-MMT and chitosan/MMT nano

composite films with and without SEO are depicted in Fig. 1.

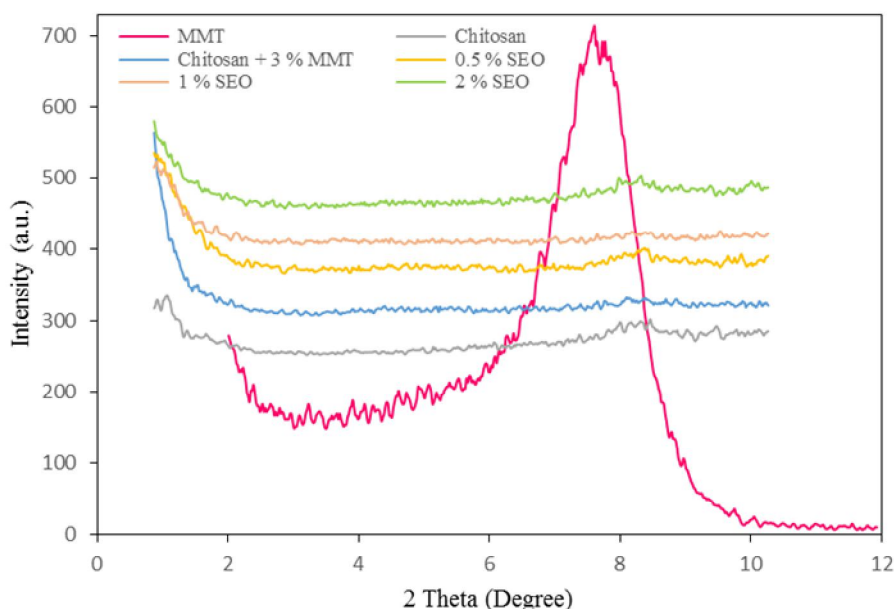


**Fig 1. XRD patterns for the pristine MMT and chitosan-based nanocomposite films incorporated with various concentrations of SEO.**

During intercalation, insertion of polymer chains into the MMT layers forced the platelets apart and increased the d-spacing. This created a shift in the diffraction peak of montmorillonite toward lower angles

regardless of the clay content (Xu *et al.*, 2006). In an exfoliated (or delaminated) nanocomposite structure, diffraction peaks of nano-clay disappear from the XRD patterns due to the lack of order between the silicate

layers (Alexandre & Dubois, 2000). The crystalline structure of chitosan is strongly dependent on its processing condition, as well as its origin and molecular constitution, such as its molecular weight and degree of deacetylation (Lavorgna, Piscitelli, Mangiacapra, & Buonocore, 2010). Pure chitosan films showed a characteristic crystallinity peak at around  $2\theta=8.42^\circ$  which was also observed in the nanocomposite films. As can be seen in Fig. 1, the crystallinity of chitosan was slightly reduced by the incorporation of MMT clay. Previous studies on the chitosan films (Abdollahi *et al.* 2012) containing MMT, have presented similar trends. MMT exhibited a single diffraction peak at ( $2\theta=7.61^\circ$ ). The reflection peak was disappeared with the incorporation of 3 wt % MMT into the chitosan solution, indicating the formation of an exfoliated structure (homogeneously dispersed structure) that was

disordered and not detectable by XRD (Xu *et al.* 2006). Moreover, addition of SEO at various concentrations did not affect the structure of chitosan/MMT films. Similar results were reported for chitosan/clay nanocomposite films incorporated with rosemary essential oil (Abdollahi *et al.* 2012) and agar/cellulose nanocomposite films formulated with savory essential oil (Atef *et al.* 2015).

#### Film microstructure

Scanning electron microscopy (SEM) allows the microstructural analysis of films and provides a better understanding of the relationships between water vapor transmission mechanisms, mechanical and optical properties with the film structural characteristics. Fig. 2 illustrates SEM micrographs of the surface and cross-section of the films.

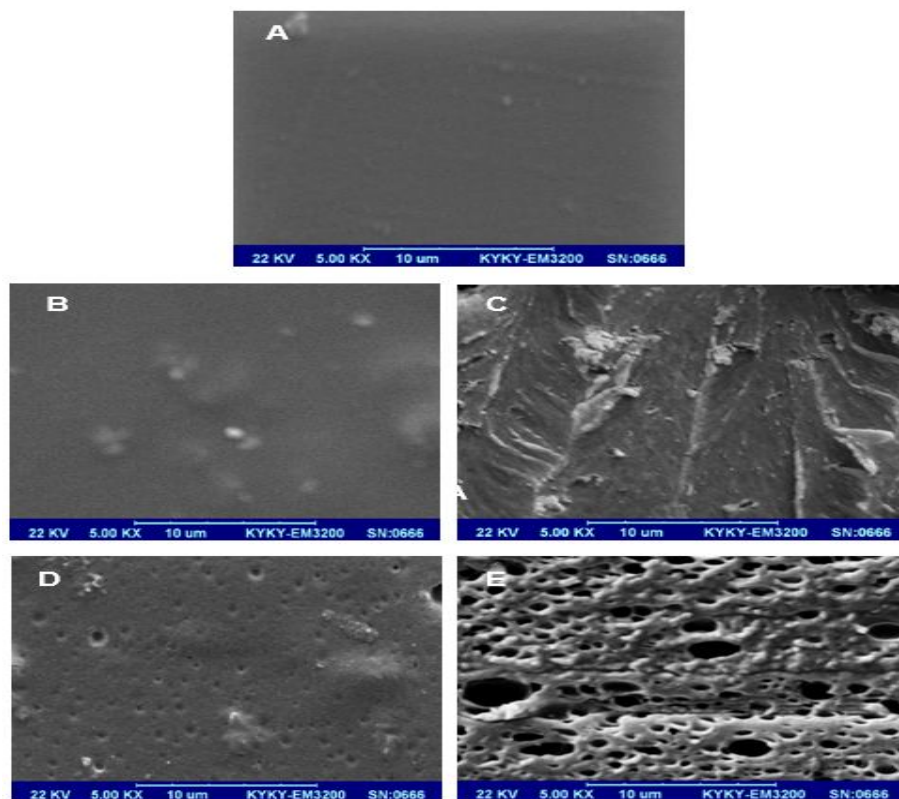


Fig. 2. SEM images of the surface (A: pure chitosan, B-C: chitosan-MMT, D: chitosan- MMT containing 2% SEO) and cross-section (D) of chitosan-MMT film containing 2% SEO.

The pure chitosan film had a compact, smooth and continuous surface (Fig. 2 A). As

seen, chitosan/MMT film had a compact, homogenous and continuous structure without irregularities, cracks or pores. This indicated that MMT nanoparticles were approximately well-dispersed in the chitosan matrix (Fig. 2 B-C). The surface and cross-section of film containing SEO were covered with micropores and seemed to be sponge-like (Fig. 2 D-E). Essential oil might have been evaporated during drying (Ahmad *et al.* 2012) leading to the formation of micro-pores throughout the film. Microscopy image revealed that the presence of SEO caused a heterogeneous structure in which oil droplets were entrapped in the continuous carbohydrate network. This could be due to the negative effect of oil

incorporation on the cohesion forces of the chitosan matrix, which enhance transparent phenomena through the film (bonilla *et al.*, 2012, Hosseini *et al.*, 2009). Thus, film microstructure might be associated with the attributes of the film, particularly water vapor permeability of the resulting film.

#### Thermo-gravimetric analysis (TGA)

TGA thermograms representing the thermal degradation behavior of chitosan nanocomposite films incorporated with SEO at different concentrations are illustrated in Fig. 3. The degradation temperatures (Td), weight loss ( $\Delta w$ ) and residue of the film samples are presented in Table 3.

**Table 3. Thermal degradation temperature (Td, °C) and weight loss ( $\Delta w$ , %) of chitosan-based nanocomposite films incorporated with various concentrations of SEO.**

SEO (% v/v)	$\Delta 1$		$\Delta 2$		$\Delta 3$		$\Delta 4$		Residue (%)
	Td <sub>1</sub>	$\Delta w_1$	Td <sub>2</sub>	$\Delta w_2$	Td <sub>3</sub>	$\Delta w_3$	Td <sub>4</sub>	$\Delta w_4$	
0.0	117.5	11.52	226.66	20.46	316.66	43.66	-	-	24.36
0.5	115.83	10.42	235.83	18.83	313.33	35.10	424.16	16.52	19.13
1	110.83	9.20	240	18.45	322.5	36.62	430.83	15.58	20.15
2	114.16	7.88	241.66	17.01	325	37.21	433.33	16.48	21.42

$\Delta w_1$ ,  $\Delta w_2$ ,  $\Delta w_3$  and  $\Delta w_4$  indicate the first, second, third and fourth stage weight loss, respectively, of film during TGA heating scan.

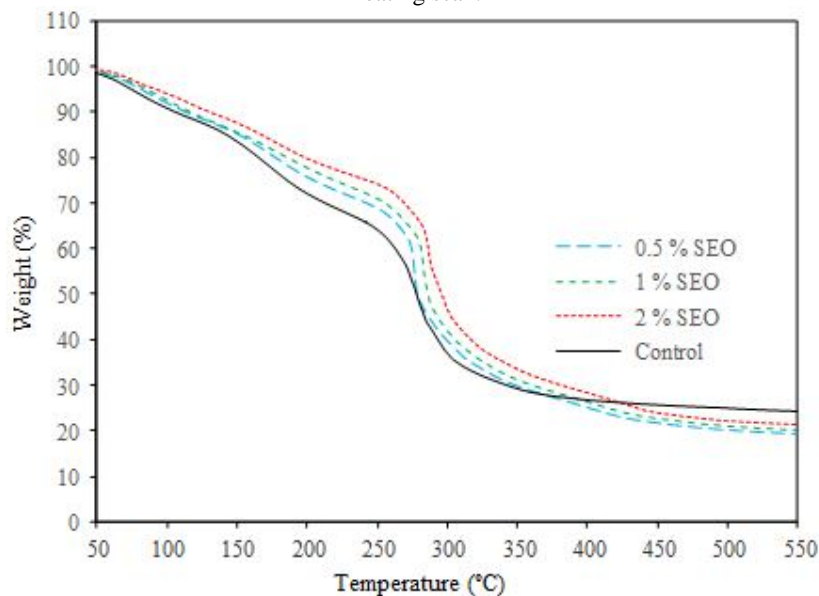


**Fig 3. TGA graph of chitosan-based nanocomposite films incorporated with various concentrations of SEO.**

The control chitosan film exhibited three main stages of weight loss. A similar result

was observed in the chitosan film (Shen *et al.* 2015). However, four main stages of weight loss were found in the films incorporated with SEO. The first stage of weight loss ( $\Delta w_1=7.88-11.52\%$ ), observed over the onset temperature ( $Td_1$ ) ranging from 110.83 to 117.50°C, is mostly associated with the evaporation of residual water and the acetic acid in the film. The second stage of weight loss ( $\Delta w_2=17.01-20.46\%$ ) was appeared at  $Td_2$  of 226.66–241.66°C. This stage of weight loss was possibly caused by the degradation of lower molecular weight components or structurally bound water in the chitosan network. The third stage of weight loss,  $\Delta w_3$  of 35.10–43.66% and  $Td_3$  of 313.13–325°C which was obtained for all film samples, mostly associated with the dehydration of saccharide rings, de-polymerization and pyrolytic decomposition of the acetylated and deacetylated units of the polysaccharide (Abdollahi, Rezaei, & Farzi, 2012). In general, the thermal degradation temperature of the second and third stages for all films containing SEO was higher than the control film. With the increase of SEO level in the films, the degradation temperature was enhanced but the weight loss decreased. An enhanced thermal stability of the chitosan samples with SEO was attributed to the interaction between chitosan and SEO, yielding a stronger polymer matrix, thus leading to the higher thermal resistance of the resulting film compared with the pure chitosan film. In the fourth stage of weight loss,  $\Delta w_4$  of 15.58–16.52% and  $Td_4$  of 424.16–433.33°C was obtained for the films containing SEO. Nevertheless, this stage ( $\Delta w_4$ ) was disappeared for the pure chitosan film. It was noted that this stage was likely associated with the loss of the thermally stable components of SEO incorporated in the polymer matrix. Overall, lower residue (or char content) from thermal degradation was observed in SEO-containing films, compared with the control film. TGA curves showed clearly that SEO at different concentrations contributed to a substantial improvement in the thermal stability of the chitosan film.

### Antibacterial activity

The antimicrobial activity of the nanocomposite films incorporated with SEO at various concentrations against the selected microorganisms is shown in Table 4. The chitosan/MMT nanocomposite film without SEO served as the control sample that did not show any antibacterial effect against all studied bacterial strains, resulting in no inhibition zones (Table 4). The results were in concordance with those of (Hosseini, Razavi, & Mousavi, 2009) who reported that the chitosan films showed no antibacterial effect against *Listeria monocytogenes*, *Staphylococcus aureus*, *Salmonella enteritidis* and *Pseudomonas aeruginosa*. According to Coma *et al.*, (2002), chitosan does not diffuse through the adjacent agar media in the agar diffusion method, as only organisms in direct contact with the active sites of chitosan are inhibited. Using the direct-contact test, the films containing 1% (v/v) SEO were not effective against *S. typhimurium*, yet exhibited a certain antibacterial effect on the growth of *B. cereus*, *S. aureus* and *E. coli* as evidenced by minimal bacterial growth around the film discs. As the concentration of SEO was increased, the zone of inhibition also was increased significantly ( $P<0.05$ ). Among the examined bacteria, *S. typhimurium* and *S. aureus* were the most resistant and most susceptible to SEO-containing films, respectively. In accordance with these results, Shojaee-Aliabadi *et al.* (2012) reported that k-carrageenan films produced with *Satureja hortensis* essential oil showed a greater inhibition zone for *S. aureus* than *B. cereus*, *E. coli*, *S. typhimurium* and *P. aeruginosa*. The antibacterial effect of SEO is attributed to its relatively high concentration of carvacrol,  $\gamma$ -terpinene and p-cymene (Hadian *et al.*, 2010). These constituents can disintegrate the external membrane of gram-negative bacteria, and thus increase the permeability of the cytoplasmic membrane (Burt, 2004). In general, SEO-containing films were obviously more effective against gram-positive bacteria than the gram-negative ones. This might be due to the impermeable outer membrane

surrounding gram negative bacteria (Fisher & Phillips, 2006).

**Table 4. Antimicrobial activity of chitosan-based nanocomposite films incorporated with various concentrations of SEO.**

SEO (% v/v)	Inhibition zone (mm <sup>2</sup> )			
	<i>S. aureus</i>	<i>B. cereus</i>	<i>E. coli</i>	<i>S. typhimurium</i>
0.0	0.00 <sup>c</sup>	0.00 <sup>c</sup>	0.00 <sup>c</sup>	0.00 <sup>b</sup>
0.5	0.00 <sup>c</sup>	0.00 <sup>c</sup>	0.00 <sup>c</sup>	0.00 <sup>b</sup>
1	45.71 ± 6.13 <sup>b</sup>	29.58 ± 4.25 <sup>b</sup>	18.73 ± 3.10 <sup>b</sup>	0.00 <sup>b</sup>
2	144.85 ± 12.97 <sup>a</sup>	98.40 ± 8.14 <sup>a</sup>	83.62 ± 7.82 <sup>a</sup>	65.12 ± 5.36 <sup>a</sup>

Values within each column with different letters are significantly different ( $P < 0.05$ ).

## Conclusions

The incorporation of SEO into the chitosan-based nanocomposite film was successfully performed to prepare antimicrobial biodegradable films. Addition of SEO significantly influenced the properties of the resulting films. The incorporation of SEO into the film decreased tensile strength and water solubility, while increased the percentage of EAB, WVP as well as the thickness of the nanocomposite films. Scanning electron microscopy showed that the microstructure of emulsified films had a critical effect on their WVP and mechanical properties. The obtained results indicated that SEO at various concentrations led to different thermal resistance for the resulting films. The films

exhibited highest inhibition against gram-positive bacteria (*S. aureus* and *B. cereus*) than gram-negative bacteria (*S. typhimurium* and *E. coli*). Overall, this study demonstrates that SEO-containing films present a good potential for being applied in food packaging. Although further studies, such as analysis of the physical stability and inhibition against other harmful microorganisms, are still needed.

## Acknowledgment

The authors gratefully acknowledge the Ramin Agriculture and Natural Resources University of Khuzestan and Iran Polymer and Petrochemical Institute for technical assistance and financial supports for this work.

## References

- Abdollahi, M., Rezaei, M., & Farzi, G. (2012). A novel active bionanocomposite film incorporating rosemary essential oil and nanoclay into chitosan. *Journal of Food Engineering*, 111(2), 343-350.
- Ahmad, M., Benjakul, S., Prodpran, T., & Agustini, T. W. (2012). Physico-mechanical and antimicrobial properties of gelatin film from the skin of unicorn leatherjacket incorporated with essential oils. *Food Hydrocolloids*, 28(1), 189-199.
- Alexandre, M., & Dubois, P. (2000). Polymer-layered silicate nanocomposites: preparation, properties and uses of a new class of materials. *Materials Science and Engineering: R: Reports*, 28(1), 1-63.
- Almasi, H., Ghanbarzadeh, B., & Entezami, A. A. (2010). Physicochemical properties of starch-CMC-nanoclay biodegradable films. *International Journal of Biological Macromolecules*, 46(1), 1-5.
- ASTM. (2002). Standard test method for tensile properties of thin plastic sheeting. In Annual book of ASTM standards designation D882. Philadelphia, PA: American Society for Testing and Materials.
- Atef, M., Rezaei, M., & Behrooz, R. (2015). Characterization of physical, mechanical, and antibacterial properties of agar-cellulose bionanocomposite films incorporated with savory essential oil. *Food Hydrocolloids*, 45, 150-157.
- Avella, M., De Vlieger, J. J., Errico, M. E., Fischer, S., Vacca, P., & Volpe, M. G. (2005).

- Biodegradable starch/clay nanocomposite films for food packaging applications. *Food Chemistry*, 93(3), 467-474.
- Benavides, S., Villalobos-Carvajal, R., & Reyes, J. E. (2012). Physical, mechanical and antibacterial properties of alginate film: effect of the crosslinking degree and oregano essential oil concentration. *Journal of Food Engineering*, 110(2), 232-239.
- Bonilla, J., Atarés, L., Vargas, M., & Chiralt, A. (2012). Effect of essential oils and homogenization conditions on properties of chitosan-based films. *Food Hydrocolloids*, 26(1), 9-16.
- Burt, S. (2004). Essential oils: their antibacterial properties and potential applications in foods—a review. *International Journal of Food Microbiology*, 94(3), 223-253.
- Coma, V., Martial-Gros, A., Garreau, S., Copinet, A., Salin, F., & Deschamps, A. (2002). Edible antimicrobial films based on chitosan matrix. *Journal of Food Science*, 67(3), 1162-1169.
- Dashipour, A., Razavilar, V., Hosseini, H., Shojaee-Aliabadi, S., German, J. B., Ghanati, K., ... & Khaksar, R. (2015). Antioxidant and antimicrobial carboxymethyl cellulose films containing *Zataria multiflora* essential oil. *International Journal of Biological Macromolecules*, 72, 606-613.
- Fisher, K., & Phillips, C. A. (2006). The effect of lemon, orange and bergamot essential oils and their components on the survival of *Campylobacter jejuni*, *Escherichia coli* O157, *Listeria monocytogenes*, *Bacillus cereus* and *Staphylococcus aureus* in vitro and in food systems. *Journal of Applied Microbiology*, 101(6), 1232-1240.
- Gennadios, A., Hanna, M. A., & Kurth, L. B. (1997). Application of edible coatings on meats, poultry and seafoods: a review. *LWT-Food Science and Technology*, 30(4), 337-350.
- Ghasemlou, M., Khodaiyan, F., & Oromiehie, A. (2011). Physical, mechanical, barrier, and thermal properties of polyol-plasticized biodegradable edible film made from kefiran. *Carbohydrate Polymers*, 84(1), 477-483.
- Hadian, J., Ebrahimi, S. N., & Salehi, P. (2010). Variability of morphological and phytochemical characteristics among *Satureja hortensis* L. accessions of Iran. *Industrial Crops and Products*, 32(1), 62-69.
- Hosseini, M. H., Razavi, S. H., & Mousavi, M. A. (2009). Antimicrobial, physical and mechanical properties of chitosan-based films incorporated with thyme, clove and cinnamon essential oils. *Journal of Food Processing and Preservation*, 33(6), 727-743.
- Hosseini, S. F., Rezaei, M., Zandi, M., & Farahmandghavi, F. (2015). Bio-based composite edible films containing *Origanum vulgare* L. essential oil. *Industrial Crops and Products*, 67, 403-413.
- Jouki, M., Yazdi, F. T., Mortazavi, S. A., & Koocheki, A. (2014). Quince seed mucilage films incorporated with oregano essential oil: physical, thermal, barrier, antioxidant and antibacterial properties. *Food Hydrocolloids*, 36, 9-19.
- Lavorgna, M., Piscitelli, F., Mangiacapra, P., & Buonocore, G. G. (2010). Study of the combined effect of both clay and glycerol plasticizer on the properties of chitosan films. *Carbohydrate Polymers*, 82(2), 291-298.
- Peng, Y., & Li, Y. (2014). Combined effects of two kinds of essential oils on physical, mechanical and structural properties of chitosan films. *Food Hydrocolloids*, 36, 287-293.
- Salarbashi, D., Tajik, S., Shojaee-Aliabadi, S., Ghasemlou, M., Moayyed, H., Khaksar, R., & Noghabi, M. S. (2014). Development of new active packaging film made from a soluble soybean polysaccharide incorporated *Zataria multiflora* Boiss and *Mentha pulegium* essential oils. *Food Chemistry*, 146, 614-622.
- Sánchez-González, L., González-Martínez, C., Chiralt, A., & Cháfer, M. (2010). Physical and antimicrobial properties of chitosan–tea tree essential oil composite films. *Journal of Food Engineering*, 98(4), 443-452.
- Sefidkon, F., Abbasi, K., & Khaniki, G. B. (2006). Influence of drying and extraction methods on yield and chemical composition of the essential oil of *Satureja hortensis*. *Food Chemistry*, 99(1), 19-23.

- Shen, Z., & Kamdem, D. P. (2015). Development and characterization of biodegradable chitosan films containing two essential oils. *International Journal of Biological Macromolecules*, 74, 289-296.
- Shojaee-Aliabadi, S., Hosseini, H., Mohammadifar, M. A., Mohammadi, A., Ghasemlou, M., Ojagh, S. M., & Khaksar, R. (2013). Characterization of antioxidant-antimicrobial  $\kappa$ -carrageenan films containing Satureja hortensis essential oil. *International Journal of Biological Macromolecules*, 52, 116-124.
- Wang, S. F., Shen, L., Tong, Y. J., Chen, L., Phang, I. Y., Lim, P. Q., & Liu, T. X. (2005). Biopolymer chitosan/montmorillonite nanocomposites: preparation and characterization. *Polymer Degradation and Stability*, 90(1), 123-131.
- Xu, Y., Ren, X., & Hanna, M. A. (2006). Chitosan/clay nanocomposite film preparation and characterization. *Journal of Applied Polymer Science*, 99(4), 1684-1691.
- Zolfi, M., Khodaiyan, F., Mousavi, M., & Hashemi, M. (2014). The improvement of characteristics of biodegradable films made from kefirin–whey protein by nanoparticle incorporation. *Carbohydrate polymers*, 109, 118-125.

## تولید و ارزیابی فیلم نانوکامپوزیتی کیتوزان- مونت‌موریلونیت حاوی اسانس مرزه (*Satureja hortensis*)

وحید علیزاده<sup>1</sup> - حسن برزگر<sup>2\*</sup> - بهزاد ناصحی<sup>3</sup> - وحید سمواتی<sup>2</sup>

تاریخ دریافت: 1396/05/06

تاریخ پذیرش: 1396/09/28

### چکیده

در تحقیق حاضر، خصوصیات فیزیکوشیمیایی و ضد میکروبی فیلم‌های فعال نانوکامپوزیتی کیتوزان-نانورس حاوی مقادیر مختلف اسانس مرزه (0/5، 1 و 2 درصد حجمی / حجمی) مورد ارزیابی قرار گرفت. با افزودن اسانس به فیلم‌ها، مقاومت به کشت، کاهش و کشش‌پذیری فیلم‌ها، به‌طور معنی‌داری افزایش پیدا کرد. نتایج نشان داد که از بین نمونه‌های فیلم مورد آزمون، فیلم شاهد دارای کمترین میزان نفوذپذیری نسبت به عبور بخار آب بود. همچنین با افزایش غلظت اسانس، حلالیت در آب و شفافیت فیلم‌ها کاهش یافت. نتایج آزمون گرما وزن‌سنجی (TGA) نشان داد که فیلم‌های حاوی اسانس مرزه نسبت به فیلم شاهد دارای دمای تخریب بالاتری هستند. در ادامه خصوصیات ساختاری و مورفولوژیکی فیلم‌های نانوکامپوزیتی، بوسیله روش پراش پرتو ایکس (XRD) و میکروسکوپ الکترونی روبشی (SEM) مورد بررسی قرار گرفت. فیلم‌های حاوی اسانس مرزه، روی باکتری‌های گرم مثبت (*Bacillus cereus* و *Staphylococcus aureus*) نسبت به باکتری‌های گرم منفی (*Escherichia coli* و *Salmonella typhimurium*) تاثیر بازدارندگی بیشتری داشتند. در نهایت نتایج نشان داد که اسانس مرزه می‌تواند به‌عنوان یک ماده ضدباکتری طبیعی در ساخت فیلم‌های زیست تخریب پذیر ضد میکروب مورد استفاده قرار گیرد.

واژه‌های کلیدی: فیلم نانوکامپوزیتی، کیتوزان، مرزه، روغن اساسی، ضد میکروب.

1، 2 و 3- دانشجوی کارشناسی ارشد، استادیار و دانشیار، گروه علوم و صنایع غذایی، دانشگاه کشاورزی و منابع طبیعی رامین خوزستان، خوزستان، ایران.  
\* - نویسنده مسئول: (Email: hbarzegar@ramin.ac.ir)

## Study on the effects of sucrose and lactose on the rheological properties of *Alyssum homolocarpum* seed gum in dilute solutions

M. A. Hesarinejad<sup>1</sup>, S. M. A. Razavi<sup>2\*</sup>, A. Koocheki<sup>2</sup>, M. A. Mohammadifar<sup>3</sup>

Received: 2016.09.26

Accepted: 2017.03.15

### Abstract

Nowadays, demands for hydrocolloids which improve the rheological properties of foods as well as retain their properties under the influence of food additives have increased. In this study, dilute solution properties were employed to understand the molecular and conformational properties of *Alyssum homolocarpum* seed gum (AHSG), in presence of sucrose and lactose. The model of Tanglertpaibul & Rao was selected as the best model for the estimation of the intrinsic viscosity. It was shown that except for water, the solutions of sucrose and lactose are poor solvents for AHSG as indicated by a decrease in intrinsic viscosity, swollen specific volume, shape function, and coil dimensions. As the sucrose and lactose concentrations increased, the coil radius decreased. The reduction in the shape and swollen volume parameters in the presence of sucrose and lactose as compared to the sugar-free solution indicated the negative effect of the opted sugars on the molecular volume of the gum. Evaluations of the dilute solution properties of the gum in sucrose and lactose solutions revealed that the existence of a conformation tending to ellipsoidal shape and the probability of the conformation of random coil with no molecular entanglements in AHSG solutions.

**Keywords:** *Alyssum homolocarpum*, intrinsic viscosity, lactose, sucrose.

### Introduction

In recent years, application of hydrocolloids has dramatically increased in the food industry. Owing to their safety, availability and low processing costs, herbal seeds have a proper potential for the extraction of hydrocolloids. Most of these seeds have starch as food supply for their embryos. Yet, some others have non-starch polysaccharides with functionalities similar to those of gums and could be used as commercial gums (Bostan, Razavi, Farhoosh, 2010). Some of these plants grow in different regions of Iran and contain some polysaccharides known as hydrocolloids (Razavi, Farhoosh, Bostan, 2007).

Qodume Shirazi (*Alyssum homolocarpum*)

is a member of Cruciferae family which has many traditional applications (Koocheki, Mortazavi, Shahidi, *et al.*, 2009). Qodume is native to some Middle East countries including Egypt, Iraq, Iran and Pakistan (Amin, 2005). Its mucilage is pharmaceutically applicable and has recently been examined as a novel source of hydrocolloid (Koocheki *et al.*, 2009b, Koocheki, Kadkhodae, Mortazavi, *et al.*, 2009a; Koocheki, Shahidi, Mortazavi, *et al.*, 2011). Due to the food fibers of hydrocolloids, they can be utilized in the formulations of food and pharmaceutical products, inspection of the characteristics of novel sources of herbal gums with appropriate properties. Optimization of AHSG extraction conditions has been carried out through the response surface methodology (Koocheki, Mortazavi, Shahidi, *et al.*, 2010). The rheological properties of the gum was studied in the stable conditions under the impact of concentration (1.5-4%), temperature (5-65°C), pH (3-9), the salts of CaCl<sub>2</sub>, MgCl<sub>2</sub>, NaCl and KCl and sucrose (0-40%) (Koocheki *et al.*, 2009b). The viscoelastic behavior of AHSG has been recently

1 And 2. PhD Student and Professor, Department of Food Science and Technology, Faculty of Agriculture, Ferdowsi University of Mashhad, Mashhad, Iran.

3. Associate Professor, Research Group for Food Production Engineering, National Food Institute, Technical University of Denmark, Søtofts Plads, 2800, Kgs. Lyngby, Denmark.

(\*-Corresponding Author: s.razavi@um.ac.ir)

DOI: 10.22067/ifstrj.v1396i0.59095

investigated in the linear viscoelastic region (LVE) as a function of temperature and concentration (Hesarinejad, Koocheki, Razavi, 2015a). The obtained mechanical spectrum demonstrated that this gum, like many commercial gums, acts as a weak gel in the studied concentration range (1.5-3%). In addition, some of the physico chemical and functional properties of this gum have been determined. These properties include thickening, gelling, stabilizing and fat replacing which represent its potential as an alternative for commercial gums in food and pharmaceutical formulations (Koocheki *et al.*, 2009b; Koocheki *et al.*, 2010; Koocheki & Kadkhodaei, 2011; Koocheki *et al.*, 2009a; Koocheki & Razavi, 2009; Koocheki, *et al.*, 2011).

One of the important properties of biopolymers is their effectiveness in developing high viscosity in aqueous solutions, even at low concentrations. Since the coils of polysaccharides are separated from each other in the dilute solutions and move independently and freely, determination of intrinsic viscosity in dilute solutions provide good knowledge concerning the fundamental properties of macromolecules in solution (Pamies, Schmidt, Martinez, & Torr, 2010). The attraction-repulsion interactions among the chain segments affect the hydration of the polysaccharide and its hydrodynamic molecular volume. Molecular volume is associated with the chain conformation of polysaccharide molecules in the respective solution. These interactions could vary either with the properties of different solvents or with the electrostatic repulsion between the chain parts via addition of some cosolutes like sugars (development of new solvents). Therefore, the change in the hydrodynamic molecular volume, conformation and macromolecular aggregations could be evaluated through the change in the intrinsic viscosity (Van Aken, 2006). The effect of some additives, such as different sugars, on the intrinsic viscosity of a wide range of hydrocolloids have been extensively studied (Richardson, Willmer &

Foster, 1998; Samavati, Razavi, Rezaei & Aminifar, 2007; Mohammad Amini & Razavi, 2012; Behrouzian, Razavi & Karazhyian, 2014; Mirabolhassani *et al.*, 2017).

In our previous research, the monosaccharide composition,  $\zeta$ -potential, particle size distribution, specific volume and molecular parameters of AHSG were verified at different temperatures (Hesarinejad, Razavi, Koocheki, 2015b). It is necessary to study the effects of different conditions on the rheological behavior of this hydrocolloid for more investigations on the molecular behavior of this gum. The actual formulation of foods may contain different ingredients. It is also essential because of the complexities of food media caused by different concentrations of ingredients such as sugars. Among sugars, the most abundant ones in food products is sucrose, afterwards the lactose is also the most important constituents present in dairy systems, which along with sucrose play a vital role in taste and texture of various food products; hence, the main objective of this study was to investigate the effects of sucrose and lactose on the rheological properties of AHSG in a dilute domain (e.g. intrinsic viscosity; molecular conformation; shape and hydration parameters; coil radius and volume) in order to understand its behavior in real systems.

## 2. Materials and Methods

AHSG was extracted under the optimal conditions ( $36.3 \pm 1^\circ\text{C}$ , pH=4 and water to seed ration of 40:1 for 1 h), purified by ethanol (Koocheki *et al.*, 2010) and then freeze-dried. Initially, the AHSG was dissolved in deionized water in the presence or absence of cosolutes (sucrose, lactose) under constant mixing (1000 rpm) using a magnetic stirrer for 30 min at room temperature. After that, the stock solutions ( $0.1 \text{ g}\cdot\text{dl}^{-1}$ ) were left at ambient temperature overnight for complete hydration. Sucrose and lactose (Merck, Germany) were used for the preparation of sugar solutions.

**Measurement of the solution's viscosities**

The viscosity of samples was measured using a Cannon-Ubbelohde capillary viscometer (Size 75, Cannon Instruments Co., Germany; viscometer constant,  $k = 0.01875 \text{ mm}^2/\text{s}^2$ ) immersed in a thermostatic water bath under precise temperature control ( $25 \pm 0.1^\circ\text{C}$ ). In this experiment, the passage time of the solvent and samples from one mark to another was measured using a chronometer and the relative viscosity of the samples ( $\eta_{rel}$ ) was calculated through the division of the sample passage time ( $t$ ) by that of the solvent ( $t_s$ ) (Eqn. 1). Next, the specific viscosity was computed by Eqn. (2):

$$\eta_{rel} = \frac{\eta}{\eta_s} = \frac{t}{t_s} \quad (1)$$

$$\eta_{sp} = \frac{\eta - \eta_s}{\eta_s} = \eta_{rel} - 1 \quad (2)$$

Intrinsic viscosity ( $[\eta]$ ) was determined by fitting the obtained data from the dilute region measurement to the models of Huggins (1942) (Eqn.3), Kraemer (1938) (Eqn.4), Tanglertpaibul and Rao (1987) (Eqn.5) and Higiroy et al (2006) (Eqns. 6 and 7):

$$\frac{\eta_{sp}}{C} = [\eta] + K'[\eta]^2 C \quad (3)$$

$$\frac{\ln \eta_{rel}}{C} = [\eta] + K''[\eta]^2 C \quad (4)$$

$$\eta_{rel} = 1 + [\eta]C \quad (5)$$

$$\eta_{rel} = e^{C[\eta]} \quad (6)$$

$$\eta_{rel} = \frac{1}{1 - C[\eta]} \quad (7)$$

where  $k'$  and  $k''$  are constants of the Huggins and Kraemer models, respectively. Intrinsic viscosity is equal to the slope of the plot of  $\ln \eta_{rel}$  against  $C$  according to equation 6 and the slope of the plot of  $1 - \frac{1}{\eta_{rel}}$  against concentration ( $C$ ) based on equation 7.

**Estimation of the molecular conformation**

The biopolymer conformation could be calculated by the  $b$  parameter form Eqn. 8

which is the slope of the logarithmic plot of  $\log \eta_{sp}$  versus concentration (Lai, Tung & Lin, 2000).

$$\eta_{sp} = aC^b \quad (8)$$

**Shape and swollen volume parameters determination**

Voluminosity or swollen specific volume ( $v_s$ ) which gives us some information about the polymer conformation under different conditions of the solvent is applied to determine the volume of the solvated polymer molecules.

For determining  $v_s$ , the Y equation -which is characterized as follows- can be plotted against concentration under different conditions, so that the  $v_s$  would be measured at  $C=0$  (the intercept) (Joseph et al., 1991).

$$Y = \frac{\eta_{rel}^{0.5} - 1}{C(1.35\eta_{rel}^{0.5} - 0.1)} \quad (9)$$

Subsequently, the shape of polymer's molecules in a solution could be estimated through  $v$  factor (Eqn 10). According to this equation, swollen specific volume and intrinsic viscosity are associated with each other in which  $v$  is referred to as the shape factor and the extent of the viscosity increment which is concerned with the shapes of polymer's particles in the solution (Antoniou *et al.*, 2010).

$$[\eta] = v.v_s \quad (10)$$

If  $v=2.5$ , the particles shapes will be spherical and if  $v>2.5$ , the particles shapes in the solution will tend to oval.

**Coil radius and volume estimation**

Based on Einstein's viscosity equation, the hydrodynamic coil radius ( $R_{coil}$ ) is obtained as follows (Antoniou *et al.*, 2010):

$$R_{coil} = \left[ \frac{3[\eta]M_w}{10\pi.N_A} \right]^{\frac{1}{3}} \quad (11)$$

Where  $M_w$  is the molecular mass,  $N_A$  represents the Avogadro's number and  $[\eta]$

denotes the intrinsic viscosity. If the assumption of the coil spherical shape is correct, the helix volume ( $V_{coil}$ ) will be determined as follows:

$$V_{coil} = \frac{4}{3} \pi R_{coil}^3 \quad (12)$$

## Results and Discussion

### Intrinsic viscosity

The difference in the rheological behavior of various hydrocolloids solutions is the result of the difference between their individual macromolecular conformations in the solution. The conformation of each macromolecule has an impact on its hydrodynamic volume. Intrinsic viscosity is applied to specify the hydrodynamic volume occupied by macromolecule (Bohdanecky and Kovar, 1982). It is also influenced by hydrodynamic properties which include a measure of the permeability of the polymer coil to solvent and chain anisotropy (Samavati, Razavi, Rezaei, and Aminifar, 2007).

The typical twin Huggins-Kraemer and triple Tanglertpaibul & Rao, Higiroy 1 & Higiroy 2 plots for AHSG's intrinsic viscosity calculation are represented in Figs. 1 and 2, respectively.

The intrinsic viscosity  $[\eta]$  of AHSG calculated by five models (Eqns. 3-7) at different concentrations of sucrose and lactose is listed in Table 1. It can be seen that AHSG did not follow the Huggins and Kramer's equations, whereas slope based relations (Tanglertpaibul & Rao, Higiroy 1 & Higiroy 2) indicated high efficiency to determine the intrinsic viscosity of AHSG, because they showed better linear fit with higher correlation coefficient ( $R^2$ ) and lower root mean square error (RMSE) values. Therefore, the estimation of the intrinsic viscosity of AHSG from the slope of the dilute region seemed to provide more reliable results

McMilan (1974) stated that the plot-slope-based determination methods of the intrinsic viscosity have higher determination coefficients and lower standard errors as compared to those which are based on

intercept (extrapolation).

Niuckerson *et al* (2004) declared as the polymer concentrations are prepared by sequential dilutions, the error of the term  $\eta_{sp}/C$  increases and attempts for fitting the data to the Huggins model will encounter problems.

Table 1. Comparison between the intrinsic viscosity values of AHSG calculated by different models as a function of sugar type and concentration (at 25°C)

Treatment	Huggins					Kraemer					Tang, & Rao					Higro 1					Higro 2						
	$[\eta]$	$R^2$	RMSE	$[\eta]$	RMS E	$[\eta]$	$R^2$	RMSE	$[\eta]$	RMS E	$[\eta]$	$R^2$	RMSE	$[\eta]$	$R^2$	RMSE	$[\eta]$	$R^2$	RMSE	$[\eta]$	$R^2$	RMSE	$[\eta]$	$R^2$	RMSE		
Control	18.38±0.08	0.97	0.14	18.29±0.12	0.95	0.09	23.11±0.19	0.99	0.00	15.83±0.19	0.99	0.00	15.83±0.19	0.99	0.01	10.75±0.11	0.99	0.02	10.75±0.11	0.99	0.02						
Sucrose (%)																											
10	11.48±0.12	0.94	0.22	11.39±0.21	0.91	0.14	13.68±0.09	0.99	0.01	9.54±0.11	0.99	0.01	9.54±0.11	0.99	0.01	6.73±0.06	0.95	0.04	6.73±0.06	0.95	0.04						
20	11.15±0.07	0.94	0.09	11.00±0.17	0.98	0.05	12.79±0.12	0.99	0.00	8.79±0.21	0.99	0.01	8.79±0.21	0.99	0.01	6.45±0.11	0.94	0.04	6.45±0.11	0.94	0.04						
30	10.75±0.11	0.89	0.19	10.66±0.14	0.83	0.14	13.79±0.02	0.97	0.00	8.35±0.19	0.99	0.01	8.35±0.19	0.99	0.01	6.24±0.10	0.94	0.04	6.24±0.10	0.94	0.04						
40	7.18±0.16	0.78	0.13	7.00±0.21	0.97	0.08	6.56±0.08	0.99	0.00	5.14±0.17	0.97	0.01	5.14±0.17	0.97	0.01	5.14±0.10	0.92	0.03	5.14±0.10	0.92	0.03						
Lactose (%)																											
2.5	15.89±0.13	0.74	0.15	15.51±0.14	0.94	0.10	17.17±0.13	0.99	0.00	11.63±0.14	0.98	0.01	11.63±0.14	0.98	0.01	8.11±0.12	0.85	0.04	8.11±0.12	0.85	0.04						
5	11.00±0.10	0.95	0.41	11.78±0.12	0.75	0.25	20.71±0.10	0.99	0.01	14.09±0.14	0.99	0.01	14.09±0.14	0.99	0.01	9.56±0.09	0.97	0.03	9.56±0.09	0.97	0.03						
10	11.86±0.16	0.85	0.39	12.16±0.22	0.61	0.18	16.82±0.11	0.99	0.01	11.43±0.08	0.99	0.01	11.43±0.08	0.99	0.01	7.81±0.14	0.97	0.03	7.81±0.14	0.97	0.03						
15	9.92±0.09	0.95	0.35	9.76±0.17	0.83	0.21	15.85±0.09	0.99	0.00	10.86±0.13	0.99	0.01	10.86±0.13	0.99	0.01	7.55±0.11	0.98	0.02	7.55±0.11	0.98	0.02						

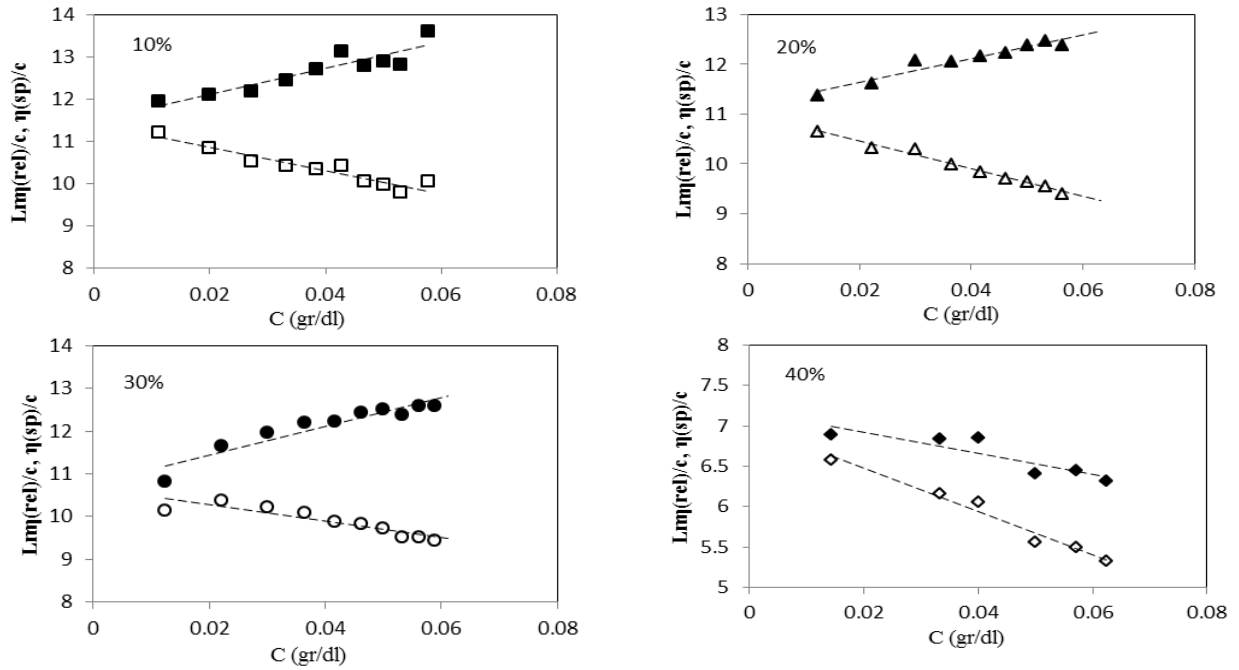


Fig 1. The plots resulted from fitting the Huggins (solid) and Kraemer (hollow) models to the data of the dilute region viscometry test of AHSG in different concentrations of sucrose (25°C).

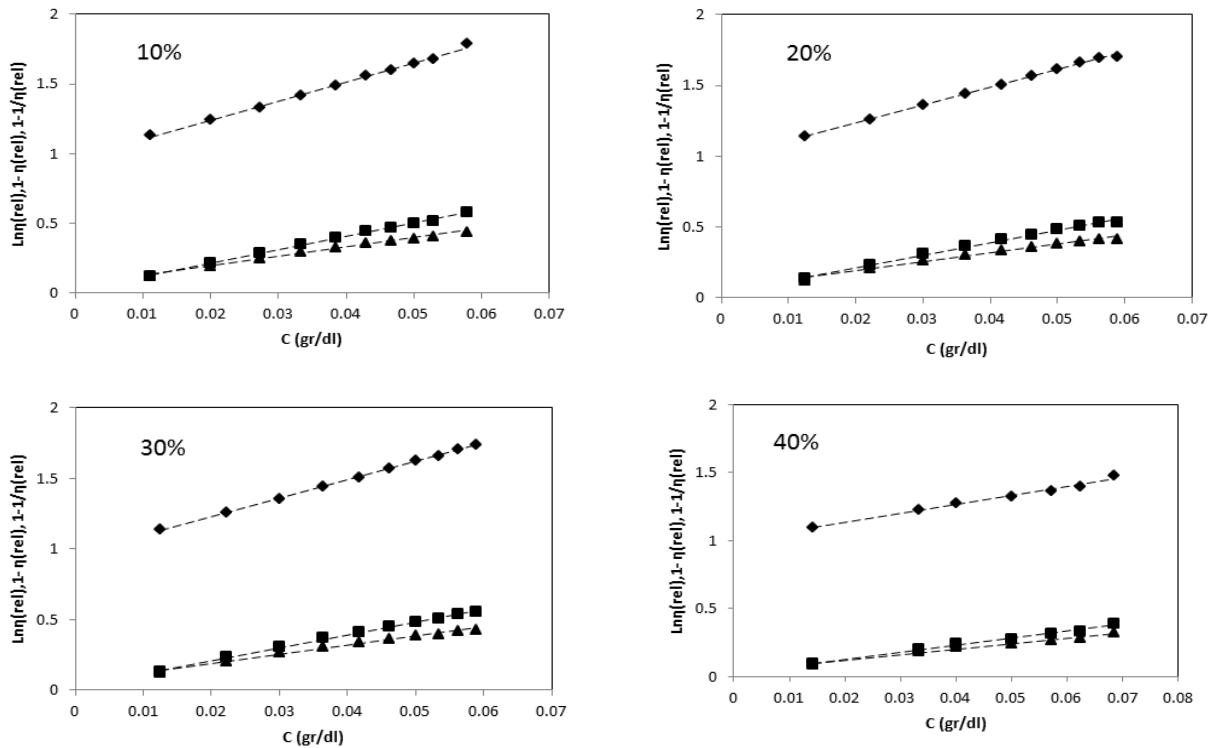


Fig 2. The curves obtained from fitting the models of Tanglertpaibul & Rao (◆), Higo 1 (■), Higo 2 (▲) to the dilute-region viscosity data of AHSG in different concentrations of sucrose (25°C).

Launay *et al* (1986) mentioned that the Huggins equation is valid only when  $\eta_{sp} < 0.7$ . The specific viscosity ranged from 0.2 to 1 in the present study. Lai *et al* (2000) and Higiro *et al* (2007) applied the models which calculate the intrinsic viscosity based on the plot slope, because the data of the two gums of *hsian-tSao* leaf gum and xanthan against concentration could not be fitted to the linear regression model.

After comparison of the  $R^2$  and RMSE values of the three slope-based models of Tanglertpaibul & Rao, Higiro1 and Higiro2 and verification of their capability in showing the difference between intrinsic viscosities in various concentrations of sucrose and lactose, the model of Tanglertpaibul & Rao was chosen as the superlative model with the highest  $R^2$  and the lowest RMSE (Table 1). Adding the lactose, the intrinsic viscosity of the AHSG solution decreased from 23.11 dl/g in the lactose-free sample to 15.85 dl/g in the 15% lactose solution. This reduction can be attributed to the impact of lactose on the reduction of the molecular associations. Slight decrease in the intrinsic viscosity of AHSG at different concentrations of lactose could be probably due to the decrease in the solvent quality.

Similar finding was also reported by Mirabolhassani *et al*, (2016) for Basil seed gum (BSG). They indicated that the intrinsic viscosity of BSG was decreased when the lactose concentration increased from 5 to 15% (w/v). Elfak *et al* (1977) observed that the intrinsic viscosities of the two hydrocolloids of guar and locust bean gum were reduced to 60% after the addition of 40% sucrose. Nonetheless, this decreasing trend was different at the concentration of 30% w/w and the rise in the solution intrinsic viscosity was observed in this concentration. The phenomenon can be explained as follows: sucrose is probably able to break down the intramolecular hydrogen bonds as a hydrogen-bond-forming agent and may cause the unfolding of the polymeric chain which in turn may lead to the viscosity increase. Similar results were reported for the cress

seed gum (Behrouzian *et al.*, 2013) and balangu seed gum (Mohammad Amini and Razavi, 2012) in the presence of lactose.

The same decreasing trend was also observed with the addition of sucrose as the intrinsic viscosity of the AHSG solution with reduction from 23.11 dl/g in the sucrose-free sample to 6.56 dl/g in the 40% sucrose sample. Similar results were reported by Michel *et al* (1984). They indicated that with the addition of sucrose to the high-methoxyl pectin hydrocolloid solution, the intrinsic viscosity decreased due to the reduction of the solvent quality. A similar phenomenon was also observed by Richardson *et al* (1998) investigating the effect of sucrose on the hydrodynamic volume of two commercial hydrocolloids (guar and locust bean gum). The reduction in the intrinsic viscosity of hydrocolloids has been reported as a function of various concentrations of  $\beta$ -glucan in maltose (Grimm *et al.*, 1995). On the other hand, Chen and Joslyn (1967) observed a dramatic increase in viscosity after investigating the effect of the sucrose solution on the intrinsic viscosity of the pectin solution in the dilute solution. They stated the equilibrium electrical conductivity of the polyelectrolytes solution was reduced as the sucrose concentration increased. They ascribed this viscosity increment to the fact that when the dielectric constant decreases, the electrostatic forces become stronger and the pure charge of the solution is reduced due to the increase in the number of the linked ions. Since, the carboxyl groups of pectin have been dissociated to a lesser extent, the electrostatic repulsion between these groups have decreased and the hydrogen bonds between these hydroxyl groups and the ones of the adjacent molecules lead to aggregation (Chen & Joslyn 1967; Elfak, Pass, Phillips, & Morley, 1977; Mohammad Amini & Razavi, 2012; Richardson *et al.*, 1998).

The differences in the intrinsic viscosity of AHSG at all concentrations of sucrose and lactose were significant ( $p < 0.05$ ). Since, AHSG intrinsic viscosity was the highest in the two solutions of 30% sucrose and 5%

lactose, it can be concluded that these two solutions are probably the best solvents for AHSG among the sugar-containing solvents. However their qualities are lower than that of the pure water (the blank sample).

#### Molecular parameters

Using the power-law equation (Eqn. 8) and the estimation of  $b$  from the slope of the log-log plot of  $\eta_{sp}$  against concentration in the dilute region, we could reach to an attitude about the conformation of polysaccharides (Lai *et al.*, 2000). This parameter ranged from 0.96 to 1.30 for AHSG in the presence of sucrose and lactose within the entire range of the examined concentrations. Researchers associate the slope values  $>1$  in the dilute region with either the conformation of the

random coil (Irani, *et al.*, 2016; Lapasin and Pricl, 1995) or entanglement (Morris *et al.*, 1981). They also related the slope values  $<1$  to the rod-like conformation (Lai and Chiang, 2002; Razmkhah *et al.*, 2016; 2017).

As observed in Table 2, the value of the dimensionless concentration or the Berry number ( $C[\eta]$ ) lay within the range of 0.09-0.81 and 0.21-0.88 after the addition of sucrose and lactose to AHSG solution, respectively. Considering these data and since the  $b$  parameter of the power-law equation was more than 1, the conformation of the randomized coil without entanglement could be predicted in AHSG solutions.

**Table 2. The molecular parameters of AHSG in the dilute region as a function of the sugar type and concentration (25°C)**

Treatment	$b$	$C[\eta]$	$\nu$ (-)	$\nu_s$ (dl g <sup>-1</sup> )	$R_{coil}$ (nm)	$V_{coil}$ (nm <sup>3</sup> )
Control	1.10±0.01	0.25-0.90	2.55	7.21	11.10	5732.50
Sucrose (%)						
10	1.06±0.00	0.15-0.79	3.10	4.40	9.26	3325.72
20	1.05±0.01	0.15-0.75	2.98	4.29	9.05	3109.35
30	1.11±0.01	0.17-0.81	3.25	4.21	9.26	3320.86
40	0.96±0.01	0.09-0.37	2.35	2.78	7.24	1594.79
Lactose (%)						
2.5	1.00±0.00	0.25-0.73	2.85	6.01	9.99	4174.17
5	1.30±0.01	0.34-0.88	4.31	4.80	10.06	5034.77
10	1.15±0.01	0.28-0.84	3.53	4.76	9.92	4089.08
15	1.21±0.01	0.21-0.67	3.66	4.32	9.72	3853.27

Standard deviation was less than 2% for the three replicates of all samples.

With the addition of sucrose to 20%, the  $b$  parameter decreased as compared to the aqueous solution and increased at the concentration of 30% and decreased again dramatically at the concentration of 40%. In the case of the lactose-containing solutions, it decreased till 2.5% and was maximized at 5% and decreased again at 10% and increased at 15%. Through the verification of the Berry number and referring to the observations of Kasaai, Charlet, & Arul (2000) and Behrouzian *et al.* (2013), it could be found out all AHSG samples are within the dilute region in the presence of sucrose and lactose solutions and it demonstrates that no

entanglement and coil-overlapping has taken place (Table 2). It seems that the two competing factors: a reduction in polymer/polymer association resulting in a decrease in the intrinsic viscosity (normally a consequence of a better solvent) and good solvents increasing the intrinsic viscosity through coil expansion were present throughout the sucrose concentration range studied (Richardson *et al.*, 1998).

Table 2 shows the voluminosity ( $\nu_s$ ) and the shape factor ( $\nu$ ) of AHSG solution in the presence of sucrose and lactose. The  $\nu_s$  of AHSG decreased with the rise in sucrose and lactose concentration, which reveals the

negative effect of the selected sugars on the volume of AHSG molecules signifying the reduction in the interactions between AHSG and water which may lead to the gum intramolecular interactions

The amount of  $\upsilon$  in the sugar-free solution (deionized water) was less than 2.5 exhibiting the spherical shape of the molecule. However, it was more than 2.5 in sucrose and lactose solutions, indicating that the molecules tended to be ellipsoidal shape. Yet, it decreased to approximately 2.35 in the sucrose concentration of 40%, showing the molecule shape tended to be spherical.

The results of the coil radius ( $R_{coil}$ ) and volume ( $V_{coil}$ ) of AHSG in the presence of various concentrations of sucrose and lactose are summarized in Table 2. As sucrose and lactose concentrations increased, the coil radius of AHSG decreased. The  $V_{coil}$  of AHSG decreased with the rise in the sugar concentration as well. The variations were more pronounced in the presence of sucrose rather than lactose. A similar phenomenon was observed in the case of Balangu seed gum in the presence of sucrose and lactose (Mohammad Amini and Razavi, 2014; Mirabolhassani *et al.*, 2016). An opposite trend as the increase in the coil radius and volume was observed in sucrose concentration of 30% and lactose concentration of 5%.

## References

- Amin, G.H., 2005. Medicinal Plants of Iran, first ed. Tehran University Publication, Tehran, Iran, p. 106 (in Persian language).
- Antoniou, E., Themistou, E., Sarkar, B., Tsianou, M., & Alexandridis, P. 2010. Structure and dynamics of dextran in binary mixtures of a good and a bad solvent. *Colloid and Polymer Science*, 288(12-13), 1301-1312.
- Behrouzian, F., Razavi, S. M., & Karazhiyan, H. 2014. Intrinsic viscosity of cress (*Lepidium sativum*) seed gum: Effect of salts and sugars. *Food Hydrocolloids*, 35, 100-105.
- Bohdanecky, M., & Kovar, J. 1982. *Viscosity of polymer solutions*. Elsevier Scientific Pub. Co..
- Bostan, A., Razavi, S. M. A., & Farhoosh, R. 2010. Optimization of hydrocolloid extraction from wild sage seed (*Salvia macrosiphon*) using response surface methodology. *International Journal of Food Properties*, 13(6), 1380-1392.
- Chen, T. S., and Joslyn, M. A. 1967. The effect of sugars on viscosity of pectin solutions, 1. Comparison of corn sirup with sucrose solutions. *Journal of colloid and interface science*, 23:399-406.
- Elfak, A. M., Pass, G., & Morley, R. G. 1977. The viscosity of dilute solutions of guar gum and

## Conclusion

In this study, the effects of sucrose and lactose in various concentrations were investigated in dilute solution properties of AHSG. After fitting different models, the Tanglertpaibul & Rao model was selected as the superlative model for the determination of the intrinsic viscosity of AHSG in the dilute solution with the highest  $R^2$  and the lowest RMSE. The intrinsic nature of the two solutions of 30% sucrose and 5% lactose were the best solvents for AHSG. Addition of sucrose and lactose decreased the intrinsic viscosity of the hydrocolloid solution via the influence on the reduction of molecule associations and reducing the solvent quality. The reduction in voluminosity and shape factor in the presence of sucrose and lactose rather than the sugar-free solution implied the negative effect of the chosen sugars on the volume of AHSG molecules. Comparing to the sugar-free solution, the rise in the shape factor value to more than 2.5 suggests the tendency of the spherical shape of the AHSG molecules to the ellipsoidal shape. As the concentrations of sucrose and lactose increased, the coil radius decreased. In general, it could be concluded that the solvent quality decreased significantly as the concentration of sucrose and lactose increased in the AHSG solution

- locust bean gum with and without added sugars. *Journal of the Science of Food and Agriculture*, 28(10), 895-899.
- Grimm, A., Krüger, E., & Burchard, W. 1995. Solution properties of  $\beta$ -D-(1, 3)(1, 4)-glucan isolated from beer. *Carbohydrate Polymers*, 27(3), 205-214.
- Hesarinejad, M.A., Koocheki, A., Razavi, S.M.A. 2015a. The viscoelastic and thermal properties of Qodume shirazi seed gum (*Alyssum homolocarpum*). *Iranian Food Science and Technology Research Journal*, 11(2): 116-128. (Abstract in English).
- Hesarinejad, M.A., Koocheki, A., Razavi, S.M.A. 2015b. *Alyssum homolocarpum* seed gum: Dilute solution and some physicochemical properties. *International journal of biological macromolecules*, 81, 418-426.
- Higiro, J., Herald, T. J., & Alavi, S. 2006. Rheological study of xanthan and locust bean gum interaction in dilute solution. *Food Research International*, 39(2), 165-175.
- Higiro, J., Herald, T.J., Alavi, S., and Bean, S. 2007. Rheological study of xanthan and locust bean gum interaction in dilute solution: Effect of salt, *Food Research International*, 40:435-447.
- Huggins, M. L. 1942. The viscosity of dilute solutions of long-chain molecules. IV. Dependence on concentration. *Journal of the American Chemical Society*, 64(11), 2716-2718.
- Irani, M., Razavi, S.M.A., Abdel-Aal, El-Sayed M., Hucl, P. and Patterson, C. A., 2016, Dilute solution properties of canary seed (*Phalaris canariensis*) starch in comparison to wheat starch, *International Journal of Biological Macromolecules*, 87, 123-129.
- Joseph, R., Devi, S., & Rakshit, A. K. 1991. Viscosity behaviour of acrylonitrile-acrylate copolymer solutions in dimethyl formamide. *Polymer international*, 26(2), 89-92.
- Kasaai, M. R., Charlet, G., & Arul, J. 2000. Master curve for concentration dependence of semi-dilute solution viscosity of chitosan homologues: the Martin equation. *Food Research International*, 33, 63-67.
- Koocheki, A., Kadkhodae, R., Mortazavi, S. A., Shahidi, F., & Taherian, A. R. 2009a. Influence of *Alyssum homolocarpum* seed gum on the stability and flow properties of O/W emulsion prepared by high intensity ultrasound. *Food Hydrocolloids*, 23(8), 2416-2424.
- Koocheki, A., Mortazavi, S. A., Shahidi, F., Razavi, S. M. A., and Taherian, A. R. 2009b. Rheological properties of mucilage extracted from *Alyssum homolocarpum* seed as a new source of thickening agent. *Journal of Food Engineering*, 91: 490-496.
- Koocheki, A., Mortazavi, S. A., Shahidi, F., Razavi, S. M. A., Kadkhodae, R., & Milani, J. 2010. Optimization of mucilage extraction from Qodume shirazi seed (*Alyssum homolocarpum*) using response surface methodology. *Journal of Food Process Engineering*, 33, 861-882.
- Koocheki, A., Shahidi, F., Mortazavi, S.A., Karimi, M., & Milani, E. 2011. Effect of Qodume Shirazi (*Alyssum Homolocarpum*) seed and xanthan gum on rheological properties of wheat flour dough and quality of bread. *Iranian Food Science and Technology Research Journal*. 7(1): 9-16. (Abstract in English)
- Koocheki, A., & Kadkhodae, R. (2011). Effect of *Alyssum homolocarpum* seed gum, Tween 80 and NaCl on droplets characteristics, flow properties and physical stability of ultrasonically prepared corn oil-in-water emulsions. *Food Hydrocolloids*, 25(5), 1149-1157.
- Koocheki, A., & Razavi, S. M. 2009. Effect of concentration and temperature on flow properties of *Alyssum homolocarpum* seed gum solutions: assessment of time dependency and thixotropy. *Food Biophysics*, 4(4), 353-364.
- Kraemer, E. O. 1938. Molecular weights of celluloses and cellulose derivates. *Industrial & Engineering Chemistry*, 30(10), 1200-1203.
- Lai, L. S., & Chiang, H. F. 2002. Rheology of decolorized hsian-tsoa leaf gum in the dilute domain. *Food Hydrocolloids*, 16(5), 427-440.
- Lai, L. S., Tung, J., & Lin, P. S. 2000. Solution properties of hsian-tsoa (*Mesona procumbens* Hemsl) leaf gum. *Food Hydrocolloids*, 14(4), 287-294.

- Lapasin, R. and Pricl, S., 1995. Rheology of Industrial Polysaccharides: Theory and Applications (Eds). Glasgow, Blackie Academic and Professional, pp. 250-494.
- Launay, B., Doublier, J. R., and Cuvelier, G. 1986. Flow properties of aqueous solution and dispersion of polysaccharides. In Mitchell, J. R., Ledward, D. A. (eds), Functional Properties of Food Macromolecules. Elsevier Applied Sci. Publisher, London, (pp. 1-78).
- McMillan, D. E. 1974. A comparison of five methods for obtaining the intrinsic viscosity of bovine serum albumin. *Biopolymers*, 13:1367-1371.
- Michel, F., Thibault, J. F., and Doublier, J. L. 1984. Viscometric and potentiometric study of high-methoxyl pectins in the presence of sucrose. *Carbohydrate Polymers*, 4:283-297.
- Mirabolhassani, S.E., Rafe, A., and Razavi, S.M.A., 2016, The influence of temperature, sucrose and lactose on dilute solution properties of basil seed gum, *International Journal of Biological Macromolecules*, 93: 623-629.
- Mohammad Amini, A., & Razavi, S. M. A. 2012. Dilute solution properties of Balangu (*Lallemantia royleana*) seed gum: effect of temperature, salt, and sugar. *International Journal of Biological Macromolecules*, 51(3), 235-243.
- Morris, E. R., Cutler, A. N., Ross-Murphy, S. B., Rees, D. A., & Price, J. 1981. Concentration and shear rate dependence of viscosity in random coil polysaccharide solutions. *Carbohydrate Polymers*, 1(1), 5-21.
- Nickerson, M. T., Paulson, A. T., and Hallett, F. R. 2004. Dilute solution properties of k-carrageenan polysaccharides: effect of potassium and calcium ions on chain conformation. *Carbohydrate Polymers*, 58: 25-33
- Pamies, R., Schmidt, R. R., Martínez, M. D. C. L., & de la Torre, J. G. 2010. The influence of mono and divalent cations on dilute and non-dilute aqueous solutions of sodium alginates. *Carbohydrate Polymers*, 80(1), 248-253.
- Razavi, S. M. A., Farhoosh, R., and Bostan, A. 2007. Functional properties of hydrocolloid extract of some domestic Iranian seeds, Research project No. 1475, Unpublished report, Ferdowsi University of Mashhad, Iran.
- Razmkhah, S., Razavi, S.M.A., and Mohammadifar, M.A., 2017, Dilute solution, flow behavior, thixotropy and viscoelastic characterization of cress seed (*Lepidium sativum*) gum fractions, *Food Hydrocolloids*, 63, 404-413.
- Razmkhah, S., Razavi, S.M.A., Mohammadifar, M.A., Tutor Ale, M. and Ahmadi Gavlighi, H., 2016, Protein-free cress seed (*Lepidium sativum*) gum: Physicochemical characterization and rheological properties, *Carbohydrate polymer*, 153, 14-24.
- Richardson, P. H., Willmer, J., & Foster, T. J. 1998. Dilute solution properties of guar and locust bean gum in sucrose solutions. *Food Hydrocolloids*, 12(3), 339-348.
- Samavati, V., Razavi, S. H., Rezaei, K. A., and Aminifar, M. 2007. Intrinsic viscosity of locust bean gum and sweeteners mixture in dilute solutions. *EJEAFChe*, 6(3): 1879- 1889.
- Tanglertpaibul, T., & Rao, M. A. 1987. Intrinsic viscosity of tomato serum as affected by methods of determination and methods of processing concentrates. *Journal of Food Science*, 52(6), 1642-1645.
- van Aken, G. A. 2006. Polysaccharides in food emulsions. In A. M. Stephen, G. O. Phillips, & P. A. Williams (Eds.), *Food polysaccharides and their applications* (2nd ed.). (pp. 521-539) London: Taylor and Francis.

## مطالعه اثر ساکارز و لاکتوز بر ویژگی‌های رئولوژیکی صمغ دانه قدومه شیرازی در ناحیه رقیق

محمدعلی حصاری نژاد<sup>1</sup> - سید محمدعلی رضوی<sup>2\*</sup> - آرش کوچکی<sup>2</sup> - محمدامین محمدی فر<sup>3</sup>

تاریخ دریافت: 1395/07/05

تاریخ پذیرش: 1395/12/25

### چکیده

امروزه تقاضا برای هیدروکلوئیدها نه تنها به منظور بهبود خواص رئولوژیکی مواد غذایی، بلکه جهت حفظ ویژگی‌های آن‌ها تحت تاثیر افزودنی‌های غذایی افزایش یافته است. در این مطالعه ویژگی‌های ناحیه رقیق صمغ دانه قدومه شیرازی برای درک خواص مولکولی و ساختمانی آن در حضور ساکارز و لاکتوز مورد بررسی قرار گرفته است. مدل تانگ و راتو به عنوان بهترین مدل برای تخمین ویسکوزیته ذاتی انتخاب شد. نتایج این پژوهش نشان داد که به جز آب، محلول‌های ساکارز و لاکتوز به دلیل کاهش ویسکوزیته ذاتی، حجم مخصوص متورم، تابع شکل، و ابعاد مارپیچ، حلال‌های ضعیفی برای صمغ دانه قدومه شیرازی هستند. با افزایش غلظت ساکارز و لاکتوز، شعاع مارپیچ کاهش می‌یابد. کاهش پارامترهای شکل و حجم متورم در حضور ساکارز و لاکتوز در مقایسه با محلول بدون قند نشان دهنده اثر منفی قندها بر حجم مولکولی صمغ است. ارزیابی ویژگی‌های ناحیه رقیق این صمغ در محلول‌های ساکارز و لاکتوز وجود کنفورماسیون بیضی شکل و احتمالاً حلقه تصادفی بدون درگیری مولکولی را در صمغ دانه قدومه شیرازی نشان داد.

**واژه‌های کلیدی:** صمغ دانه قدومه شیرازی، ویسکوزیته ذاتی، لاکتوز، ساکارز

1 و 2- دانشجوی دکترا و استاد، گروه علوم و مهندسی صنایع غذایی، دانشکده کشاورزی، دانشگاه فردوسی مشهد  
3- دانشیار، گروه تحقیقاتی مهندسی تولید مواد غذایی، موسسه ملی غذا، دانشگاه تکنیکال دانمارک، لونگبو، دانمارک  
(\* - نویسنده مسئول: s.razavi@um.ac.ir (Email:))

# نشریه پژوهش های علوم و صنایع غذایی ایران

با شماره پروانه 124/847 و درجه علمی - پژوهشی شماره 3/11/810 از وزارت علوم، تحقیقات و فناوری  
88/5/10

بهمن - اسفند 1396

شماره 6

جلد 13

درجه علمی - پژوهشی این نشریه طی نامه 3/11/47673 از وزارت علوم، تحقیقات و فناوری تا سال 1393 تمدید شده است.  
90/4/14

صاحب امتیاز: دانشگاه فردوسی مشهد

مدیر مسئول: دکتر ناصر شاهنوشی

سر دبیر: دکتر سید محمد علی رضوی

کارشناس امور اجرایی: دکتر مسعود تقی زاده

اعضای هیئت تحریریه:

استاد، اقتصاد کشاورزی ( دانشگاه فردوسی مشهد)

استاد، مهندسی و خواص بیوفیزیک مواد غذایی، دانشگاه فردوسی مشهد

استادیار، مهندسی مواد غذایی، دانشگاه فردوسی مشهد

استاد، تکنولوژی لبنیات، دانشگاه تهران

استاد، شیمی مواد غذایی، دانشگاه فردوسی مشهد

استاد، میکروبیولوژی، دانشگاه فردوسی مشهد

استاد، تکنولوژی لبنیات، دانشگاه ارومیه

دانشیار، میکروبیولوژی، دانشگاه علوم کشاورزی و منابع طبیعی گرگان

استاد، مهندسی و خواص بیوفیزیک مواد غذایی، دانشگاه فردوسی مشهد

استاد، شیمی مواد غذایی، دانشگاه تربیت مدرس

استاد، میکروبیولوژی مواد غذایی، دانشگاه فردوسی مشهد

دانشیار، بسته بندی مواد غذایی، دانشگاه فردوسی مشهد

دانشیار، مهندسی و خواص بیوفیزیک مواد غذایی، دانشگاه شیراز

استاد، شیمی مواد غذایی، دانشگاه فردوسی مشهد

استاد، میکروبیولوژی، دانشکده داروسازی دانشگاه علوم پزشکی مشهد

دانشیار، مهندسی و خواص بیوفیزیک مواد غذایی، دانشگاه علوم کشاورزی و

منابع طبیعی گرگان

دانشیار، شیمی مواد غذایی، دانشگاه صنعتی اصفهان

استاد، میکروبیولوژی و بیوتکنولوژی، دانشگاه فردوسی مشهد

دانشیار، تکنولوژی مواد غذایی، دانشگاه فردوسی مشهد

چاپ: چاپخانه دانشگاه فردوسی مشهد

قیمت: 5000 ریال (دانشجویان 2500 ریال)

دکتر محمدرضا احسانی

دکتر هاشم پورآذرنگ

دکتر محمداقبر حبیبی نجفی

دکتر اصغر خسروشاهی

دکتر مرتضی خمیری

دکتر سید محمد علی رضوی

دکتر محمد علی سحری

دکتر فخری شهیدی

دکتر ناصر صداقت

دکتر عسگر فرحناکی

دکتر رضا فرهوش

دکتر بی بی صدیقه فضلی بزاز

دکتر مهدی کاشانی نژاد

دکتر مهدی کدیور

دکتر سید علی مرتضوی

دکتر محمدجواد وریدی

ناشر: دانشگاه فردوسی مشهد

شمارگان: 250 نسخه

نشانی: مشهد - کد پستی 91775 صندوق پستی 1163

دانشگاه فردوسی مشهد، دانشکده کشاورزی - گروه علوم و صنایع غذایی - دفتر نشریه پژوهش های علوم و صنایع غذایی ایران.

تلفن: 20-8795618 داخلی 321 نمابر: 8787430

این نشریه در پایگاههای زیر نمایه شده است:

پایگاه استنادی علوم ایران (ISC)، پایگاه اطلاعات علمی جهاد دانشگاهی (SID)، بانک اطلاعات نشریات کشور (MAGRAN)

پست الکترونیکی: ifstrj@um.ac.ir

این نشریه در سایت [http://jm.um.ac.ir/index.php/food\\_tech/index](http://jm.um.ac.ir/index.php/food_tech/index) به صورت مقاله کامل نمایه شده است.

# بِسْمِ اللَّهِ الرَّحْمَنِ الرَّحِيمِ

## مندرجات

- 92 بهینه‌سازی ویژگی‌های بافتی پنیر فتای فراپالایش آنالوگ تولید شده از ترکیبات لبنی و غیرلبنی  
علی‌اکبر غلامحسین پور - مصطفی مظاهری تهرانی - سید محمدعلی رضوی
- 104 اثر دوره تابش و توان مایکروویو در خشک کردن برنج  
حسن جعفری - داوود کلاتری - محسن آزادبخت
- 116 تغییرات کشش سطحی و گرانی نانوامولسیون روغن ماهی تولید شده با روش فراصوت طی انبارمانی  
مریم نژادمنصوری - سید محمدهاشم حسینی - مهرداد نیاکوثری - غلامحسین یوسفی - محمدتقی گلمکانی
- 130 اثر اولتراسوند حمام و پروب در ترکیب با محلول‌های آب نمک و آب نمک-پلی فسفات بر خواص کیفی و بافتی گوشت گاو  
محمدحسین نانلی - رضا اسماعیل‌زاده کناری
- 143 تولید و ارزیابی فیلم نانو کامپوزیتی کیتوزان - مونت‌موریلونیت حاوی اسانس مرزه (*Satureja hortensis*)  
وحید علیزاده - حسن برزگر - بهزاد ناصحی - وحید سمواتی
- 155 مطالعه اثر ساکارز و لاکتوز بر ویژگی‌های رئولوژیکی صمغ دانه قدومه شیرازی در ناحیه رقیق  
محمدعلی حصارینژاد - سید محمدعلی رضوی - آرش کوچکی - محمدامین محمدی فر



# نشریه علمی - پژوهشی پژوهش‌های علوم و صنایع غذایی ایران



جلد ۱۳ شماره ۶  
سال ۱۳۹۶



شاپا: ۴۱۶۱-۱۷۳۵

شماره پیاپی ۴۸

## عنوان مقالات

- ۱۱۲..... بهینه‌سازی ویژگی‌های بافتی پنیر فتای فراپالایش آنالوگ تولید شده از ترکیبات لبنی و غیرلبنی  
علی اکبر غلامحسین پور - مصطفی مظاهری تهرانی - سید محمدعلی رضوی
- ۱۰۴..... اثر دوره تابش و توان مایکروویو در خشک کردن برنج  
حسن جعفری - داوود کلاتری - محسن آزادبخت
- ۱۱۶..... تغییرات کشش سطحی و گرانیوی نانوامولسیون روغن ماهی تولید شده با روش فراصوت طی انبارمانی  
مریم نژادمنصوری - سید محمدهاشم حسینی - مهرداد نیاکوثری - غلامحسین یوسفی - محمدتقی گل‌مکانی
- اثر اولتراسوند حمام و پروب در ترکیب با محلول‌های آب نمک و آب نمک-پلی فسفات بر خواص کیفی و  
بافتی گوشت گاو .....  
محمدحسین نائلی - رضا اسماعیل‌زاده کناری
- ۱۴۳..... تولید و ارزیابی فیلم نانو کامپوزیتی کیتوزان-مونت‌موریلونیت حاوی اسانس مرزه (*Satureja hortensis*)  
وحید علیزاده - حسن برزگر - بهزاد ناصحی - وحید سمواتی
- ۱۵۵..... مطالعه اثر ساکارز و لاکتوز بر ویژگی‌های رئولوژیکی صمغ دانه قدومه شیرازی در ناحیه رقیق  
محمدعلی حصاری نژاد - سید محمدعلی رضوی - آرش کوچکی - محمدامین محمدی فر